THE USE OF BIOPOLYMERS FOR TISSUE ENGINEERING

A Dissertation

Submitted to the Faculty

of

Purdue University

by

Nelda M. Vázquez Portalatín

In Partial Fulfillment of the

Requirements for the Degree

of

Doctor of Philosophy

December 2019

Purdue University

West Lafayette, Indiana

THE PURDUE UNIVERSITY GRADUATE SCHOOL
STATEMENT OF DISSERTATION APPROVAL

Dr. Alyssa Panitch, Co-Chair

Weldon School of Biomedical Engineering

Department of Biomedical Engineering, University of California, Davis

Currently at UC Davis

Dr. Julie C. Liu, Co-Chair

Davidson School of Chemical Engineering

Dr. Sarah Calve

Weldon School of Biomedical Engineering

Dr. Gert Breur

Department of Veterinary Clinical Sciences

Approved by:

Dr. George R. Wodicka

Head of the Departmental Graduate Program

To Mom, Dad, and Leilany

This would not be possible if it were not for you

ACKNOWLEDGMENTS

Pursuing and achieving my Ph.D. would not have been possible without the support, encouragement, and advice of many people. First, I would like to thank my family for always encouraging me to pursue my dreams no matter where they take me. To my late father, Julio A. Vázquez Cruz, thank you for showing me what dedication and passion are and for always encouraging me to be the best I can be. To my mom, Nelda I. Portalatín Padua, and sister, Leilany Vázquez Portalatín, thank you for your immense support, encouragement, and enthusiasm. I would not be here if it weren't for you.

My time as a graduate student at Purdue and a visiting graduate student at UC Davis has been a time for personal growth and intellectual stimulation. I would like to thank my advisor, Dr. Alyssa Panitch, for giving me the opportunity to pursue my Ph.D. and for her advice and guidance. I would also like to thank my co-advisor, Dr. Julie Liu, for her advice and guidance throughout the years. I am grateful to my committee members, Dr. Sarah Calve and Dr. Gert Breur, for their critical insight and feedback. I would also like to acknowledge the Purdue and UC Davis staff in Biomedical Engineering for their help during my time as a graduate student. I am grateful to the Panitch lab members for the feedback, discussions, and friendship throughout the years.

There are several people I would like to thank for their encouragement, support, feedback, and friendship throughout my Ph.D. tenure. Thanks to Dr. Katherine Clayton, Dr. Nimisha Bajaj, Dr. Joyatee Sarker, Dr. Rucha Joshi, and Carolina Vivas Valencia for their amazing friendship and support throughout the entirety of my Ph.D. Your incredible dedication to others and your achievements are a testament to the amazing people you are. You have been a great influence and have empowered me to continue on pursuing my dreams.

I am also grateful to Dr. Alba Alfonso García, Tima Dehghani, Alena Casella, Charlotte Vorwald, Dr. Nuala del Piccolo, and Vanessa Franco Carvalho Dartora. Your friendship and laughs have made me feel at home during my last years as a visiting graduate student at UC Davis. I am lucky to have met you.

Finally, I would like to acknowledge my funding sources (Purdue University George Washington Carver Fellowship) for providing financial support during my Ph.D.

My time as a Ph.D. student would not have been the same without you. Thank you all for being there.

TABLE OF CONTENTS

Page

Page

Page

Page

LIST OF TABLES

LIST OF FIGURES

ABSTRACT

Vázquez Portalatín, Nelda M. Ph.D., Purdue University, December 2019. The Use of Biopolymers for Tissue Engineering. Major Professors: Alyssa Panitch, Julie C. Liu.

Osteoarthritis (OA) is a degenerative joint disease characterized by cartilage damage and loss in the joints that affects approximately 27 million adults in the US. Tissue that is damaged by OA is a major health concern since cartilage tissue has a limited ability to self-repair due to the lack of vasculature in cartilage and low cell content. Tissue engineering efforts aim towards the development of cartilage repair strategies that mimic articular cartilage and are able to halt the progression of the disease as well as restore cartilage to its normal function.

This study harnesses the biological activity of collagen type II, present in articular cartilage, and the superior mechanical properties of collagen type I by characterizing gels made of collagen type I and II blends (1:0, 3:1, 1:1, 1:3, and 0:1). The collagen blend hydrogels were able to incorporate both types of collagen and retain chondroitin sulfate (CS) and hyaluronic acid (HA). Cryoscanning electron microscopy images showed that the 3:1 ratio of collagen type I to type II gels had a lower void space percentage (36.4%) than the 1:1 gels (46.5%) and the complex modulus was larger for the 3:1 gels (G*=5.0 Pa) compared to the 1:1 gels (G*=1.2 Pa). The 3:1 blend consistently formed gels with superior mechanical properties compared to the other blends and has the potential to be implemented as a scaffold for articular cartilage engineering.

Following the work done to characterize the collagen scaffolds, we studied whether an aggrecan mimic, CS-GAH$_b$, composed of CS and HA binding peptides, GAH, and not its separate components, is able to prevent glycosaminoglycan (GAG) and

collagen release when incorporated into chondrocyte-embedded collagen gels. Bovine chondrocytes were cultured and embedded in collagen type I scaffolds with CS, GAH, CS and GAH, or CS-GAH$_b$ molecules. Gels composed of 3:1 collagen type I and II with CS or CS-GAH$_b$ were also studied. The results obtained showed CS-GAH$_b$ is able to decrease GAG and collagen release and increase GAG retention in the gels. CS-GAH$_b$ also stimulated cytokine production during the initial days of scaffold culture. However, the addition of CS-GAH$_b$ into the chondrocyte embedded collagen scaffolds did not affect ECM protein expression in the gels. The incorporation of collagen type II into the collagen type I scaffolds did not significantly affect GAG and cytokine production and ECM protein synthesis, but did increase collagen release. The results suggest the complex interaction between CS-GAH$_b$, the chondrocytes, and the gel matrix make these scaffolds promising constructs for articular cartilage repair.

Finally, we used Dunkin Hartley guinea pigs, a commonly used animal model of osteoarthritis, to determine if high frequency ultrasound can ensure intra-articular injections of the aggrecan mimic are accurately positioned in the knee joint. A high-resolution small animal ultrasound system with a 40 MHz transducer was used for image-guided injections. We assessed our ability to visualize important anatomical landmarks, the needle, and anatomical changes due to the injection. From the ultrasound images, we were able to visualize clearly the movement of anatomical landmarks in 75% of the injections. The majority of these showed separation of the fat pad (67.1%), suggesting the injections were correctly delivered in the joint space. The results demonstrate this image-guided technique can be used to visualize the location of an intra-articular injection in the joints of guinea pigs and we are able to effectively inject the aggrecan mimic into knee joints.

All of the work presented here suggests that the addition of the aggrecan mimic to collagen I and collagen I and II scaffolds has shown that this type of construct could be useful for treating cartilage damage in the future.

1. INTRODUCTION

1.1 Background and Significance

Osteoarthritis (OA) is a degenerative joint disease characterized by cartilage damage and loss in the joints. Approximately 27 million adults in the US suffer from this disease [1], with knee OA being one of the top 5 causes of disability among adults [2]. OA patients exhibit pain, swelling and stiffness, all of which may limit the movement in the affected joints. The prevalence of this disease has resulted in a total annual cost of $89.1 billion in the US [2], most of which is spent on OA treatments. Tissue that is damaged by OA is a major health concern since cartilage tissue has a limited ability to self-repair due to the lack of vasculature in cartilage and low cell content [3]. Tissue engineering efforts aim towards the development of cartilage repair strategies that mimic articular cartilage and are able to halt the progression of the disease as well as restore the damaged cartilage.

1.2 Articular Cartilage

Articular cartilage is the connective tissue that forms the smooth, gliding surface of the diarthrodial joints. It is composed of a chondrocyte secreted extracellular matrix (ECM) that lacks blood vessels, nerves, and lymphatic vessels [4]. This ECM is mainly composed of collagen type II, glycosaminoglycans (GAGs), proteoglycans, and water (Figure 1.1). The ECM also contains proteins and other types of collagen in reduced amounts. The chondrocytes in articular cartilage are responsible for maintaining ECM production and homeostasis [5]. These chondrocytes produce collagen molecules that are able to crosslink and stabilize the matrix [5]. The interactions between the crosslinked matrix and proteoglycans results in a reinforcement of the

porous solid matrix. The negative charge of the proteoglycans causes water to be retained inside the matrix making up the fluid phase of articular cartilage. This fluid phase, which also contains gases, small proteins, metabolites, and a high concentration of cations to balance the negatively charged proteoglycans, confers articular cartilage with viscoelasticity and biomechanical properties, such as low-friction, high compressive strength [6], and the abilities to distribute load and deform and reform [7]. Loss of these main components, as is observed in OA, leads to a debilitated matrix with compromised biomechanical properties.

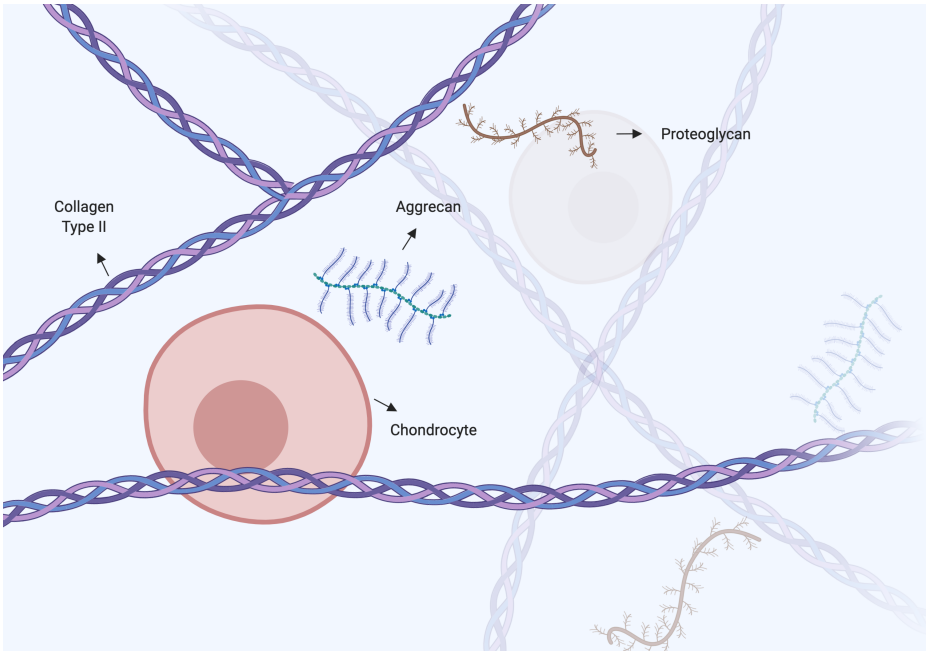

Figure 1.1.: Illustration of the articular cartilage extracellular matrix with chondrocytes, collagen type II, aggrecan and other proteoglycans. Illustration created with biorender.com.

1.2.1 Collagen

Collagen type II is the most abundant type of collagen found in articular cartilage. It makes up 90-95% of the collagen present in the ECM [8]. Collagen type II is made up of triple $\alpha 1$(II) helical strands that form fibrils that together form the collagen

network that contains the ECM proteoglycans [8–10]. Collagen types I, IV, V, VI, IX, X, and XI are also present in the ECM. These other types of collagen help stabilize and organize the collagen type II network that interacts with the proteoglycan aggregates [11]. These collagens are also involved in pericellular matrix (PCM), the matrix that surrounds each chondrocyte within the ECM, organization by interacting with cartilage proteoglycans [12,13]. Moreover, these collagens are able to anchor the chondrocytes to the PCM in articular cartilage [13] and mediate cell-matrix interactions and intermolecular interactions [13–16]. These interactions confer the cartilage its compressive stiffness and strength [17–20].

1.2.2 Proteoglycans

Proteoglycans are glycoconjugates that have GAG side chains attached to a central core protein. Proteoglycans contribute 4-7% wet weight of the ECM [21]. Among the cartilage proteoglycans, aggrecan is one of the most crucial to the proper functioning of articular cartilage. Aggrecan, the largest aggregating proteoglycan present in the ECM, is composed of chondroitin sulfate (CS), keratin sulfate (KS), and O-linked oligosaccharides side chains attached laterally along the length of a core protein (Figure 1.2) [22]. A globular region, located towards the N-terminus of the core protein, called the G1 domain is able to bind to a minimum of 10 disaccharides of hyaluronic acid (HA) through a link protein. This interaction between the G1 domain, link protein, and HA allows many aggrecan molecules to bind to a single HA chain leading to the formation of large multimolecular aggregates [22, 23]. The G1 domain is followed by a short extended region known as the interglobular domain (IGD). This IGD contains proteolytic cleavage sequences that are attacked by proteinases such as matrix metalloproteinases (MMPs) and aggrecanases during cartilage degradation [4, 22]. The IGD is followed by a G2 domain, the second globular domain from the N-terminus, that contains KS chains. A KS domain and a CS domain are found between the G2 and G3 domains. These KS and CS domains have approxi-

mately 30 KS and 100 CS chains attached [22, 24]. The G3 domain, the last domain in aggrecan, is composed of an epidermal growth factor-like module, a carbohydrate recognition domain, a complement binding protein-like module, and a tail. The G3 domain is responsible for facilitating the attachment of GAG chains and enhancing the secretion of the product [22]. All of these components anchor aggrecan within the ECM and, due to their negative charge, provide cartilage with its osmotic properties and resistance to compression [25, 26]. Other smaller proteoglycans present in articular cartilage such as decorin and fibromodulin are involved in fibrillogenesis and interfibril interactions [17, 27–33].

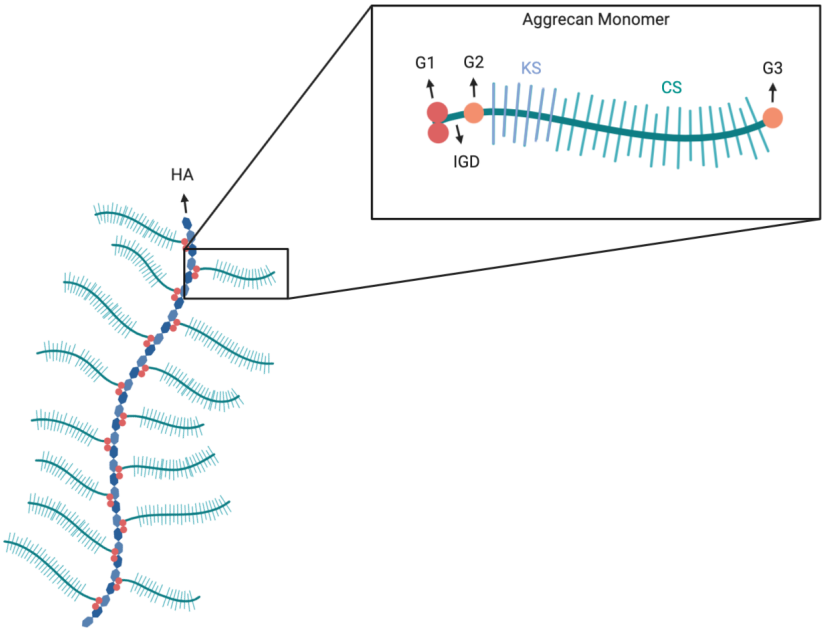

Figure 1.2.: Illustration of the aggrecan molecule. The closeup image shows the aggrecan monomer with its different components. G1, G2, G3: globular domains; KS: keratin sulfate; CS: chondroitin sulfate; IGD: interglobular domain. Illustration created with biorender.com.

1.2.3 Articular Cartilage Architecture

Articular cartilage is structurally organized into four different zones: the superficial, middle, deep, and calcified zones [5]. These zones exhibit different composition, organization, cell morphology, and mechanical properties. The superficial zone is a dense layer made up of elongated chondrocytes and collagen fibrils that show parallel alignment to the surface [5]. It expresses different proteins that protect and lubricate the zone to obtain a smooth surface that is shear-resistant [34]. The superficial zone is followed by the middle zone which makes up the majority of the articular cartilage. The middle zone has a lower concentration of collagen, a higher compressive modulus, less organization, and chondrocytes with a more circular morphology [4, 25]. Following the middle zone, the deep zone holds even thicker collagen fibrils that show perpendicular alignment to the articular surface. The chondrocytes in this zone show a parallel arrangement to the collagen fibrils. This layer contains the largest amount of proteoglycans and highest compressive modulus, when compared to the other zones [4, 25].

1.3 Osteoarthritis

As previously mentioned, articular cartilage is the connective tissue and load-bearing surface in all synovial joints and is primarily composed of ECM and chondrocytes. These components along with the articular cartilage architecture allow cartilage to lubricate the surface of joints and facilitate distribution of loads. These key functions result in a low-friction movement of opposing joint surfaces allowing for painless movement [35]. However, several factors such as age, obesity, and traumatic injury can lead to articular cartilage degradation [7]. In OA, the ECM of cartilage is shown to degrade as a lesion starting from the articular surface and progressing to the subchondral bone (Figure 1.3). As the ECM degrades, the joint suffers swelling and loss of mechanical properties, all of which limit movement and decrease quality of life. The National Arthritis Data Workgroup states that approximately 27 million

adults in the United States suffer from this disease [1], with knee OA being one of the top 5 causes of disability among adults [2]. The prevalence of this disease in the US has resulted in a total annual cost of $89.1 billion [2], most of which is spent on OA treatments.

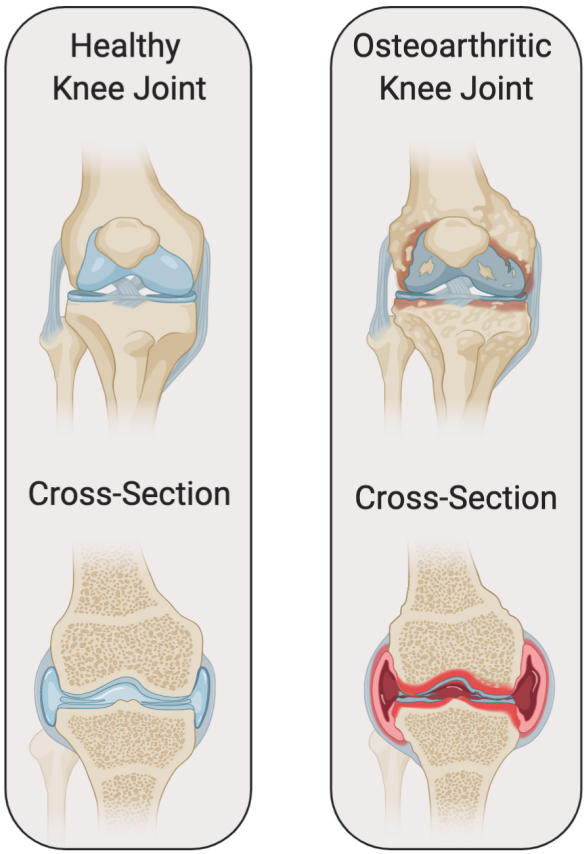

Figure 1.3.: Illustration of healthy and osteoarthritic knee joints and their cross-sections. In OA, cartilage degradation is observed as a lesion starting from the articular surface and progressing to the subchondral bone. Illustration created with biorender.com.

1.3.1 OA Pathology

During OA, the ECM undergoes biochemical and mechanical changes that cause articular cartilage degradation. Inflammation plays a big role in OA and can be

triggered by several factors such as age, obesity, and traumatic injury [7]. This inflammation affects the chondrocytes responsible for maintaining ECM production and homeostasis and induces their catabolic activities [5, 36]. Interleukin 1β (IL-1β), a proinflammatory cytokine highly upregulated during OA, significantly increases the expression of matrix degrading proteins known as matrix metalloproteinases (MMPs) (MMP-1, -3, -13) and a disintegrin and metalloproteinase with a thrombospondin type 1 motif (ADAMTS) (ADAMTS-4, -5) in chondrocytes [37–39]. In healthy cartilage, aggrecan protects collagen type II from degradation by obstructing proteolytic enzymes from diffusing into the cartilage [40]. However, in early OA, ADAMTS-4 and ADAMTS-5 are responsible for cleaving aggrecan in the IGD (Glu373 Ala374) and releasing the GAG-rich region into the surrounding environment [41–43]. The loss of aggrecan affects the mechanical properties of the tissue and exposes collagen type II to enzymatic degradation. The MMPs are then able to cleave collagen type II [37, 44, 45]. Once the collagen is lost, the articular cartilage is not able to repair itself [46]. The degraded fragments in the tissue further stimulate proteolytic enzyme production, thus, perpetuating the cycle of OA (Figure 1.4). The upregulation of catabolic activities in OA is accompanied by a downregulation of growth factors such as transforming growth factor β (TGF-β), sex determining region Y-box 9 (SOX9), insulin-like growth factor (IGF), and connective tissue growth factor (CTGF) involved in ECM synthesis [47–50]. The downregulation of these factors results in a reduction of anabolic activities furthering the progression of OA [48].

1.3.2 Current OA Treatments

Since there is no cure for OA, current treatments aim to alleviate symptoms and prevent progression of the disease. Depending on the severity of the disease, there is a wide range of treatments available to the patients. Common treatments range from exercise and diet control to pharmacological and surgical interventions. Current pharmacological options available for pain relief include analgesics, non-steroidal

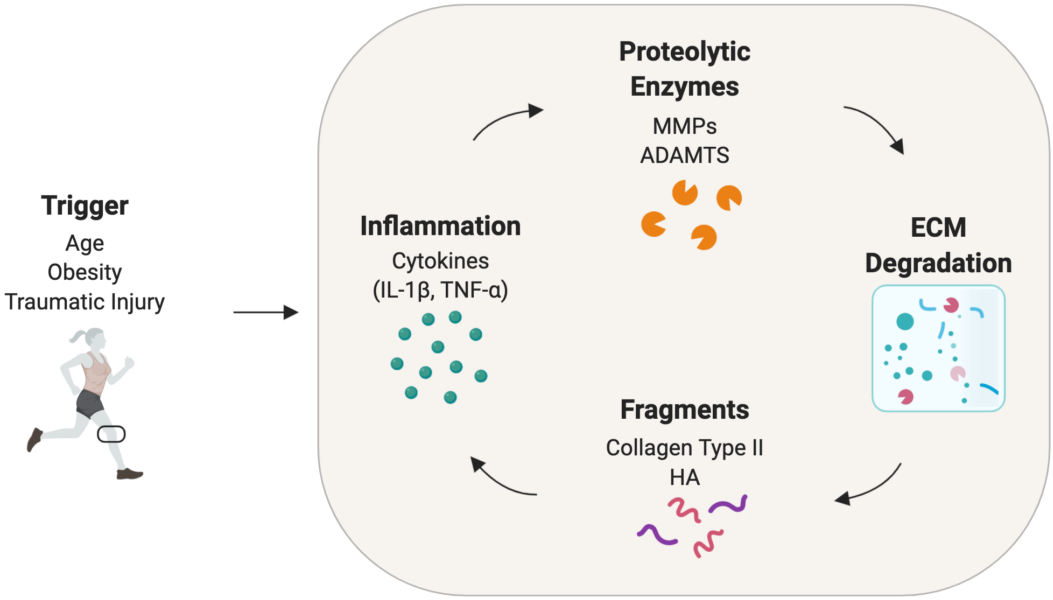

Figure 1.4.: Inflammatory cycle of OA. A trigger, such as a sports injury, induces an inflammatory response that stimulates the production of proteolytic enzymes and a decrease in growth factors. An imbalance in these factors results in damage to the ECM which releases fragments into the surrounding environment. These fragments further stimulate an inflammatory response, thus, perpetuating the cycle of OA. Illustration created with biorender.com.

anti-inflammatory drugs (NSAIDs), and cyclooxygenase-2 (COX-2) inhibitors [25]. However, these drugs should be taken in low doses since they have presented several side effects such as gastric ulcerations and bleeding, increased risk of mild loss of renal function, and hypertension [25]. Other pharmacological treatment options include intra-articular injections of corticosteroids and HA. These injections are limited due to their residence time in the joint space. Patients require multiple injections for these treatments to be efficient in relieving pain [51].

Current surgical interventions to repair damaged articular cartilage include arthroscopic lavage and debridement, microfracture, marrow stimulation techniques, osteochondral autografts and allografts, autologous chondrocyte implantation (ACI), and total knee arthroplasty [52, 53]. These methods, however, pose several complications

and require long rehabilitation. The osteochondral autograft and allograft techniques have resulted in donor site morbidity and implant rejection [53]. The microfracture and marrow stimulation techniques have resulted in subchondral bone loss and axis malalignment [54]. Total knee arthroplasty has proven to be very successful, but patients that undergo this treatment have to limit their activity [55]. Even though these treatments have shown to relieve pain, they are not able to modify the disease and protect the cartilage from further degradation.

1.4 Biomaterials for Articular Cartilage Tissue Engineering

Many biomaterials are being used to design scaffolds whose aim is to repair damaged articular cartilage [56–59]. Naturally derived materials have been widely used because they possess similar characteristics to the tissue components in cartilage. For the most part, they are biocompatible [60–65] and biodegradable [65–68]. However, their biomechanical properties are not ideal [69–72]. Synthetic materials have been used as an alternative to naturally derived materials because of the control researchers possess over their biomechanical properties [68, 73, 74]. Even though synthetic materials possess useful characteristics for tissue engineering, especially the higher mechanical properties, they also pose some concerns in terms of their biocompatibility [68, 75, 76] and far less complex structures when compared to natural articular cartilage. Tables 1.1 and 1.2 present a summary of the advantages and limitations of common naturally occuring materials and synthetic materials, respectively.

Special consideration is given to the materials when developing a scaffold. The materials, individually or combined, should exhibit adequate properties in a matrix (porosity, adhesion, biodegradability, biocompatibility, stability, cohesiveness, and structural organization) for its successful implementation. For the work presented here, we chose to work with naturally occuring materials, particularly collagen and HA.

Table 1.1.: Advantages and limitations of naturally occurring materials for articular cartilage repair.

Type of Material	**Advantages**	**Limitations**
Collagen	Biocompatibility (without telopeptides) [60, 61, 77]; Porosity can be controlled [69, 70]; Adhesive qualities [70, 78, 79]; Can carry different cells [78, 79]	Weak mechanical properties [69, 70]; Cytotoxic [80,81]; Bioincompatibility (with telopeptides) [60, 61, 77]; Inferior release kinetics when compared to HA-based scaffolds [82]
Fibrin	Biocompatibility [62]; Adhesive qualities [83, 84]; Biodegradability [66]	Cytotoxic potential [72]; Poor mechanical properties [72]
HA	Can carry different cells [85]; Superior release kinetics when compared to collagen-based matrices [86]	Immunogenic [73, 87]
Chitosan	Biocompatibility [63, 88]; Biodegradability [67, 88–90]; Pore size can be controlled [91]; Adhesive qualities [88]	Low cell viability [92]; Low scaffold strength [91]
Alginate	Biocompatibility [64]; Low toxicity [93]; Biodegradability [68]	Does not support cell metabolism [94]; Poor cell adhesion [68]; Poor mechanical properties [71]

continued on next page

Table 1.1.: *continued*

Type of Material	**Advantages**	**Limitations**
Agarose	Can serve as a cell carrier [95]	Poor mechanical properties [71]
Decellularized ECM	Constructive remodeling [96]; Biocompatibility [65]; Biodegradability [65]; Can serve as a cell carrier [86, 97]	Decellularization process can affect mechaninal properties [98]
ECM: extracellular matrix; HA: hyaluronic acid		

Table 1.2.: Advantages and limitations of synthetic materials for articular cartilage repair.

Type of Material	**Advantages**	**Limitations**
PEG	Biocompatibility [99, 100]; Non-toxic [99, 100]; Can serve as a cell carrier [101]; Pore size can be controlled [101]	Low biodegradability [102]; Non-adhesive qualities [103]; Lacks the complex organization of the ECM
PLGA	Good mechanical properties [73,74]; Biodegradability [104]; Biocompatibility [68, 104]; Can serve as cell carriers [104]	Lacks the complex organization of the ECM

continued on next page

Table 1.2.: *continued*

Type of Material	Advantages	Limitations
PLA	Biocompatibility [68]; Biodegradability [68]; Good mechanical properties [68]; Can serve as cell carriers [105];	Immunogenic [68]; Lacks the complex organization of the ECM
Carbon fibers	Can serve as cell carriers [106]; Can carry non-biological molecules [106]	Immunogenic [75, 76]; Lacks the complex organization of the ECM

PEG: poly(ethylene glycol); ECM: extracellular matrix; PLGA: poly(lactic-co-glycolic acid); PLA: polylactic acid

1.5 Current Commercially Available Collagen Scaffolds for Cartilage Repair

There are several collagen-based matrix-associated autologous chondrocyte implantation (MACI) products in the cartilage tissue engineering clinical market. The NOVOCART® 3D scaffold is based on a collagen type I sponge with a bilayer structure and has shown cartilage repair in a study conducted two years after implantation [107,108]. Another product on the market is MACI® which is a membrane made up of collagen type I and III [107,109]. When compared to microfracture, MACI® was able to heal more effectively [109]. CaReS® scaffolds, made of collagen type I, yielded comparable results to microfracture 3 years after implantation [107, 110]. It did, however, show improvement when compared to patients prior to implantation [110]. Also on the market, NeoCart® is a collagen type I gel loaded into collagen type I sponges that was able to show greater clinical efficacy than microfracture after two

years [107, 111]. Even though these products have shown to improve cartilage repair and are comparable or better than microfracture, there are still areas left for improvement. All of these products are based on collagen type I and do not incorporate collagen type II. Incorporation of collagen type II could help maintain chondrocyte morphology and stimulate cartilaginous tissue synthesis.

1.6 Collagen Scaffolds for Articular Cartilage Repair

When developing scaffolds for cartilage repair, the composition and architecture of the native environment is very important. The articular cartilage network and its components provide the tissue with its shear-resistance and compressive strength [4, 25, 34]. Many biomaterials are being used to design scaffolds whose aim is to repair damaged articular cartilage [56–59]. Scaffolds with a network reminiscent of native cartilage could provide the mechanical properties associated with the articular cartilage function.

Collagen is one of the key components in articular cartilage [5]. Hence, collagen type I has been extensively studied and used to develop scaffolds for tissue engineering for over 20 years [108–125]. The collagen structure and composition - a triple helix with ligands [126]- provides an adhesion surface where cells can migrate and differentiate [127]. These collagen fibrils also allow growth factor loading and interactions to take place [128] and can serve as carriers of different types of cells, such as chondrocytes [78, 107, 120, 129] and mesenchymal stem cells (MSCs) [79]. It has been shown that these scaffolds increase healing responses in rabbits [130], chickens [131], and horses [132]. Additionally, its abundant availability [133], biocompatibility [134], and wide clinical approval [107, 134, 135] are some of the advantages this material offers [134]. Collagen type I has, however, a limited chondrogenic ability [107, 115, 134, 136, 137].

Even though collagen type I has been extensively used in articular cartilage tissue engineering, collagen type I is not the most prevalent collagen in cartilage. Col-

lagen type II makes up 90-95% of the collagen produced by the chondrocytes in the ECM, making collagen type II a promising material for articular tissue engineering [8, 138]. For this reason, recent constructs have been designed incorporating collagen type II [97, 112, 113, 115, 124, 137, 139–159]. Collagen type II has been shown to stabilize chondrocyte morphology [107, 112, 139, 141], as well as stimulate chondrogenic differentiation of mesenchymal stem cells (MSCs) and collagen type II synthesis [115,137,145,147,148,151,154,156,158]. Similar to collagen type I, collagen type II use in tissue constructs also has disadvantages. Collagen type II is potentially arthritogenic [107,160,161] and has limited clinical approval [107,120]. Collagen type II also forms fibrils of smaller diameter and contains more carbohydrates than collagen type I [162]. Collagen type II has an abundance of bulky disaccharide groups that prevent the formation of highly ordered fibrils with a large diameter [162]. Without crosslinking, scaffolds composed of collagen type II exhibit poor mechanical properties [163]. Different alternatives, including the addition of other materials and types of collagen, are being explored to improve the mechanical properties of scaffolds for tissue repair.

1.7 GAGs in Scaffolds for Cartilage Repair

The presence of GAGs in articular cartilage has motivated scientists to use them to synthesize scaffolds or incorporate them in scaffolds for cartilage repair. As previously mentioned, HA is a nonimmunogenic biocompatible GAG present in articular cartilage [164]. Scaffolds consisting of HA have been used as carriers for chondrocytes and MSCs [165] and chondrocytes have shown to be able to maintain their morphology for long periods of time [166]. For instance, Kawasaki *et al* showed that HA-treated cells resulted in a 1.5-fold increase in cell proliferation versus untreated cells [167]. Moreover, sulphated HA allows better cell adhesion and spreading than non-sulphated HA [168]. HA is also involved in cell-cell and cell-matrix interactions, thus, aiding in cell development [169]. However, HA undergoes esterification to ob-

tain a crosslinked porous network with the required physical organization [170] to synthesize a scaffold, causing biocompatibility issues [168]. Low molecular weight HA can also induce immune responses: macrophage and neutrophil activation and proimmflamatory cytokine production [73, 87].

Past works have studied GAG interaction [117, 118, 124, 139, 141, 171–173] and incorporation into collagen type I gels [117, 118, 123, 124, 139, 141, 172–175] as well as GAG effects on chondrocyte cultures [123, 139, 141, 175, 176]. GAG incorporation and production in scaffolds containing collagen type II have also been studied [124, 139, 141, 142, 149, 152]. Several groups have constructed chondrocyte seeded collagen type II scaffolds with CS and demonstrated their superior ability to stimulate GAG synthesis and preserve chondrocyte morphology in comparison to collagen type I gels [139, 141].

The work presented herein focuses on the incorporation of GAGs and aggrecan mimetic molecules into collagen I scaffolds and collagen I and II blend hydrogels.

1.8 Aggrecan Peptidoglycan

Aggrecan has shown to be a component of major importance in articular cartilage. As formerly stated, aggrecan is responsible for protecting collagen type II from degradation and confers cartilage some of its mechanical properties. Our lab has designed and synthesized an aggrecan mimic (CS-BMPH-GAH) by attaching HA binding peptides to a CS backbone via a heterobifunctional crosslinker N- (β-Maleimidopropionic acid) hydrazide, trifluoroacetic acid salt (BMPH) (Figure 1.5) [177]. This aggrecan mimic was able to bind to HA in solution and significantly increase the storage modulus when compared to CS and HA solutions [177]. When incorporated in collagen type I constructs with HA, these mimetic molecules also showed an increase in compressive strength in contrast to collagen type I only gels and collagen type I gels with HA and CS [122, 177]. Additionally, these gels with CS-BMPH-GAH were shown to significantly reduce collagen and HA degradation in the presence of hyaluronidase and

MMP-1 [177]. Sharma *et al* further examined the efficacy of these aggrecan mimics in *ex vivo* and *in vivo* OA models [178]. In an OA environment, these molecules were able to prevent CS degradation and lower cytokine IL-1β production in human OA synovial fluid *ex vivo* models. In *in vivo* rat models, the aggrecan mimic was able to preserve GAG and cartilage in articular cartilage tissue sections from rat knee joints [178]. Thus, CS-BMPH-GAH molecules are able to functionally mimic aggrecan [122, 177].

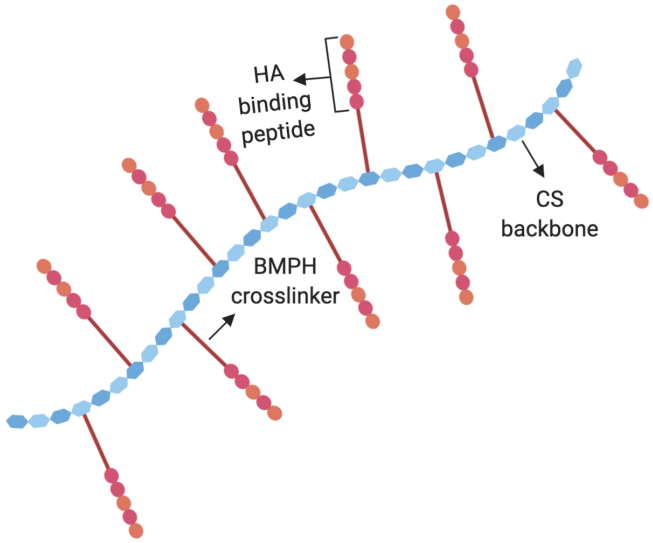

Figure 1.5.: Illustration of the aggrecan mimic. The aggrecan mimic is made up of an average of 10 moles of an HA binding peptide attached to a chondroitin sulfate (CS) backbone via a heterobifunctional crosslinker (BMPH). Illustration created with biorender.com.

1.9 Thesis Outline and Contributions

Tissue engineering efforts aim towards the development of cartilage repair strategies that mimic articular cartilage. With this in mind, the work presented here took into account the articular cartilage components and the protective role of aggrecan in cartilage degradation to develop a scaffold composed of collagen type I and II that also incorporates the aggrecan mimic to halt the progression of OA and stimulate cartilage repair.

Chapter 2 focuses on the development and characterization of hydrogels composed of blends of collagen type I to collagen type II and whether the addition of collagen type I to a collagen type II hydrogel affected the amount of protein incorporated into the gels, the mechanical properties of the gels, and the structure of the collagen network. The effects of adding HA and/or CS on gel formation were also investigated. This chapter consists of a manuscript by Nelda Vázquez Portalatín, Claire E. Kilmer, Alyssa Panitch, and Julie C. Liu, published in Biomacromolecules, Volume 17, Issue 10, 2016. Authors Claire Kilmer and I contributed equally to this work. Claire Kilmer performed the molecular assays and I performed all other experiments.

Chapter 3 characterizes a new aggrecan mimic synthesis process and studies the effects of the mimetic molecule and its separate components on chondrocytes embedded in collagen type I constructs. This chapter also explores the effects of the addition of collagen type II to the chondrocyte embedded collagen type I gels with CS or the aggrecan mimic. LC MS/MS was performed by Michelle Salemi from the University of California Davis Proteomics Core Facility. Proteomic analysis was done by Michelle Salemi and me. I designed and performed all other experiments and data analysis presented.

Chapter 4 seeks to determine if high-frequency ultrasound could be used to ensure intra-articular injections of the aggrecan mimic are correctly deposited in the knee joint. Dunkin Hartley guinea pigs were used for this study. Dr. Gert Breur participated in data analysis, injection assistance, and editing. Dr. Alyssa Panitch

was involved in data analysis, editing, and providing financial support. Dr. Craig Goergen and I participated in data collection and analysis, injection assistance, and writing. Dr. Craig Goergen was also involved in editing.

Chapter 5 summarizes the findings presented in the previous chapters and briefly outlines the scope of future work.

1.10 References

[1] Reva C. Lawrence, David T. Felson, Charles G. Helmick, Lesley M. Arnold, Richard A. Deyo, Sherine Gabriel, R. Hirsch, M. C. Hochberg, G. G. Hunder, J. M. Jordan, J. N. Katz, H. M. Kremers, and F Wolfe. Estimates of the prevalence of arthritis and other rheumatic conditions in the United States. Part II. *Arthritis Rheum*, 58:26–35, 2008.

[2] Ryan Bitton. The economic burden of osteoarthritis. *The American journal of managed care*, 15(8 Suppl):S230–S235, 2009.

[3] Zimin Wang and Jiang Peng. Articular cartilage tissue engineering: Development and future: A review. *Journal of Musculoskeletal Pain*, 22:68–77, 2014.

[4] T. Aigner and L. McKenna. Molecular pathology and pathobiology of osteoarthritic cartilage. *Cellular and Molecular Life Sciences*, 59(1):5–18, 2002.

[5] Andrew D. Pearle, Russell F. Warren, and Scott A. Rodeo. Basic science of articular cartilage and osteoarthritis, 2005.

[6] Syam P. Nukavarapu and Deborah L. Dorcemus. Osteochondral tissue engineering: Current strategies and challenges. *Biotechnology Advances*, 31:706–721, 2013.

[7] D. T. Felson, R. C. Lawrence, P. A. Dieppe, R. Hirsch, C. G. Helmick, J. M. Jordan, R. S. Kington, N. E. Lane, M. C. Nevitt, Y. Zhang, M. Sowers, T. McAlindon, T. D. Spector, A. R. Poole, S. Z. Yanovski, G. Ateshian, L. Sharma, J. A. Buckwalter, K. D. Brandt, and J. F. Fries. Osteoarthritis: New insights - Part 1: The disease and its risk factors. In *Annals of Internal Medicine*, volume 133, pages 635–646, 2000.

[8] Hemanth Akkiraju and Anja Nohe. Role of chondrocytes in cartilage formation, progression of osteoarthritis and cartilage regeneration. *Journal of Developmental Biology*, 3:177–192, 2015.

[9] Richard Mayne. Cartilage Collagens: What Is Their Function, and Are They Involved in Articular Disease? *Arthritis & Rheumatism*, 32(3):241–246, 1989.

[10] A R Poole, M Kobayashi, T Yasuda, S Laverty, F Mwale, T Kojima, T Sakai, C Wahl, S El-Maadawy, G Webb, E Tchetina, and W Wu. Type II collagen degradation and its regulation in articular cartilage in osteoarthritis. *Annals of the Rheumatic Diseases*, 61(Suppl 2):ii78–ii81, nov 2002.

[11] Richard J. Wenstrup, Jane B. Florer, Eric W. Brunskill, Sheila M. Bell, Inna Chervoneva, and David E. Birk. Type V Collagen Controls the Initiation of Collagen Fibril Assembly. *The Journal of Biological Chemistry*, 279(51):53331–53337, dec 2004.

[12] Gerald N. Smith Jr., Karen A. Hasty, and Kenneth D. Brandt. Type XI Collagen is Associated with the Chondrocyte Surface in Suspension Culture. *Matrix*, 9(3):186–192, jun 1989.

[13] Yunyun Luo, Dovile Sinkeviciute, Yi He, Morten Karsdal, Yves Henrotin, Ali Mobasheri, Patrik Önnerfjord, and Anne Bay-Jensen. The minor collagens in articular cartilage. *Protein & Cell*, 8(8):560–572, aug 2017.

[14] Martin Pfaff, Monique Aumailley, Ulrich Specks, Joachim Knolle, Hans Günter Zerwes, and Rupert Timpl. Integrin and Arg-Gly-Asp Dependence of Cell Adhesion to the Native and Unfolded Triple Helix of Collagen Type VI. *Experimental Cell Research*, 206(1):167–176, may 1993.

[15] Katsuhiko Arai, Yuko Nagashima, Taeko Takemoto, and Toshio Nishiyama. Mechanical Strain Increases Expression of Type XII Collagen in Murine Osteoblastic MC3T3-E1 Cells. *Cell Structure and Function*, 33(2):203–210, 2008.

[16] Drew W. Taylor, Nazish Ahmed, Justin Parreno, Gregory P. Lunstrum, Allan E. Gross, Eleftherios P. Diamandis, and Rita A. Kandel. Collagen Type XII and Versican Are Present in the Early Stages of Cartilage Tissue Formation by Both Redifferentating Passaged and Primary Chondrocytes. *Tissue Engineering Part A*, 21(3-4):683–693, feb 2015.

[17] Alice J Sophia Fox, Asheesh Bedi, and Scott A Rodeo. The Basic Science of Articular Cartilage: Structure, Composition, and Function. *Sports Health*, 1(6):461–468, 2009.

[18] David Eyre. Collagen of articular cartilage. *Arthritis research*, 4(1):30–35, 2002.

[19] Laura E. Niklason. Understanding the Extracellular Matrix to Enhance Stem Cell-Based Tissue Regeneration. *Cell Stem Cell*, 22(3):302–305, mar 2018.

[20] Nicole A Zelenski, Holly A Leddy, Johannah Sanchez-Adams, Jinzi Zhang, Paolo Bonaldo, Wolfgang Liedtke, and Farshid Guilak. Type VI Collagen Regulates Pericellular Matrix Properties, Chondrocyte Swelling, and Mechanotransduction in Mouse Articular Cartilage. *Arthritis & rheumatology*, 67(5):1286–1294, may 2015.

[21] Van C. Mow, Anthony Ratcliffe, and A. R. Poole. *Biomaterials*.

[22] Chris Kiani, Liwen Chen, Yao Jiong Wu, Albert J Yee, and Burton B Yang. *Cell Research*.

[23] H Muir. The chondrocyte, architect of cartilage. Biomechanics, structure, function and molecular biology of cartilage matrix macromolecules. *BioEssays : news and reviews in molecular, cellular and developmental biology*, 17(12):1039–1048, 1995.

[24] SL Carney and H Muir. The structure and function of cartilage. *Physiological Reviews*, 65(3):858–910, 1988.

[25] Mohit Kapoor and Nizar N. Mahomed. *Osteoarthritis: Pathogenesis, diagnosis, available treatments, drug safety, regenerative and precision medicine*. Springer International Publishing, 2015.

[26] T E Hardingham, A J Fosang, and J Dudhia. The structure, function and turnover of aggrecan, the large aggregating proteoglycan from cartilage. *European journal of clinical chemistry and clinical biochemistry : journal of the Forum of European Clinical Chemistry Societies*, 32(4):249–257, 1994.

[27] Renato V Iozzo and Liliana Schaefer. Proteoglycan form and function: A comprehensive nomenclature of proteoglycans. *Matrix Biology*, 42:11–55, 2015.

[28] Joseph P. R. O. Orgel, Aya Eid, Olga Antipova, Jordi Bella, and John E. Scott. Decorin Core Protein (Decoron) Shape Complements Collagen Fibril Surface Structure and Mediates Its Binding. *PLoS ONE*, 4(9):e7028, sep 2009.

[29] Charles C. Reed and Renato V. Iozzo. The role of decorin in collagen fibrillogenesis and skin homeostasis. *Glycoconjugate Journal*, 19:249–255, may 2003.

[30] Claus Rühland, Elke Schönherr, Horst Robenek, Uwe Hansen, Renato V. Iozzo, Peter Bruckner, and Daniela G. Seidler. The glycosaminoglycan chain of decorin plays an important role in collagen fibril formation at the early stages of fibrillogenesis. *FEBS Journal*, 274(16):4246–4255, aug 2007.

[31] Arif T Jan, Eun J Lee, and Inho Choi. Fibromodulin: A regulatory molecule maintaining cellular architecture for normal cellular function. *The International Journal of Biochemistry & Cell Biology*, 80:66–70, 2016.

[32] Douglas R Keene, James D San Antonio, Richard Mayne, David J McQuillan, George Sarris, Samuel A Santoro, and Renato V Iozzo. Decorin Binds Near the C Terminus of Type I Collagen. *The Journal of Biological Chemistry*, 275(29):21801–21804, 2000.

[33] K G Vogel, M Paulsson, and D Heinegård. Specific inhibition of type I and type II collagen fibrillogenesis by the small proteoglycan of tendon. *The Biochemical journal*, 223(3):587–597, nov 1984.

[34] Tannin A. Schmidt, Nicholas S. Gastelum, Quynhhoa T. Nguyen, Barbara L. Schumacher, and Robert L. Sah. Boundary lubrication of articular cartilage: role of synovial fluid constituents. *Arthritis and rheumatism*, 56(3):882–91, mar 2007.

[35] Joseph a Buckwalter, Henry J Mankin, and Alan J Grodzinsky. Articular cartilage and osteoarthritis, 2005.

[36] M J Benito, D J Veale, O FitzGerald, W B van den Berg, and B Bresnihan. Synovial tissue inflammation in early and late osteoarthritis. *Annals of the rheumatic diseases*, 64(9):1263–1267, sep 2005.

[37] R. Clark Billinghurst, Leif Dahlberg, Mirela Ionescu, Agnes Reiner, Robert Bourne, Cecil Rorabeck, Peter Mitchell, John Hambor, Oliver Diekmann, Harald Tschesche, Jeffrey Chen, Hal Van Wart, and A. Robin Poole. Enhanced cleavage of type II collagen by collagenases in osteoarthritic articular cartilage. *Journal of Clinical Investigation*, 99(7):1534–1545, 1997.

[38] Ruo Hua Song, Micky D. Tortorella, Anne Marie Malfait, James T. Alston, Zhiyong Yang, Elizabeth C. Arner, and David W. Griggs. Aggrecan degradation in human articular cartilage explants is mediated by both ADAMTS-4 and ADAMTS-5. *Arthritis and Rheumatism*, 56(2):575–585, 2007.

[39] Linda Troeberg and Hideaki Nagase. Proteases involved in cartilage matrix degradation in osteoarthritis, 2012.

[40] Michael A Pratta, Wenqing Yao, Carl Decicco, Micky D Tortorella, Riu-Qin Liu, Robert A Copeland, Ronald Magolda, Robert C Newton, James M Trzaskos, and Elizabeth C Arner. *The Journal of Biological Chemistry*.

[41] Christopher B. Little, Clare T. Meeker, Suzanne B. Golub, Kate E. Lawlor, Pamela J. Farmer, Susan M. Smith, and Amanda J. Fosang. Blocking aggrecanase cleavage in the aggrecan interglobular domain abrogates cartilage erosion and promotes cartilage repair. *Journal of Clinical Investigation*, 117:1627–1636, 2007.

[42] John D Sandy and Christie Verscharen. Analysis of aggrecan in human knee cartilage and synovial fluid indicates that aggrecanase (ADAMTS) activity is responsible for the catabolic turnover and loss of whole aggrecan whereas other protease activity is required for C-terminal processing in vivo. *Biochemical Journal*, 358(3):615–626, sep 2001.

[43] J. D. Sandy. A contentious issue finds some clarity: On the independent and complementary roles of aggrecanase activity and MMP activity in human joint aggrecanolysis. *Osteoarthritis and Cartilage*, 14(2):95–100, 2006.

[44] A J Fosang and T E Hardingham. *The Biochemical Journal*.

[45] L C Tetlow, D J Adlam, and D E Woolley. Matrix metalloproteinase and proinflammatory cytokine production by chondrocytes of human osteoarthritic cartilage: associations with degenerative changes. *Arthritis and rheumatism*, 44(3):585–94, mar 2001.

[46] Morten a Karsdal, Suzi H Madsen, Claus Christiansen, Kim Henriksen, Amanda J Fosang, and Bodil C Sondergaard. Cartilage degradation is fully reversible in the presence of aggrecanase but not matrix metalloproteinase activity. *Arthritis Research & Therapy*, 10(3):R63, 2008.

[47] Jin Nam, Priyangi Perera, Jie Liu, Bjoern Rath, James Deschner, Robert Gassner, Timothy A. Butterfield, and Sudha Agarwal. Sequential alterations in catabolic and anabolic gene expression parallel pathological changes during progression of monoiodoacetate-induced arthritis. *PLoS ONE*, 6(9), 2011.

[48] Maricela Maldonado and Jin Nam. The role of changes in extracellular matrix of cartilage in the presence of inflammation on the pathology of osteoarthritis, 2013.

[49] E N Blaney Davidson, E L Vitters, P M van der Kraan, and W B van den Berg. Expression of transforming growth factor-beta (TGFbeta) and the TGF-beta signalling molecule SMAD-2P in spontaneous and instability-induced osteoarthritis: role in cartilage degradation, chondrogenesis and osteophyte formation. *Annals of the rheumatic diseases*, 65(11):1414–21, 2006.

[50] E N Blaney Davidson, A Scharstuhl, E L Vitters, P M van der Kraan, and W B van den Berg. Reduced transforming growth factor-beta signaling in cartilage of old mice: role in impaired repair capacity. *Arthritis research & therapy*, 7(6):R1338–47, 2005.

[51] N Bellamy, J Campbell, V Robinson, T Gee, R Bourne, and G Wells. Intraarticular corticosteroid for treatment of osteoarthritis of the knee. *The Cochrane database of systematic reviews*, (2):CD005328, 2006.

[52] J Winslow Alford and Brian J Cole. Cartilage restoration, part 1: basic science, historical perspective, patient evaluation, and treatment options. *The American journal of sports medicine*, 33(2):295–306, feb 2005.

[53] C T Laurencin, a M Ambrosio, M D Borden, and J a Cooper. Tissue engineering: orthopedic applications. *Annual review of biomedical engineering*, 1:19–46, 1999.

[54] M J Angel, P Razzano, and D A Grande. Defining the challenge. The basic science of articular cartilage repair and response to injury. *Sports Medicine and Arthroscopy Review*, 11:168–181, 2003.

[55] Elizabeth S. Tetteh, Sarvottam Bajaj, and Neil S Ghodadra. Basic science and surgical treatment options for articular cartilage injuries of the knee. *The Journal of orthopaedic and sports physical therapy*, 42(3):243–53, mar 2012.

[56] Rozlin Abdul Rahman, Muhammad Aa'zamuddin Ahmad Radzi, Norhamiza Mohamad Sukri, Noorhidayah Md Nazir, and Munirah Sha'ban. Tissue engineering of articular cartilage: from bench to bed-side. *Tissue Engineering and Regenerative Medicine*, 12:1–11, 2015.

[57] Kota Uematsu, Koji Hattori, Yoshiyuki Ishimoto, Jun Yamauchi, Takashi Habata, Yoshinori Takakura, Hajime Ohgushi, Takeshi Fukuchi, and Masao Sato. Cartilage regeneration using mesenchymal stem cells and a three-dimensional poly-lactic-glycolic acid (PLGA) scaffold. *Biomaterials*, 26:4273–4279, 2005.

[58] Stephanie J. Bryant, Ryan J. Bender, Kevin L. Durand, and Kristi S. Anseth. Encapsulating chondrocytes in degrading PEG hydrogels with high modulus: Engineering gel structural changes to facilitate cartilaginous tissue production. *Biotechnology and Bioengineering*, 86:747–755, 2004.

[59] E Sachlos and J T Czernuszka. Making tissue engineering scaffolds work. *European Cells & Materials*, 5:29–39, 2003.

[60] Edward E Luck and John R Daniels. Non-Antigenic Collagen and Articles of Manufacture, 1980.

[61] A. K. Lynn, I. V. Yannas, and W. Bonfield. Antigenicity and immunogenicity of collagen. *Journal of Biomedical Materials Research - Part B*, 71B:343–354, 2004.

[62] Huang Fang, Songlin Peng, Anmin Chen, Fengfeng Li, Kai Ren, and Ning Hu. Biocompatibility studies on fibrin glue cultured with bone marrow mesenchymal stem cells in vitro. *Journal of Huazhong University of Science and Technology - Medical Science*, 24:272–274, 2004.

[63] Makarand V. Risbud and Ramesh R. Bhonde. Polyacrylamide-chitosan hydrogels: In vitro biocompatibility and sustained antibiotic release studies. *Drug Delivery: Journal of Delivery and Targeting of Therapeutic Agents*, 7:69–75, 2000.

[64] Honghyun Park, Sun Woong Kang, Byung Soo Kim, David J. Mooney, and Kuen Yong Lee. Shear-reversibly crosslinked alginate hydrogels for tissue engineering. *Macromolecular Bioscience*, 9:895–901, 2009.

[65] Kim E.M. Benders, P. René van Weeren, Stephen F. Badylak, Daniël B.F. Saris, Wouter J.A. Dhert, and Jos Malda. Extracellular matrix scaffolds for cartilage and bone regeneration. *Trends in Biotechnology*, 31(3):169–176, 2013.

[66] Y. Xu, Y. F. Song, and Z. X. Lin. Transplantation of muscle-derived stem cells plus biodegradable fibrin glue restores the urethral sphincter in a pudendal nerve-transected rat model. *Brazilian Journal of Medical and Biological Research*, 43:1076–1083, 2010.

[67] J. Berger, M. Reist, J. M. Mayer, O. Felt, N. A. Peppas, and R. Gurny. Structure and interactions in covalently and ionically crosslinked chitosan hydrogels for biomedical applications. *European Journal of Pharmaceutics and Biopharmaceutics*, 57:19–34, 2004.

[68] Ghassem Amoabediny, Nasim Salehi-Nik, and Bentolhoda Heli. The Role of Biodegradable Engineered Scaffold in Tissue Engineering. In Prof. Rosario Pignatello, editor, *Biomaterials Science and Engineering*. 2011.

[69] Shunji Yunoki, Toshiyuki Ikoma, and Junzo Tanaka. Development of collagen condensation method to improve mechanical strength of tissue engineering scaffolds. *Materials Characterization*, 61:907–911, 2010.

[70] Julie Glowacki and Shuichi Mizuno. Collagen scaffolds for tissue engineering. *Biopolymers*, 89:338–344, 2008.

[71] Hani a. Awad, M. Quinn Wickham, Holly a. Leddy, Jeffrey M. Gimble, and Farshid Guilak. Chondrogenic differentiation of adipose-derived adult stem cells in agarose, alginate, and gelatin scaffolds. *Biomaterials*, 25(16):3211–3222, 2004.

[72] Job L C Van Susante, Pieter Buma, Lein Schuman, George N. Homminga, Wim B. Van Den Berg, and Rene P H Veth. Resurfacing potential of heterologous chondrocytes suspended in fibrin glue in large full-thickness defects of femoral articular cartilage: An experimental study in the goat. *Biomaterials*, 20:1167–1175, 1999.

[73] Guoping Chen, Takashi Ushida, and Tetsuya Tateishi. A biodegradable hybrid sponge nested with collagen microsponges. *Journal of Biomedical Materials Research*, 51:273–279, 2000.

[74] Wenda Dai, Zhenjun Yao, Jian Dong, Naoki Kawazoe, Chi Zhang, and Guoping Chen. Cartilage tissue engineering with controllable shape using a poly(lactic-co-glycolic acid)/collagen hybrid scaffold. *Journal of Bioactive and Compatible Polymers*, 28:247–257, 2013.

[75] R. J. Minns and M. Flynn. Intra-articular implant of filamentous carbon fibre in the experimental animal. *Journal of Bioengineering*, 2:279–286, 1978.

[76] J Mortier and M Engelhardt. Foreign body reaction to a carbon fiber implant in the knee - Case report and literature survey. *ZEITSCHRIFT FUR ORTHOPADIE UND IHRE GRENZGEBIETE*, 138:390–394, 2000.

[77] F. O. Schmitt, L. Levine, M. P. Drake, A. L. Rubin, D. Pfahl, and P. F. Davison. THE ANTIGENICITY OF TROPOCOLLAGEN. *Proceedings of the National Academy of Sciences of the United States of*, 51:493–497, 1964.

[78] Shigeyuki Wakitani, Tatsuhiko Goto, Randell G Young, Joseph M Mansour, D Ph, Victor M Goldberg, and Arnold I Caplan. Defects with Allograft Articular Chondrocytes. 4(4):429–444, 1998.

[79] G. I. Im, D. Y. Kim, J. H. Shin, C. W. Hyun, and W. H. Cho. Repair of cartilage defect in the rabbit with cultured mesenchymal stem cells from bone marrow. *Journal of Bone and Joint Surgery - Series B*, 83B:289–294, 2001.

[80] Esther Middelkoop, Henry J.C. de Vries, Lisette Ruuls, Vincent Everts, Charles H.R. Wildevuur, and Wiete Westerhof. Adherence, proliferation and collagen turnover by human fibroblasts seeded into different types of collagen sponges. *Cell and Tissue Research*, 280:447–453, 1995.

[81] M. J.A. van Luyn, P. B. van Wachem, L. Olde Damink, P. J. Dijkstra, J. Feijen, and P. Nieuwenhuis. Relations between in vitro cytotoxicity and crosslinked dermal sheep collagens. *Journal of Biomedical Materials Research*, 26:1091–1110, 1992.

[82] Robert F. Valentini and Hyun D. Kim. Retention and activity of BMP-2 in hyaluronic acid-based scaffolds in vitro. *Journal of Biomedical Materials Research*, 59:573–584, 2002.

[83] P Visna, L Pasa, R Hart, J Kocis, I Cizmár, and J Adler. [Treatment of deep chondral defects of the knee using autologous chondrocytes cultured on a support–results after one year]. *Acta chirurgiae orthopaedicae et traumatologiae Cechoslovaca*, 70(6):356–362, 2003.

[84] P. Visna, L. Pasa, I. Cizmár, R. Hart, and J. Hoch. Treatment of Deep Cartilage Defects of the Knee Using Autologous Chondrograft Transplantation and by Abrasive Techniques A Randomized Controlled Study. *Acta Chirurgica Belgica*, 104(6):709–714, jan 2004.

[85] W. M. Kuś, A. Górecki, P. Strzelczyk, and P. Swiader. Carbon fiber scaffolds in the surgical treatment of cartilage lesions. *Annals of Transplantation: Quarterly of the Polish Transplantation Society*, 4:101–102, 1999.

[86] Yi Yi Gong, Ji Xin Xue, Wen Jie Zhang, Guang Dong Zhou, Wei Liu, and Yilin Cao. A sandwich model for engineering cartilage with acellular cartilage sheets and chondrocytes. *Biomaterials*, 32:2265–2273, 2011.

[87] Jennie Baier Leach, Kathryn A. Bivens, Charles W. Patrick, and Christine E. Schmidt. Photocrosslinked hyaluronic acid hydrogels: Natural, biodegradable tissue engineering scaffolds. *Biotechnology and Bioengineering*, 82:578–589, 2003.

[88] Pamela J. VandeVord, Howard W.T. Matthew, Stephen P. DeSilva, Lois Mayton, Bin Wu, and Paul H. Wooley. Evaluation of the biocompatibility of a chitosan scaffold in mice. *Journal of Biomedical Materials Research*, 59:585–590, 2002.

[89] Kenji Tomihata and Yoshito Ikada. In vitro and in vivo degradation of films of chitin and its deacetylated derivatives. *Biomaterials*, 18:567–575, 1997.

[90] Jianbiao Ma, Hongjun Wang, Binglin He, and Jiatong Chen. A preliminary in vitro study on the fabrication and tissue engineering applications of a novel chitosan bilayer material as a scaffold of human neofetal dermal fibroblasts. *Biomaterials*, 22:331–337, 2001.

[91] Sundararajan V. Madihally and Howard W.T. Matthew. Porous chitosan scaffolds for tissue engineering. *Biomaterials*, 20:1133–1142, 1999.

[92] Jin Shu Mao, Yuan Lu Cui, Xiang Hui Wang, Yi Sun, Yu Ji Yin, Hui Ming Zhao, and Kang De Yao. A preliminary study on chitosan and gelatin polyelectrolyte complex cytocompatibility by cell cycle and apoptosis analysis. *Biomaterials*, 25:3973–3981, 2004.

[93] Mohammad Kazem Ghahramanpoor, Sayed Alireza Hassani Najafabadi, Majid Abdouss, Fatemeh Bagheri, and Mohamadreza Baghaban Eslaminejad. A hydrophobically-modified alginate gel system: Utility in the repair of articular cartilage defects. *Journal of Materials Science: Materials in Medicine*, 22:2365–2375, 2011.

[94] Yulia Sapir, Olga Kryukov, and Smadar Cohen. Integration of multiple cell-matrix interactions into alginate scaffolds for promoting cardiac tissue regeneration. *Biomaterials*, 32:1838–1847, 2011.

[95] Andrea Y. Thompson, Karl A. Piez, and Saeid M. Seyedin. Chondrogenesis in agarose gel culture. A model for chondrogenic induction, proliferation and differentiation. *Experimental Cell Research*, 157:483–494, 1985.

[96] Stephen F. Badylak. The extracellular matrix as a biologic scaffold material. *Biomaterials*, 28:3587–3593, 2007.

[97] ZuFu Lu, Behrouz Zandieh Doulabi, ChunLing Huang, Ruud A Bank, and Marco N Helder. Collagen type II enhances chondrogenesis in adipose tissue-derived stem cells by affecting cell shape. *Tissue engineering. Part A*, 16:81–90, 2010.

[98] Benjamin D. Elder, Sriram V. Eleswarapu, and Kyriacos A. Athanasiou. Extraction techniques for the decellularization of tissue engineered articular cartilage constructs. *Biomaterials*, 30:3749–3756, 2009.

[99] Esther J. Lee, F. Kurtis Kasper, and Antonios G. Mikos. Biomaterials for Tissue Engineering. *Annals of Biomedical Engineering*, 42(2):323–337, feb 2014.

[100] Norma A. Alcantar, Eray S. Aydil, and Jacob N. Israelachvili. Polyethylene glycol-coated biocompatible surfaces. *Journal of Biomedical Materials Research*, 51:343–351, 2000.

[101] Silvia Orsi, Daniela Guarnieri, and Paolo A. Netti. Design of novel 3D gene activated PEG scaffolds with ordered pore structure. *Journal of Materials Science: Materials in Medicine*, 21:1013–1020, 2010.

[102] Sachiko Kaihara, Shuichi Matsumura, and John P. Fisher. Synthesis and characterization of cyclic acetal based degradable hydrogels. *European Journal of Pharmaceutics and Biopharmaceutics*, 68:67–73, 2008.

[103] Stephanie M. Willerth and Shelly E. Sakiyama-Elbert. Approaches to neural tissue engineering using scaffolds for drug delivery. *Advanced Drug Delivery Reviews*, 59:325–338, 2007.

[104] Cheryl V. Rahman, Gisela Kuhn, Lisa J. White, Giles T.S. Kirby, Oommen P. Varghese, Jane S. Mclaren, Helen C. Cox, Felicity R.A.J. Rose, Ralph Muller, Jons Hilborn, and Kevin M. Shakesheff. PLGA/PEG-hydrogel composite scaffolds with controllable mechanical properties. *Journal of Biomedical Materials Research - Part B Applied Biomaterials*, 101B:648–655, 2013.

[105] G. Georgiou, L. Mathieu, D. P. Pioletti, P. E. Bourban, J. A.E. Månson, J. C. Knowles, and S. N. Nazhat. Polylactic acid-phosphate glass composite foams as scaffolds for bone tissue engineering. *Journal of Biomedical Materials Research - Part B Applied Biomaterials*, 80:322–331, 2007.

[106] E. B. Hunziker. Articular cartilage repair: Basic science and clinical progress. A review of the current status and prospects. *Osteoarthritis and Cartilage*, 10:432–463, 2001.

[107] Vincent Irawan, Tzu-Cheng Sung, Akon Higuchi, and Ikoma Toshiyuki. Collagen Scaffolds in Cartilage Tissue Engineering and Relevant Approaches for Future Development. *Tissue Engineering and Regenerative Medicine*, 15(6):673–697, 2018.

[108] Lukas Zak, Christian Albrecht, Barbara Wondrasch, Harald Widhalm, György Vekszler, Siegfried Trattnig, Stefan Marlovits, and Silke Aldrian. Results 2 years after matrix-associated autologous chondrocyte transplantation using the Novocart 3D scaffold: An analysis of clinical and radiological data. *American Journal of Sports Medicine*, 2014.

[109] D Saris, A Price, Widuchowski W, and Bertrand-Marchand M. Matrix-Applied Characterized Autologous Cultured Chondrocytes Versus Microfracture: Two-Year Follow-up of a Prospective Randomized Trial. *Am J Sports Med*, 42(6):1384–1394, 2014.

[110] Maximilian Petri, Maximilian Broese, Annika Simon, Emmanouil Liodakis, Max Ettinger, Daniel Guenther, Johannes Zeichen, Christian Krettek, Michael Jagodzinski, and Carl Haasper. CaReS® (MACT) versus microfracture in treating symptomatic patellofemoral cartilage defects: A retrospective matched-pair analysis. *Journal of Orthopaedic Science*, 2013.

[111] Dennis C. Crawford, Thomas M. DeBerardino, and Riley J. Williams. NeoCart, an autologous cartilage tissue implant, compared with microfracture for treatment of distal femoral cartilage lesions: An FDA phase-II prospective, randomized clinical trial after two years. *Journal of Bone and Joint Surgery - Series A*, 2012.

[112] Stefan Nehrer, Howard A. Breinan, Arun Ramappa, Sonya Shortkroff, Gretchen Young, Tom Minas, Clement B. Sledge, Ioannis V. Yannas, and Myron Spector. Canine chondrocytes seeded in type I and type II collagen implants investigated in vitro. *Journal of Biomedical Materials Research*, 1997.

[113] Stefan Nehrer, Howard A Breinan+, Arun Ramappa, Gretchen Young, Sonya Shortkroff, Libby K Louie+, Clement B Sledge, Ioannis V Yannas+, and Myron Spector. Matrix collagen type and pore size influence behaviour of seeded canine chondrocytes. *Biomaterials*, 18:769–776, 1997.

[114] M. Ochi, Y. Uchio, K. Kawasaki, S. Wakitani, and J. Iwasa. Transplantation of cartilage-like tissue made by tissue engineering in the treatment of cartilage defects of the knee. *The Journal of Bone and Joint Surgery*, 2002.

[115] C. W. Chen, Y. H. Tsai, W. P. Deng, S. N. Shih, C. L. Fang, J. G. Burch, W. H. Chen, and W. F. Lai. Type I and II collagen regulation of chondrogenic differentiation by mesenchymal progenitor cells. *Journal of Orthopaedic Research*, 23(2):446–453, 2005.

[116] Laurent Galois, Sandrine Hutasse, Delphine Cortial, Cécile F. Rousseau, Laurent Grossin, Marie Clarie Ronziere, Daniel Herbage, and Anne Marie Freyria. Bovine chondrocyte behaviour in three-dimensional type I collagen gel in terms of gel contraction, proliferation and gene expression. *Biomaterials*, 2006.

[117] Kate Stuart and Alyssa Panitch. Influence of chondroitin sulfate on collagen gel structure and mechanical properties at physiologically relevant levels. *Biopolymers*, 89:841–851, 2008.

[118] Kate Stuart and Alyssa Panitch. Characterization of gels composed of blends of collagen l, collagen III, and chondroitin sulfate. *Biomacromolecules*, 10:25–31, 2009.

[119] C. Albrecht, B. Tichy, S. Nürnberger, S. Hosiner, L. Zak, S. Aldrian, and S. Marlovits. Gene expression and cell differentiation in matrix-associated chondrocyte transplantation grafts: A comparative study. *Osteoarthritis and Cartilage*, 2011.

[120] Akon Higuchi, Qing Dong Ling, Shih Tien Hsu, and Akihiro Umezawa. Biomimetic cell culture proteins as extracellular matrices for stem cell differentiation, 2012.

[121] Turgay Efe, Christina Theisen, Susanne Fuchs-Winkelmann, Thomas Stein, Alan Getgood, Marga B. Rominger, Jürgen R.J. Paletta, and Markus D. Schofer. Cell-free collagen type I matrix for repair of cartilage defects-clinical and magnetic resonance imaging results. *Knee Surgery, Sports Traumatology, Arthroscopy*, pages 1915–1922, 2012.

[122] Shaili Sharma, Alyssa Panitch, and Corey P. Neu. *Acta Biomaterialia*.

[123] Tyler Novak, Sherry L Voytik-Harbin, and Corey P Neu. Cell encapsulation in a magnetically aligned collagen GAG copolymer microenvironment. *Acta Biomaterialia*, 11:274–282, 2015.

[124] Nelda Vazquez-Portalatín, Claire E Kilmer, Alyssa Panitch, and Julie C Liu. Characterization of Collagen Type I and II Blended Hydrogels for Articular Cartilage Tissue Engineering. *Biomacromolecules*, 17:3145–3152, 2016.

[125] Guang Zhen Jin and Hae Won Kim. Effects of Type I Collagen Concentration in Hydrogel on the Growth and Phenotypic Expression of Rat Chondrocytes. *Tissue Engineering and Regenerative Medicine*, 2017.

[126] Matthew D. Shoulders and Ronald T. Raines. Collagen Structure and Stability. *Annual Review of Biochemistry*, 78:929–958, 2009.

[127] H. K. Kleinman, R. J. Klebe, and G. R. Martin. Role of collagenous matrices in the adhesion and growth of cells. *Journal of Cell Biology*, 88:473–485, 1981.

[128] Brian C. Toolan, Sally R. Frenkel, James M. Pachence, Laurie Yalowitz, and Harold Alexander. Effects of growth-factor-enhanced culture on a chondrocyte-collagen implant for cartilage repair. *Journal of Biomedical Materials Research*, 31:273–280, 1996.

[129] Tsuguharu Takahashi, Toru Ogasawara, Yukiyo Asawa, Yoshiyuki Mori, Eiju Uchinuma, Tsuyoshi Takato, and Kazuto Hoshi. Three-Dimensional Microenvironments Retain Chondrocyte Phenotypes During Proliferation Culture. *Tissue Engineering*, 2007.

[130] D. P. Speer, M. Chvapil, R. G. Volz, and M. D. Holmes. Enhancement of healing in osteochondral defects by collagen sponge implants. *Clinical Orthopaedics and Related Research*, 144:326–335, 1979.

[131] C. Perka, O. Schultz, K. Lindenhayn, R. S. Spitzer, M. Muschik, M. Sittinger, and G. R. Burmester. Joint cartilage repair with transplantation of embryonic chondrocytes embedded in collagen-fibrin matrices. *Clinical and Experimental Rheumatology*, 18:13–22, 2000.

[132] A. J. Nixon, A. E. Sams, G. Lust, D. Grande, and H. O. Mohammed. Temporal matrix synthesis and histologic features of a chondrocyte-laden porous collagen cartilage analogue. *American Journal of Veterinary Research*, 54:349–356, 1993.

[133] K Gelse, E Pöschl, and T Aigner. Collagens-structure, function, and biosynthesis.

[134] Brian J Huang, Jerry C Hu, and Kyriacos A Athanasiou. Cell-based tissue engineering strategies used in the clinical repair of articular cartilage. *Biomaterials*, 98:1–22, 2016.

[135] E. B. Hunziker. Articular cartilage repair: Basic science and clinical progress. A review of the current status and prospects. *Osteoarthritis and Cartilage*, 2002.

[136] J. Farjanel, G. Schürmann, and P. Bruckner. Contacts with fibrils containing collagen I, but not collagens II, IX, and XI, can destabilize the cartilage phenotype of chondrocytes. *Osteoarthritis and Cartilage*, 2001.

[137] Z. F. Lu, B. Zandieh Doulabi, P. I. Wuisman, R. A. Bank, and M. N. Helder. Influence of collagen type II and nucleus pulposus cells on aggregation and differentiation of adipose tissue-derived stem cells. *Journal of Cellular and Molecular Medicine*, 2008.

[138] M A Cremer, E F Rosloniec, and A H Kang. The cartilage collagens: a review of their structure, organization, and role in the pathogenesis of experimental arthritis in animals and in human rheumatic disease. *Journal of molecular medicine (Berlin, Germany)*, 76(3-4):275–88, mar 1998.

[139] S. Nehrer, H.A. Breinan, A. Ramappa, H-P. Hsu, T. Minas, S. Shortkroff, C.B. Sledge, I.V. Yannas, and M. Spector. Chondrocyte-seeded collagen matrices implanted in a chondral defect in a canine model. *Biomaterials*, 19:2313–2328, 1998.

[140] Howard A Breinan, Scott D Martin, Hu-Ping Hsu, and Myron Spector. Healing of Canine Articular Cartilage Defects Treated with Microfracture, a Type-I1 Collagen Matrix, or Cultured Autologous Chondrocytes. *Journal of Orthopaedic Research*, 18:781–789, 2000.

[141] J. S. Pieper, P. M. Van Der Kraan, T. Hafmans, J. Kamp, P. Buma, J. L C Van Susante, W. B. Van Den Berg, J. H. Veerkamp, and T. H. Van Kuppevelt. Crosslinked type II collagen matrices: Preparation, characterization, and potential for cartilage engineering. *Biomaterials*, 23:3183–3192, 2002.

[142] Pieter Buma, Jeroen S Pieper, Tony Van Tienen, Job L C Van Susante, Peter M Van Der Kraan, Jacques H Veerkamp, Wim B Van Den Berg, Rene P H Veth, and Toin H Van Kuppevelt. Cross-linked type I and type II collagenous matrices for the repair of full-thickness articular cartilage defects-A study in rabbits. *Biomaterials*, 24:3255–3263, 2003.

[143] C. R. Lee, A. J. Grodzinsky, H. P. Hsu, and M. Spector. Effects of a cultured autologous chondrocyte-seeded type II collagen scaffold on the healing of a chondral defect in a canine model. *Journal of Orthopaedic Research*, 21:272–281, 2003.

[144] Takahiro Ohno, Keizo Tanisaka, Yosuke Hiraoka, Takashi Ushida, Tamotsu Tamaki, and Tetsuya Tateishi. Effect of type I and type II collagen sponges as 3D scaffolds for hyaline cartilage-like tissue regeneration on phenotypic control of seeded chondrocytes in vitro. *Materials Science and Engineering C*, 2004.

[145] D Bosnakovski, M Mizuno, G Kim, S Takagi, M Okumura, and T Fujinaga. Chondrogenic differentiation of bovine bone marrow mesenchymal stem cells (MSCs) in different hydrogels: Influence of collagen type II extracellular matrix on MSC chondrogenesis. *Biotechnology and Bioengineering*, 93:1152–1163, 2006.

[146] H J Pulkkinen, V Tiitu, P Valonen, E.-R Hämäläinen, M J Lammi, and I Kiviranta. Recombinant human type II collagen as a material for cartilage tissue engineering. *The International Journal of Artificial Organs*, 31(11):960–969, 2008.

[147] Elise Duval, Sylvain Leclercq, Jean Marc Elissalde, Magali Demoor, Philippe Galéra, and Karim Boumédiene. Hypoxia-inducible factor 1α inhibits the fibroblast-like markers type I and type III collagen during hypoxia-induced chondrocyte redifferentiation: Hypoxia not only induces type II collagen and aggrecan, but it also inhibits type I and type III collagen i. *Arthritis and Rheumatism*, 2009.

[148] Anne-Marie Freyria, Marie-Claire Ronzière, Delphine Cortial, Laurent Galois, Daniel Hartmann, Daniel Herbage, and Frédéric Mallein-Gerin. Comparative phenotypic analysis of articular chondrocytes cultured within type I or type II collagen scaffolds. *Tissue Engineering Part A*, 15:1233–1245, 2009.

[149] H J Pulkkinen, V Tiitu, P Valonen, J S Jurvelin, M J Lammi, and I Kiviranta. Engineering of cartilage in recombinant human type II collagen gel in nude mouse model in vivo. *Osteoarthritis and Cartilage*, 18:1077–1087, 2010.

[150] Marijn Rutgers, Daniel B Saris, Lucienne A Vonk, Mattie H Van Rijen, Vanessa Akrum, Danielle Langeveld, Antonette Van Boxtel, Wouter J Dhert, and Laura B Creemers. Effect of Collagen Type I or Type II on Chondrogenesis by Cultured Human Articular Chondrocytes. *Tissue Engineering Part A*, 19(1-2):59–65, 2013.

[151] Amos Matsiko, John P. Gleeson, and Fergal J. O'Brien. Scaffold Mean Pore Size Influences Mesenchymal Stem Cell Chondrogenic Differentiation and Matrix Deposition. *Tissue Engineering Part A*, 2014.

[152] Leena-Stiina Kontturi, Elina Järvinen, Virpi Muhonen, Estelle C Collin, Abhay S Pandit, Ilkka Kiviranta, Marjo Yliperttula, and Arto Urtti. An injectable, in situ forming type II collagen/hyaluronic acid hydrogel vehicle for chondrocyte delivery in cartilage tissue engineering. *Drug Deliv. and Transl. Res.*, 4:149–158, 2014.

[153] Lu Yuan, Bao Li, Jirong Yang, Yilu Ni, Yingying Teng, Likun Guo, Hongsong Fan, Yujiang Fan, and Xingdong Zhang. Effects of composition and mechanical property of injectable collagen I/II composite hydrogels on chondrocyte behaviors. *Tissue Engineering Part A*, 22:899–906, 2016.

[154] Henrique V. Almeida, Binulal N. Sathy, Ivan Dudurych, Conor T. Buckley, Fergal J. O'Brien, and Daniel J. Kelly. Anisotropic Shape-Memory Alginate Scaffolds Functionalized with Either Type I or Type II Collagen for Cartilage Tissue Engineering. *Tissue Engineering Part A*, 23:55–68, 2017.

[155] Mariana Lazarini, Pedro Bordeaux-Rego, Renata Giardini-Rosa, Adriana S. S. Duarte, Mariana Ozello Baratti, Alessandro Rozim Zorzi, João Batista de Miranda, Carlos Lenz Cesar, Ângela Luzo, and Sara Teresinha Olalla Saad. Natural Type II Collagen Hydrogel, Fibrin Sealant, and Adipose-Derived Stem Cells as a Promising Combination for Articular Cartilage Repair. *CARTILAGE*, 8(4):439–443, 2017.

[156] M. Tamaddon, M. Burrows, S. A. Ferreira, F. Dazzi, J. F. Apperley, A. Bradshaw, D. D. Brand, J. Czernuszka, and E. Gentleman. Monomeric, porous type II collagen scaffolds promote chondrogenic differentiation of human bone marrow mesenchymal stem cells in vitro. *Scientific Reports*, 2017.

[157] Yongli Gao, Bao Li, Weili Kong, Lu Yuan, Likun Guo, Chuan Li, Hongsong Fan, Yujiang Fan, and Xingdong Zhang. Injectable and self-crosslinkable hydrogels based on collagen type II and activated chondroitin sulfate for cell delivery. *International journal of biological macromolecules*, 118:2014–2020, 2018.

[158] Claire E Kilmer. *Collagen Type I and II Blend Hydrogels for Articular Cartilage Tissue Engineering*. PhD thesis, Purdue University, 2019.

[159] H J Pulkkinen, V Tiitu, P Valonen, J S Jurvelin, L Rieppo, J Töyräs, T S Silvast, M J Lammi, and I Kiviranta. Repair of osteochondral defects with recombinant human type II collagen gel and autologous chondrocytes in rabbit.

[160] Andreas R. Klatt, Brigitte Paul-Klausch, Gabriele Klinger, Getrud Kühn, Joerg H. Renno, Marc Banerjee, Gebhart Malchau, and Klaus Wielckens. *Journal of Orthopaedic Research*.

[161] Mary B. Goldring. Chondrogenesis, chondrocyte differentiation, and articular cartilage metabolism in health and osteoarthritis. *Therapeutic Advances in Musculoskeletal Disease*, 2012.

[162] K Kuhn. The classical collagens: Types I, II, and III. In Mayne, R.; Curgeson, R. E, editor, *Structure and function of collagen types*, pages 1–37. Academic Press, New York, 1987.

[163] Laura Calderon, Estelle Collin, Diego Velasco-Bayon, Mary Murphy, Damien O'Halloran, and Abhay Pandit. Type II collagen-hyaluronan hydrogel: a step towards a scaffold for intervertebral disc tissue engineering. *European cells & materials*, 20:134–148, 2010.

[164] W. Y.J. Chen and G. Abatangelo. Functions of hyaluronan in wound repair. *Wound Repair and Regeneration*, 7:79–89, 1999.

[165] M. Radice, P. Brun, R. Cortivo, R. Scapinelli, C. Battaliard, and G. Abatangelo. Hyaluronan-based biopolymers as delivery vehicles for bone-marrow- derived mesenchymal progenitors. *Journal of Biomedical Materials Research*, 50:101–109, 2000.

[166] Brunella Grigolo, Gina Lisignoli, Anna Piacentini, Mauro Fiorini, Pietro Gobbi, Giovanni Mazzotti, Manuela Duca, Alessandra Pavesio, and Andrea Facchini. Evidence for redifferentiation of human chondrocytes grown on a hyaluronan-based biomaterial (HYAFF®11): Molecular, immunohistochemical and ultrastructural analysis. *Biomaterials*, 23:1187–1195, 2002.

[167] Kenzo Kawasaki, Mitsuo Ochi, Yuji Uchio, Nobuo Adachi, and Masahiko Matsusaki. Hyaluronic acid enhances proliferation and chondroitin sulfate synthesis in cultured chondrocytes embedded in collagen gels. *Journal of Cellular Physiology*, 179:142–148, 1999.

[168] Rolando Barbucci, Agnese Magnani, Roberto Rappuoli, Stefania Lamponi, and Marco Consumi. Immobilisation of sulphated hyaluronan for improved biocompatibility. *Journal of Inorganic Biochemistry*, 79:119–125, 2000.

[169] R. Barbucci, A. Magnani, S. Lamponi, D. Pasqui, and S. Bryan. The use of hyaluronan and its sulphated derivative patterned with micrometric scale on glass substrate in melanocyte cell behaviour. *Biomaterials*, 24:915–926, 2003.

[170] Karen L. Goa and Paul Benfield. Hyaluronic Acid: A Review of its Pharmacology and Use as a Surgical Aid in Ophthalmology, and its Therapeutic Potential in Joint Disease and Wound Healing. *Drugs*, 47:536–566, 1994.

[171] B Obrink and A Wasteson. Nature of the interaction of chondroitin 4-sulphate and chondroitin sulphate-proteoglycan with collagen. *Biochemistry Journal*, 121:227–233, 1971.

[172] J. E. Lee, J. C. Park, Y. S. Hwang, J. K. Kim, J. G. Kim, and H. Suh. Characterization of UV-irradiated dense/porous collagen membranes: morphology, enzymatic degradation, and mechanical properties. *Yonsei Medical Journal*, 42:172–179, 2001.

[173] Timothy Douglas, Sascha Heinemann, Carolin Mietrach, Ute Hempel, Susanne Bierbaum, Dieter Scharnweber, and Hartmut Worch. Interactions of collagen types I and II with chondroitin sulfates A-C and their effect on osteoblast adhesion. *Biomacromolecules*, 8:1085–1092, 2007.

[174] J. S. Pieper, T. Hafmans, J. H. Veerkamp, and T. H. Van Kuppevelt. Development of tailor-made collagen-glycosaminoglycan matrices: EDC/NHS crosslinking, and ultrastructural aspects. *Biomaterials*, 21(6):581–593, 2000.

[175] Job L.C. Van Susante, Jeroen Pieper, Pieter Buma, Toin H. Van Kuppevelt, Henk Van Beuningen, Peter M. Van Der Kraan, Jacques H. Veerkamp, Wim B. Van Den Berg, and René P.H. Veth. Linkage of chondroitin-sulfate to type I collagen scaffolds stimulates the bioactivity of seeded chondrocytes in vitro. *Biomaterials*, 2001.

[176] a Shimazu, a Jikko, M Iwamoto, T Koike, W Yan, Y Okada, M Shinmei, S Nakamura, and Y Kato. Effects of hyaluronic acid on the release of proteoglycan from the cell matrix in rabbit chondrocyte cultures in the presence and absence of cytokines. *Arthritis and rheumatism*, 36:247–53, 1993.

[177] Jonathan C. Bernhard and Alyssa Panitch. Synthesis and characterization of an aggrecan mimic. *Acta Biomaterialia*, 8:1543–1550, 2012.

[178] Shaili Sharma, Aeju Lee, Kuiwon Choi, Kwangmeyung Kim, Inchan Youn, Stephen B. Trippel, and Alyssa Panitch. *Macromolecular Bioscience*.

2. CHARACTERIZATION OF COLLAGEN TYPE I AND II BLENDED HYDROGELS FOR ARTICULAR CARTILAGE TISSUE ENGINEERING

This chapter consists of a manuscript by Vazquez-Portalatin N, Kilmer CE, Panitch A, and Liu JC, published in Biomacromolecules, Volume 17, Issue 10, 2016.

2.1 Abstract

Biomaterials that provide signals present in the native extracellular matrix have been proposed as scaffolds to support improved cartilage regeneration. This study harnesses the biological activity of collagen type II and the superior mechanical properties of collagen type I by characterizing gels made of collagen type I and II blends. The collagen blend hydrogels were able to incorporate both types of collagen and retained chondroitin sulfate and hyaluronic acid. Cryoscanning electron microscopy images showed that the 3:1 ratio of collagen type I to type II gels had a lower void space percentage (36.4%) than the 1:1 gels (46.5%). The complex modulus was larger for the 3:1 gels (G*=5.0 Pa) compared to the 1:1 gels (G*=1.2 Pa). The 3:1 blend consistently formed gels with superior mechanical properties compared to the other blends and has the potential to be implemented as a scaffold for articular cartilage engineering.

2.2 Introduction

Osteoarthritis (OA) is a debilitating condition that affects over 27 million Americans and is defined by degradation in articular cartilage extracellular matrix (ECM) [1]. Patients suffer from pain and stiffness in the joints associated with the onset of

OA. Tissue that is damaged by OA is a major health concern since cartilage tissue has a limited ability to self-repair due to the lack of vasculature in cartilage and low cell content [2].

Tissue engineering seeks to repair damaged cartilage by introducing an optimized combination of cells, scaffold, and bioactive factors that can be transplanted into a patient [3]. To prevent rejection and to provide a favorable environment for the attachment of cells, it is important to ensure that the biomaterial used for the scaffold is biocompatible. In addition, scaffold properties can induce the differentiation of encapsulated cells to a specific lineage [3]. Finally, the mechanical properties of the scaffold must match those of the surrounding tissue [4].

Many different biomaterial scaffolds are being studied as a way to repair damaged articular cartilage due to OA [5]. For example, hydrogel scaffolds made of collagen promote the formation of cartilage by encapsulating cells and mimicking native tissue [6]. The conservation of the structure and sequence of collagen across species has facilitated the biomedical application of collagen from many different sources [7]. Collagen type I hydrogels with embedded mesenchymal stem cells (MSCs) promote differentiation to chondrocytes and repair cartilage defects [6]. However, it has been shown that collagen type II hydrogels promote the differentiation of embedded MSCs to chondrocytes more efficiently than collagen type I gels [8, 9]. Collagen type II stimulates a more rounded cell shape, which is an important determinant for stem cell differentiation [10]. In addition, collagen type II and alginate hydrogels have been shown to initiate and maintain the differentiation of MSCs to chondrocytes without the addition of other bioactive molecules [9].

Collagen type II makes up 90-95% of the collagen produced by chondrocytes in the ECM and is a promising scaffold material for use in articular cartilage [11]. However, when compared to collagen type I, collagen type II is glycosylated to a greater extent [12,13]. The high number of bulky disaccharide groups in collagen type II appears to hinder the formation of highly ordered fibrils [12,13]. Without cross-linking, collagen type II exhibits poor mechanical properties when forming a hydrogel on its own [14].

Previous studies have blended collagen types to change the mechanical properties of collagen hydrogels [15].

During fibrillogenesis, collagen organization is affected by pH, ionic strength, and interactions with other components in the matrix. Previously, our lab created and characterized hydrogels made from collagen type I and III blends for use in skin and vasculature tissue engineering, and the addition of collagen type III increased the rate of collagen fibrillogensis [15]. Many different studies have investigated the effects of glycosaminoglycans (GAGs), an important nonfibrillar component of the native cartilage tissue ECM, on the rate of fibrillogenesis and collagen fibril diameter, and the conflicting data is summarized in the referenced paper [16]. GAGs attach to a protein core to form proteoglycans, which comprise 4-7% of the wet weight of healthy cartilage, and allow articular cartilage to withstand compressive forces [17,18]. Creating a collagen blend hydrogel with GAGs would thus more closely mimic the native structure of articular cartilage [19]. In this study, we sought to examine the effects of GAGs on collagen fibrillogenesis and to determine the amount of GAGs incorporated into the collagen hydrogel. Thus, we are interested in the interactions between a blend of collagen type I, collagen type II, and GAGs such as chondroitin sulfate (CS) and hyaluronic acid (HA).

The objective of this study was to create a hydrogel with a blend of collagen types I and II, and it was hypothesized that these blended hydrogels would have superior mechanical properties compared to gels made with collagen type II alone. We investigated whether the addition of collagen type I to a collagen type II hydrogel altered the amount of protein incorporated into the gels, the gels mechanical properties, and the structure of the collagen network. In addition, we examined the effects of adding HA and/or CS on gel formation.

2.3 Materials and Methods

2.3.1 Gel Preparation

Collagen type I, which was extracted from rat tail, was purchased from BD Biosciences (Franklin Lakes, NJ). Lyophilized chicken sternal collagen type II and hyaluronic acid ((1.5-1.8) x 10^6 Da) were purchased from Sigma-Aldrich (Saint Louis, MO). Sodium chondroitin sulfate from shark cartilage was purchased from Seikagaku (Tokyo, Japan). Stock solutions of both collagen types I and II were prepared in 20 mM acetic acid at a concentration of 5 mg/mL. The pH values of the solutions were raised to 7.4 with the addition of 10x phosphate buffered saline (PBS), 1 M NaOH, and 1x PBS, and the final concentrations of the collagen solutions were 4 mg/mL. The gels were prepared with collagen type I: collagen type II ratios of 1:0, 3:1, 1:1, 1:3, and 0:1 (Table 2.1). Glycosaminoglycans (e.g., CS or HA) were dissolved in 1x PBS to a concentration of 10 mg/mL and were added prior to polymerization. Gels were made with CS, HA, or a 1:1 ratio of CS to HA at a final concentration of 0.2 mg/mL of added glycosaminoglycans.

Table 2.1.: Concentration of collagen type I and collagen type II in different ratio blends.

Gel Ratio	Collagen I (mg/ml)	Collagen II (mg/ml)
1:0	4	0
3:1	3	1
1:1	2	2
1:3	1	3
0:1	0	4

2.3.2 Collagen Incorporation into a Gel

The amount of collagen incorporated into the gels was determined using a previously described method [15, 20]. Briefly, the samples were heated at 37 °C overnight to ensure that the solutions had polymerized. The gel was centrifuged for 15 min at 11000g. The supernatant was separated from the pellet by decanting. The supernatant from each sample was tested ($n = 3$) for the total amount of collagen present using a bicinchoninic acid (BCA) assay (Pierce, Rockford, IL) following the manufacturers protocol. Standard curves with different concentrations for each collagen type I to collagen type II ratio (1:0, 3:1, 1:1, 1:3, and 0:1) were used to determine the amount of collagen present within the supernatant. The amount of protein in the gel was calculated indirectly as the total amount of collagen prepared minus the amount of collagen in the supernatant.

A modified enzyme-linked immunosorbent assay (ELISA) was then performed to measure the amount of collagen type II in the supernatant ($n = 3$). A standard curve was created by adsorbing collagen with different ratios of collagen types I and II on a 96-well plate with a high binding surface (Corning, Corning, NY). The supernatant from the hydrogels and different ratio blends of collagen type I and II were diluted to a total protein concentration of 10 μg/mL. All samples and standards were then diluted 1:100 in 1x PBS and adsorbed onto the surface of a 96-well plate for 24 h at 4 °C. The wells were rinsed three times with blocking buffer (5% nonfat powdered milk in 1x PBS), blocked with blocking buffer for 2 h at room temperature, and rinsed three more times with blocking buffer. The plate was incubated for 24 h at 4 °C with a primary antibody for collagen type II (Abcam 34712, Cambridge, MA). The wells were rinsed with blocking buffer before being incubated with an HRP-conjugated secondary antibody (Life Technologies 16035, Carlsbad, CA) for 2 h at room temperature. A substrate reagent solution from a Substrate Reagent Pack (R&D Systems, Minneapolis, MN) was added to each well and incubated for 20 min at room temperature. A stopping solution of 2 N H_2SO_4 was added to each well, and

the absorbance was determined on a Spectromax M5 plate reader (Molecular Devices, Sunnyvale, CA) at 450 nm. Using the standard curves with the different collagen ratios, the ratios of collagen type I to collagen type II in our samples were quantified. The amounts of collagen types I and II in the gels were calculated indirectly by using the measured total protein concentration in the supernatant and the amounts of collagen types I and II in the supernatant.

2.3.3 CS and HA Incorporation into a Gel

A dimethylmethylene blue assay (DMMB) was performed to measure the amount of CS in the supernatant from gels made with varied amounts of HA or CS ($n = 3$). Specifically, 20 μL of the supernatant were mixed with 180 μL of DMMB reagent. The absorbance was measured on a plate reader at 525 nm. A standard curve of CS was created to quantify the amount of CS in the supernatants. The amount of CS retained in the gel was calculated indirectly.

A hyaluronic acid sandwich ELISA assay (Echelon Biosciences, Salt Lake City, UT) was performed following the manufacturers protocol. Samples and standards were prepared in 1x assay buffer, and 100 μL was incubated in each well of the HA detection plate for 1 h. The plate was washed three times with 1x Tris Buffered Saline (TBS) before 100 μL of HA detector was incubated for 1 h. After three more washes with 1x TBS, 100 μL of 3,3,5,5-Tetramethylbenzidine (TMB) solution was added and allowed to develop for 20 min. Finally, 50 μL of 2 N H_2SO_4 was added to stop the reaction before absorbance was read at 450 nm.

2.3.4 Cryoscanning Electron Microscopy (cryoSEM)

Samples for cryoSEM were prepared as previously described [13]. Briefly, collagen gels (n = 2-4) with different ratios of collagen type I to II were prepared on SEM holders and were incubated overnight at 37 °C to allow polymerization of the proteins. Samples with a 3:1 ratio of collagen type I to collagen type II with added CS, HA, or

a 1:1 ratio of CS to HA were also prepared for cryoSEM imaging. The sample holders were then moved to the cryo holder, frozen in liquid nitrogen slush, moved to a Gatan Alto 2500 prechamber (Gatan Inc., Pleasanton, CA), cooled to -155 °C, and fractured. The samples were sublimated at -90 °C for 10-15 min and sputter-coated for 120 s with platinum. Afterward, the samples were transferred to the microscope cryostage, which had been cooled to -145 °C, for imaging. All samples were imaged with an FEI NOVA nanoSEM field emission SEM (FEI, Hillsboro, OR) using the TLD (through the lens) or ET (Everhart-Thornley) detector operating at 5 kV accelerating voltage.

Fibril diameter measurements ($n \geq 782$) were analyzed using ImageJ software (National Institutes of Health, Bethesda, MD). As previously described, a perpendicular line was drawn across a fibril to obtain a measurement [15]. Three blinded individuals took 10 fibril diameter measurements per image, and each individual analyzed three or more images of each type of gel.

ImageJ software was also used to obtain void space information ($n \geq 15$) from the cryoSEM images. A Diameter J plugin was used to segment the images and determine the fraction of image containing void space.

2.3.5 Rheology

An ARG2 rheometer (TA Instruments, New Castle, DE) was used to perform rheological analysis with a 20 mm cone geometry. Gels ($n = 4$) were subjected to frequency sweeps from 0.01 to 1 Hz using a controlled stress of 0.5 Pa.

2.3.6 Statistics

The data are represented as a mean with error bars corresponding to one standard deviation. Single factor analysis of variance (ANOVA) and Tukey's post hoc tests were performed for the total protein concentration in the gels, the percentage of CS retained, and rheology data. Nested factorial models were used to perform ANOVA and Tukey's *post hoc* tests to analyze the fibril diameter and void space percentage

data. For all statistical tests, a value of $\alpha = 0.05$ was chosen, and significance was chosen to be a p-value at or below 0.05.

2.4 Results and Discussion

The total amount of protein in the supernatant was measured using a BCA assay and was used to calculate the total amount of protein in the gel. As the ratio of collagen type I to collagen type II decreased and thus the amount of collagen type II used to create the hydrogel increased, there was a statistical decrease in the final protein concentrations in the gels (Figure 2.1A). An ELISA was used to measure the amount of collagen type II in the supernatant, and this information was used to calculate the amounts of collagens type I and II in both the supernatant and gel. As the ratio of collagen type I to collagen type II in the starting solution decreased, the amounts of collagen types I and II incorporated in the gel respectively decreased and increased (Figures 2.1B and 2.1C). The amount of collagen type I in the gel decreased proportionally as the ratio of collagen type I to collagen type II decreased. However, the amount of collagen type II was not inversely proportional to the ratio of collagen type I to collagen type II. Instead, there was no statistically significant difference in the amount of collagen type II incorporated in the gel when the ratio of collagen type I to collagen type II was decreased from 1:3 to 0:1. A subset of the gels were immunostained for collagen type II to verify collagen type II incorporation in the gel (Figure S 2.6). As expected, when more collagen type II was incorporated in the gel, an increase in fluorescence signal was observed. Since the amount of collagen type II incorporated in 0:1 gels did not differ from the 1:3 gels, the 0:1 gels were no longer considered in future experiments.

Next, we investigated whether the final protein concentrations in the blended collagen gels were altered due to the addition of HA and/or CS. The final protein concentration in the supernatant was measured for three different ratios of collagen type I to collagen type II (3:1, 1:1, and 1:3). Gels had no HA or CS added or were

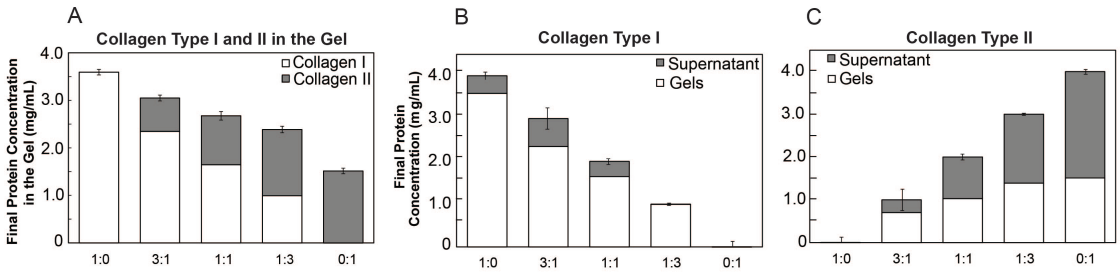

Figure 2.1.: (A) Final collagen concentration in the gel at different ratio blends uses white bars to represent collagen type I found in fibrillary form and gray bars to represent collagen type II measured in fibrillary form. Data ($n = 3$) are represented as the mean $\pm$ the standard deviation of the total concentration of collagen (both collagen types I and II) in the gel. An ANOVA and Tukey's honestly significant difference *post hoc* test were performed and indicate a significant difference in the total protein concentration in the gel between each ratio ($p < 0.05$). The final concentration of collagen in the gel and supernatant for (B) collagen type I and (C) collagen type II. The white bars represent collagen content in fibrillar form, whereas the gray bars represent collagen measured in the supernatant ($n = 3$). The error bars represent the standard deviation of the amount of collagen type II in the supernatant.

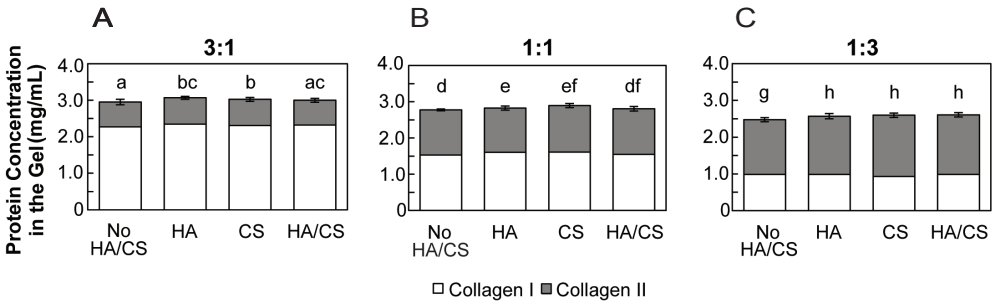

Figure 2.2.: Final protein concentration in the fibrils at different ratio blends of collagen type I and collagen type II with the addition of HA, CS, or both HA and CS. The gels were created containing a (A) 3:1, (B) 1:1, or (C) 1:3 ratio of collagen type I to collagen type II. An ANOVA and Tukey's honestly significant difference *post hoc* tests were performed. Different letters indicate groups with significantly different total protein concentrations incorporated in the gel ($p < 0.05$). Data ($n = 3$) are represented as the mean $\pm$ the standard deviation.

supplemented with HA, CS, or a combination of both HA and CS. When only HA or only CS was included, there was a significant increase in the total amount of protein incorporated into the gel. Thus, the addition of HA and/or CS did not negatively impact the total concentration of protein in the 3:1, 1:1, or 1:3 gels and therefore did not inhibit gel formation (Figure 2.2). The increase of protein incorporated into the gels upon addition of only CS is consistent with experiments performed by Stuart *et al.* using collagen type I gels [16]. Stuart and co-workers found that adding CS decreased the amount of collagen in the supernatant and thus resulted in more collagen incorporated into the gel [16]. In previous experiments, CS also increased the rate of fibrillogenesis of collagen type I and resulted in fibrils of smaller diameter [21]. These results also indicated that the addition of CS increased the number and shape of nucleation sites and promoted the aggregation of collagen molecules end-to-end [22].

The percentage of CS retained in the gel was calculated using the supernatants from the gels supplemented with CS or both HA and CS (Figure 2.3A). There was a statistically significant difference in the percentage of CS retained when adding only CS to gels made with different ratios of collagen type I to II. In addition, there was a

statistical difference in the percentage of CS retained when adding a 1:1 ratio of CS to HA to the different gel blends tested (3:1, 1:1, and 1:3). The interactions between CS and collagen are known to be ionic since increasing ionic strength reduces the binding of CS [23,24]. Furthermore, collagen type II is believed to bind more CS than collagen type I due to a stronger ionic interaction between collagen type II and GAGs. For example, Pieper *et al.* attempted unsuccessfully to remove GAGs from bovine tracheal cartilage collagen type II by washing with a high ionic strength solution [25]. In this study, the amount of collagen type II in the supernatant significantly increased with a decrease in the ratio of collagen I to collagen II (Figure 2.1), and these results could explain the significant decrease in the percentage of CS retained within the gel. When comparing the percentage of CS retained for gels with only CS added to gels with CS and HA added, there was no statistical difference for the 3:1 gels, but there were a statistical difference for the 1:1 and 1:3 gels.

The percentage of HA retained in the gel was calculated using the supernatants from the gels supplemented with HA or both HA and CS (Figure 2.3B). There was no significant difference between the three different hydrogel blends when HA was added. When HA and CS were added, there was also no significant difference between the three different ratios. There were statistical differences between gels that had HA added and gels that had both CS and HA added for the 3:1 and 1:3 gels. However, there was no statistical difference between the 1:1 gels that had CS compared to 1:1 gels that had HA. The HA that was used for these experiments was high-molecular-weight HA ((1.5 - 1.8) x 10^6 Da). High-molecular-weight HA chains form topological interactions between chains that reduce their mobility [26]. Collagen molecules are separated from the HA molecules due to the reduction in mobility and topological hindrance. The separated collagen molecules then begin to nucleate and aggregate to form fibrils without interacting with the HA molecules. In addition, HA is known to form aggregates with ECM molecules. The aggregates of ECM molecules form a viscous barrier that inhibits the displacement of macromolecules in chondrocyte cultures [27]. These previous findings suggest that, in our experiments, supplemented

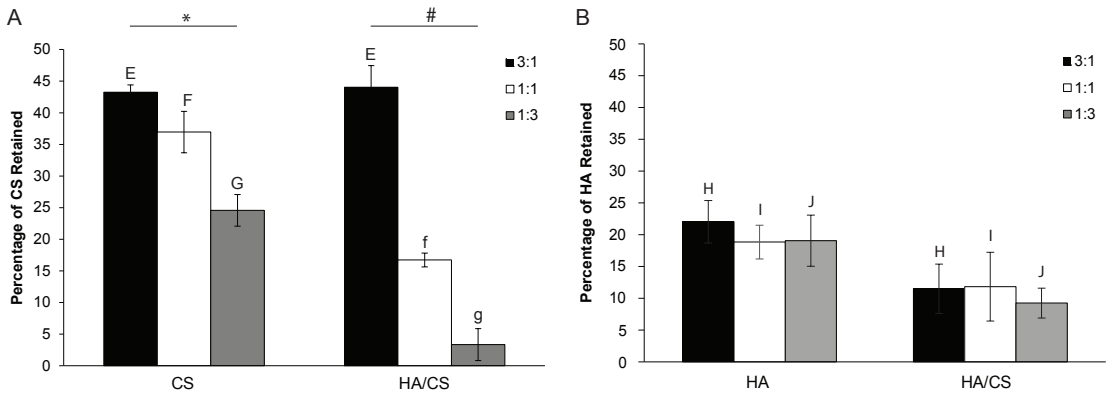

Figure 2.3.: Percentage of (A) CS and (B) HA retained in the fibrils. Gels were created using varying ratios of collagen type I to II (3:1, 1:1, and 1:3) with either CS, HA, or both CS and HA added into the gels. ANOVA and Tukey's honestly significant difference *post hoc* tests were performed. The * indicates significant differences ($p < 0.05$) between the three different hydrogel blends when CS is added. The # indicates significant differences ($p < 0.05$) between the three different hydrogel blends when HA and CS are added. EE indicates there is no statistical difference ($p > 0.05$) between the 3:1 gels. Ff and Gg indicate that there were statistical differences ($p < 0.05$) between the 1:1 and 1:3 gels, respectively. There is no significant difference ($p > 0.05$) between the three different hydrogel blends when either HA or HA and CS were added. Hh and Jj indicate that there were statistical differences ($p < 0.05$) between the 3:1 and 1:3 gels, respectively. II indicates there is no statistical difference ($p > 0.05$) between the 1:1 gels. Data ($n = 3$) are represented as the mean $\pm$ the standard deviation.

HA interacts with the added CS and precludes the CS from being incorporated within the collagen gels. The 1:3 blend was not pursued in further experiments due to the significant decrease in CS incorporated into the gels when compared to the 3:1 and 1:1 gels.

CryoSEM was performed to observe the network and structure of the collagen fibrils in the gels. Figure 2.4A shows representative cryoSEM images of different ratio blends of collagen type I to collagen type II. In these images, collagen fibrils and the networks these fibrils form within the gels can be seen. Furthermore, qualitatively, the fibril diameters appear to be similar between the gels, but the void space seems to increase with the addition of collagen type II. Thick lamellar-like structures are

also present in the SEM images, and similar structures have been observed in other SEM images of collagen hydrogels [15].

To quantify our observations, the collagen fibril diameters were measured using ImageJ software, and the diameter distribution in the gels at different ratio blends is presented in Figure 2.4B. The 1:0, 3:1, and 1:1 gels showed unimodal distributions, and the average fibril diameter showed no significant differences among the different blends (Figure S 2.7). ImageJ, along with a DiameterJ plugin, was used to obtain the void space percentage in the gels (Figure 2.4C). The 1:1 gels showed a significant increase in void space percentage (46.5%) compared to gels with ratios of 1:0 (35.1%) and 3:1 (36.4%).

CryoSEM images of 3:1 collagen type I to collagen type II gels with no GAGs or supplemented with CS, HA, or both CS and HA were also analyzed to examine the collagen fibril network within the gels (Figure S 2.8A). The collagen fibril diameters (Figure S 2.8B) and void space percentage (Figure S 2.8C) were measured using ImageJ software, and there were no significant differences observed.

The unimodal distribution shape of fibrils (Figure 2.4B) obtained in this study is similar to what was previously shown for gels composed of collagen type I only and collagen type I and collagen type III blends [15, 16, 28, 29]. However, gels composed of only collagen type I have also shown bimodal distributions [15, 16, 30]. The fibril diameter ranges exhibited by collagen type I only gels (up to 0.65 μm) and collagen type I and II blends (up to 0.6 μm) were larger than those previously reported for gels composed of collagen type I only (up to 0.4 μm) [16, 29] and collagen type I and III blends (up to 0.2 μm) [15]. The addition of collagen type II to the blends did not significantly affect the average fibril diameter with or without the addition of GAGs (Figures S 2.7 and S 2.8B).

The void space percentage results obtained for the gels without GAGs (Figure 2.4C) are similar to previous studies that showed gels composed of 70% collagen type I and 30% collagen type III or gels composed of 30% collagen type I and 70% collagen type III had an increase in void space percentage ($\sim$45-50%) compared to

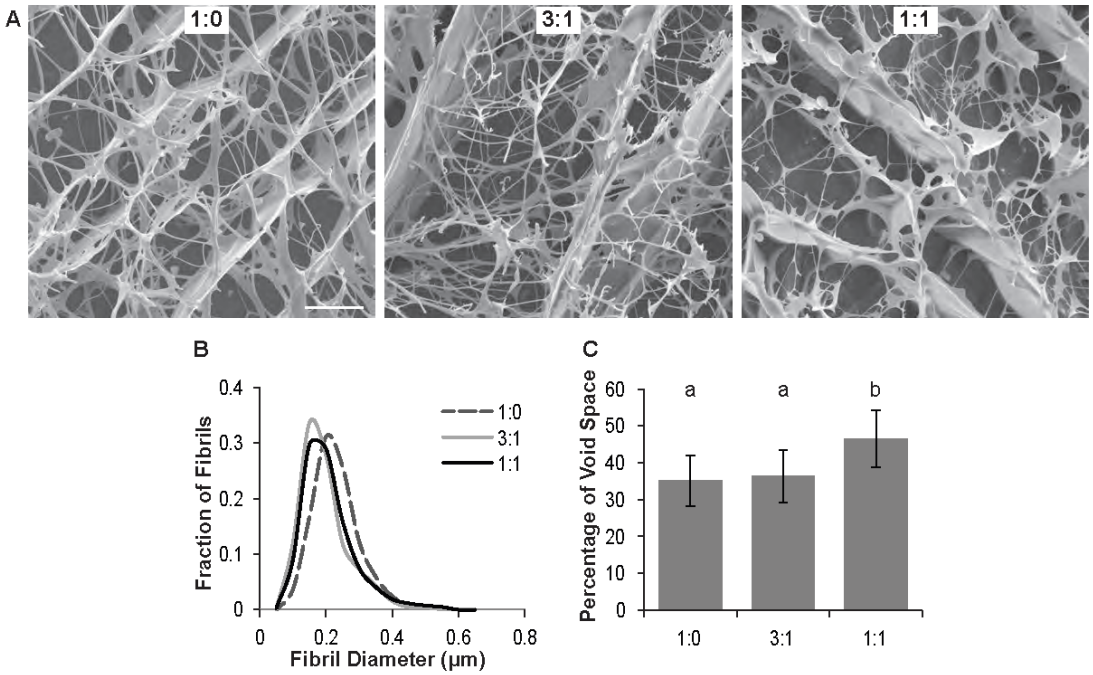

Figure 2.4.: Collagen networks for different ratio blends. (A) Representative cryoSEM images of different ratio blends of collagen type I to collagen type II show the collagen fibril network within the gels. Scale bar represents 5 μm. (B) Distribution of collagen fibril diameters in the gels at different ratio blends. (C) Percentage of void space for the gels based on cryoSEM images obtained at 10 000x magnification. ANOVA and Tukey's *post hoc* tests were performed on the percentage of void space data by using nested factorial models. The different letters indicate groups with a significant difference ($p < 0.05$) in the percentage of void space in the gels. Data ($n \geq 15$) for void space percentage are represented as the mean $\pm$ the standard deviation.

gels composed of collagen type I only (30%) [15]. The significant increase in void space percentage as the ratio of collagen type I to collagen type II in the blends decreased suggests that the collagen type II addition limits fibril formation. Collagen type II may coat the fibrils formed by collagen type I and inhibit lateral aggregation of fibrils as has been shown for collagen type I and III gels [31]. This interaction between collagen type I and II could affect the stability of the gel and, thus, its mechanical properties.

Another explanation for the results seen from the analysis of the SEM images could be due to the fact that addition of collagen type II reduced the total collagen concentration in the gel (Figure 2.1A) and also reduced the collagen type I concentration (Figure 2.1B). A previous study showed that hydrogels have statistically similar fibril diameters when polymerized with varying collagen type I concentrations [32], and these results are consistent with the results seen with the collagen type I and II blend hydrogels in this study. In addition, similar to the results seen for the blended collagen I and II hydrogels, another study showed that decreasing the collagen type I concentration increased the void space [33].

Frequency sweeps from 0.01 to 1 Hz were performed to characterize and understand the mechanical properties of these gels. The frequency sweeps showed that at 1 Hz, the 1:0, 3:1, and 1:1 gels respectively had average storage moduli (G') of 21.2 $\pm$ 5.9, 4.9 $\pm$ 1.0, and 1.2 $\pm$ 0.2 Pa (Figure 2.5) ; loss moduli (G") of 2.4 $\pm$ 0.5, 1.2 $\pm$ 0.1, and 0.3 $\pm$ 0.1 Pa (Figure 2.5); and complex moduli (G*) of 21.4 $\pm$ 5.9, 5.0 $\pm$ 0.9, and 1.2 $\pm$ 0.2 Pa (Figure S 2.9). The addition of collagen type II to the gels significantly decreased their stiffness, and this result could be attributed to a decrease in total protein concentration in the gel (Figure 2.1A) and the increase in void space (Figure 2.4C). Previously performed studies showed concentration-dependent changes in mechanical properties [34, 35]. In particular, single collagen type I fibrils or collagen type I and agarose blend hydrogels demonstrated that higher collagen type I concentrations increased the mechanical properties [34, 35]. Other studies with collagen type I membranes [36], collagen type I hydrogels [12], and collagen type I/III blended

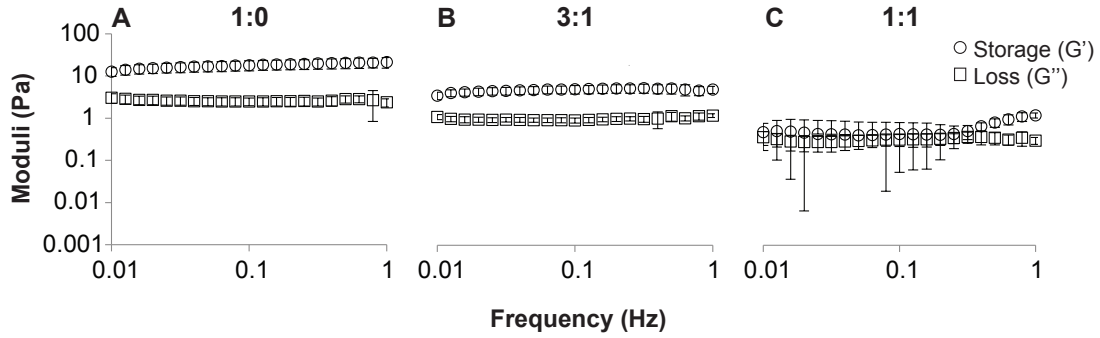

Figure 2.5.: Frequency sweeps of storage and loss moduli of gels prepared from mixtures of (A) 1:0, (B) 3:1, and (C) 1:1 collagen type I to collagen type II. ANOVA and Tukey's *post hoc* tests were performed. At 1 Hz, a significant difference ($p < 0.05$) was observed between the storage moduli for the three different gel blends. At 1 Hz, the loss modulus for the 1:1 gels was significantly different ($p < 0.05$) from the loss moduli of the 1:0 and 3:1 gels. Data ($n = 4$) are represented as the mean $\pm$ the standard deviation.

hydrogels [11] correlated an increase in porosity, or void space, with a decrease in the respective mechanical properties of tensile stress [36]; stiffness [12]; and storage, loss, and complex moduli [11].

The decrease in stiffness with increasing collagen II also suggests that the ability of collagen type II to alter network structure and fibril growth can affect the gels' mechanical properties. Previous work has shown that collagen type III also alters fibril formation of collagen I and, thus, the mechanical properties of the gel [15]. However, collagen gels composed of collagen type I and III blends exhibit higher mechanical properties than the gels composed of collagen types I and II shown here. At 1 Hz, gels composed of collagen type I and III blends exhibited a storage moduli range of 115-175 Pa and a loss moduli range of 15-25 Pa. Similarly, collagen type I gels had a storage moduli of $\sim$170 Pa and loss moduli of $\sim$24 Pa [15]. In another study, Stuart and coworkers found their collagen type I gels exhibited a storage modulus of $\sim$145 Pa and a loss modulus of $\sim$23 Pa [16]. While these collagen type I gels exhibited higher mechanical properties than the 1:0 gels presented herein, Shayegan *et al.* have

also seen lower storage moduli (0.1 - 0.3 Pa) and loss moduli (0.7 - 1.0 Pa) for collagen type I gels at 4mg/ml to 5 mg/ml concentrations [37]. The difference in mechanical properties of these gels could be attributed to different collagen type I sources, gel preparation methods, and protein concentrations. Other studies have improved the mechanical properties of their gels by incorporating HA [26, 30, 38], dermatan sulfate [26], and other crosslinking agents [38–40]. Calderon *et al.* demonstrated that noncrosslinked collagen type II gels exhibited significantly lower compressive stress (27.6 ± 6.5 kPa) and compressive modulus (1.4 ± 0.35 kPa) than those that had been crosslinked (48.9-188.1 kPa and 2.4-10.3 kPa, respectively) [14]. Halloran *et al.* have also presented similar results where noncrosslinked atelocollagen type II scaffolds showed lower storage moduli than gels that had been crosslinked with microbial transglutaminase [38].

In this study, our goal was to develop and characterize collagen blend gels that would harness the biological activity of collagen type II, which is the most abundant type of collagen produced by chondrocytes and has the ability to initiate and maintain the differentiation of MSCs to chondrocytes without added bioactive molecules [8–11]. There is growing interest in making scaffolds for tissue engineered cartilage that utilizes collagen type II, and many current studies utilize collagen type II as a cross-linked sponge [41–43]. Due to the fact that collagen type II exhibits poor mechanical properties when forming a hydrogel on its own, studies have explored ways to enhance the mechanical properties of collagen type II hydrogels by developing composite scaffolds [14, 44, 45]. From the experiments conducted, the 3:1 gels were able to incorporate both collagen type I and collagen type II within the gels. It is important to note that an antibody was able to detect collagen type II, and therefore it is likely that collagen type II would be accessible to cells embedded in the scaffolds. The 3:1 gels also retained a significantly higher amount of CS, which allows articular cartilage to withstand compressive forces, than the other blends. Adding GAGs to the collagen gels creates a more biologically relevant scaffold for articular cartilage tissue engineering. Moreover, compared to the 1:1 gels, the 3:1 gels exhibited lower

void space percentages and higher storage, loss, and complex moduli. Thus, based on all these properties, the 3:1 collagen type I to collagen type II blend has the potential to be implemented as a scaffold to effectively engineer articular cartilage tissue.

2.5 Conclusion

In this study, we created hydrogels composed of different ratios of collagen type I to collagen type II to elucidate their unique properties. We demonstrated that the addition of collagen type II alters gel formation, network structure, and mechanical properties. From the five different blends we created, the 3:1 collagen type I to collagen type II ratio blend has the potential to be implemented effectively for use in tissue engineering. Future work will focus on encapsulating cells and adding growth factors within these hydrogels.

2.6 Acknowledgements

This work was supported by the Purdue School of Chemical Engineering, Weldon School of Biomedical Engineering, Purdue University Graduate School (Ross Fellowship to C.K. and George Washington Carver Fellowship to N.V.), and the National Institutes of Health (NIAMS R21AR065644). The authors thank Dr. Thomas Kuczek and Yunfan Li from the Purdue University Statistics Department for their assistance with the statistical models and tests performed and Dr. Shaili Sharma for her editorial assistance.

2.7 Supporting Information

Collagen Type II Incorporation Materials and Methods

Collagen type II in the gel was visualized using immunostaining with a primary antibody for collagen type II (Abcam 34712, Cambridge, MA). The gels were fixed in 3% paraformaldehyde for 1 h. After fixation, the gels were rinsed three times

with 1x PBS, blocked with blocking buffer (5% nonfat powdered milk in 1x PBS) for 1 h at room temperature, and rinsed three times with 1x PBS. The gels were incubated with the primary antibody for 24 h at 4 °C. The gels were rinsed with 1x PBS before being incubated with a goat anti-rabbit AlexaFluor® 555 (Cell Signaling Technology 4413S, Danvers, MA) for 24 h at 4 °C. All confocal images were obtained using a 20x objective on a Nikon Ti-EC-1 Plus microscope (Nikon, Melville, NY). Nikon NIS-Elements AR software (version 3.2) was utilized to analyze fluorescence images.

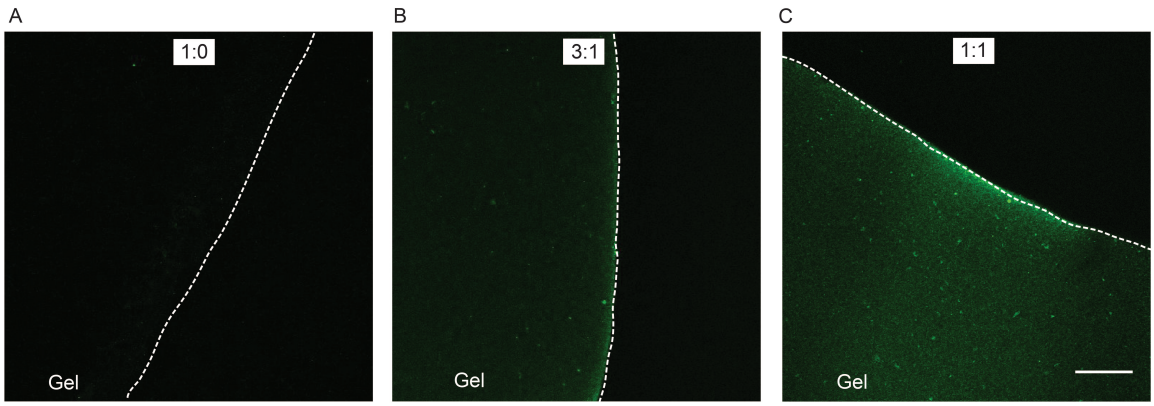

Figure S 2.6.: Representative images of immunostaining for collagen type II (green) hydrogels at different blends of (A) 1:0, (B) 3:1, and (C) 1:1 ratios of collagen type I to collagen type II. The boundary of the gel is indicated with the white, dashed line, and the side containing the gel is notated in the figure. Scale bar represents 100 μm.

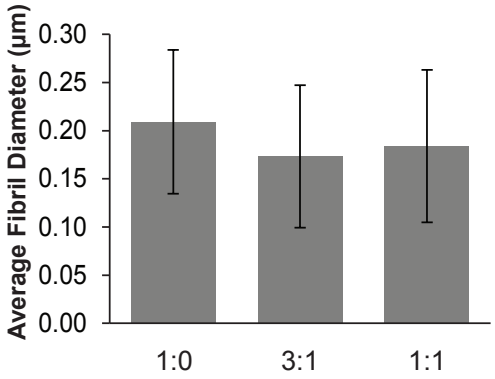

Figure S 2.7.: Average fibril diameter in the gels at different ratio blends. ANOVA and Tukey's *post hoc* tests were performed on the average fibril diameter data by using nested factorial models. For the average fibril diameter data, there were no significant differences observed between the different blends. Data ($n \geq 782$) are represented as the mean $\pm$ the standard deviation.

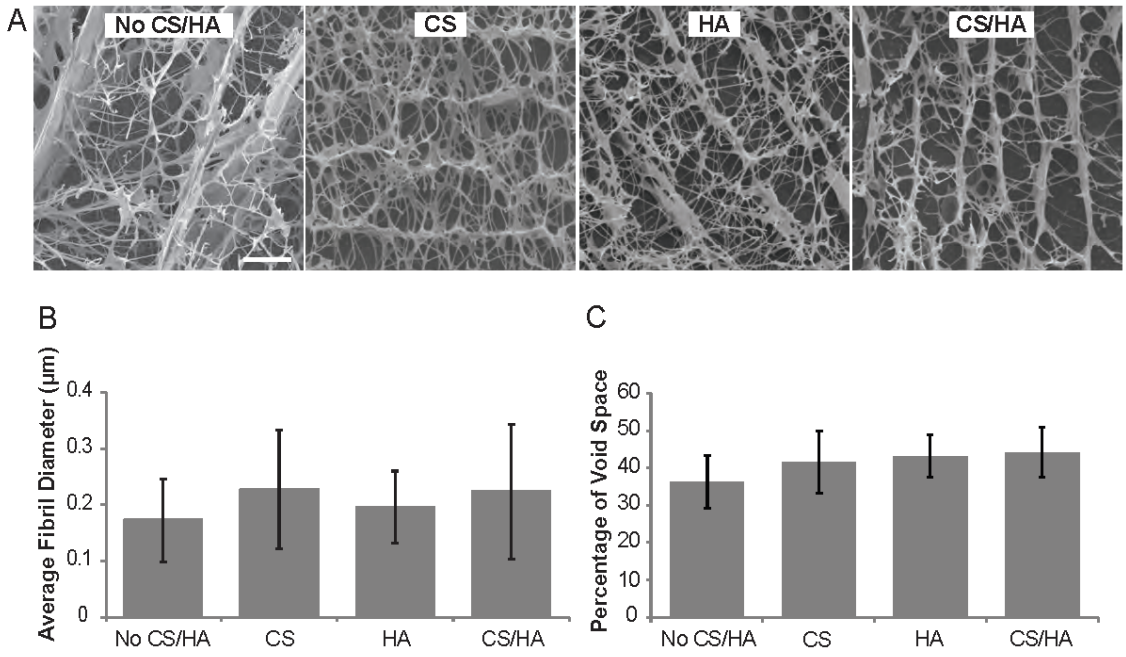

Figure S 2.8.: Effect of adding GAGs in collagen networks of different ratio blends. (A) Representative cryoSEM images of 3:1 collagen type I to collagen type II gels with no GAGs added or supplemented with CS, HA, or both CS and HA show the collagen fibril network within the gels. Scale bar represents 5 μm. (B) Average fibril diameter and (C) percentage of void space for the gels based on cryoSEM images obtained at 10,000x magnification. ANOVA and Tukey's *post hoc* tests were performed on the average fibril diameter and the percentage of void space data by using nested factorial models. There were no significant differences observed between gels that had no GAGs added or gels supplemented with CS, HA, or both CS and HA ($p > 0.05$). Data ($n \geq 58$ for fibril diameter, $n \geq 8$ for void space percentage) are represented as the mean $\pm$ the standard deviation.

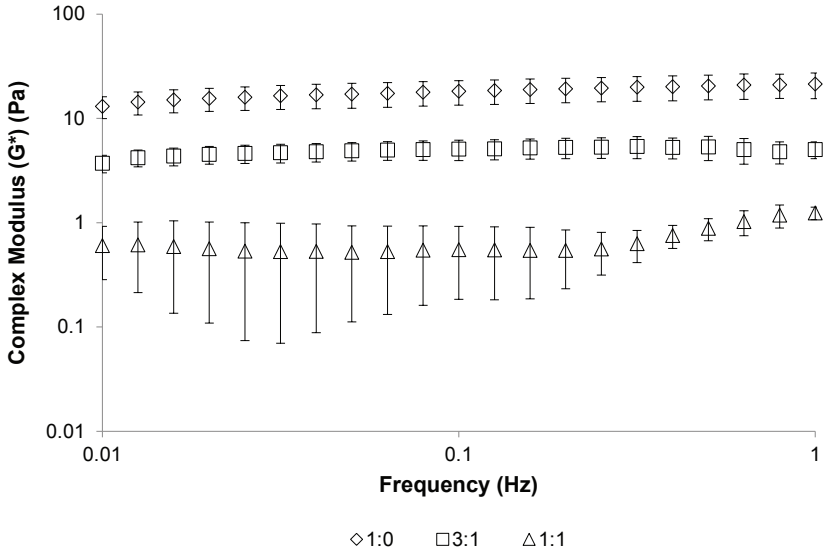

Figure S 2.9.: Complex modulus of gels prepared from mixtures of 1:0, 3:1, and 1:1 collagen type I to collagen type II. ANOVA and Tukey's *post hoc* tests were performed. At 1 Hz, a significant difference ($p < 0.05$) was observed between the complex moduli for the three different ratios. Data ($n = 4$) are represented as the mean $\pm$ the standard deviation.

2.8 References

[1] Reva C. Lawrence, David T. Felson, Charles G. Helmick, Lesley M. Arnold, Richard A. Deyo, Sherine Gabriel, R. Hirsch, M. C. Hochberg, G. G. Hunder, J. M. Jordan, J. N. Katz, H. M. Kremers, and F Wolfe. Estimates of the prevalence of arthritis and other rheumatic conditions in the United States. Part II. *Arthritis Rheum*, 58:26–35, 2008.

[2] Zimin Wang and Jiang Peng. Articular cartilage tissue engineering: Development and future: A review. *Journal of Musculoskeletal Pain*, 22:68–77, 2014.

[3] Amos Matsiko, Tanya J. Levingstone, and Fergal J. O'Brien. Advanced strategies for articular cartilage defect repair. *Materials*, 6:637–668, 2013.

[4] D W Hutmacher. Scaffolds in tissue engineering bone and cartilage. *Biomaterials*, 21:2529–2543, 2000.

[5] Rozlin Abdul Rahman, Muhammad Aa'zamuddin Ahmad Radzi, Norhamiza Mohamad Sukri, Noorhidayah Md Nazir, and Munirah Sha'ban. Tissue engineering of articular cartilage: from bench to bed-side. *Tissue Engineering and Regenerative Medicine*, 12:1–11, 2015.

[6] Pouya Mafi, Sandip Hindocha, Rafi Mafi, and Wasim S Khan. Evaluation of biological protein-based collagen scaffolds in cartilage and musculoskeletal tissue engineering- A systematic review of the literature. *Current Stem Cell Research & Therapy*, 7:302–309, 2012.

[7] Joydeep Basu and John W. Ludlow. Biomaterials for TE/RM products. In *Developments in tissue engineered and regenerative medicine products: A practical approach*, pages 23–24. Woodhead Publishing Limited, Philadelphia, 2012.

[8] ZuFu Lu, Behrouz Zandieh Doulabi, ChunLing Huang, Ruud A Bank, and Marco N Helder. Collagen type II enhances chondrogenesis in adipose tissue-derived stem cells by affecting cell shape. *Tissue engineering. Part A*, 16:81–90, 2010.

[9] D Bosnakovski, M Mizuno, G Kim, S Takagi, M Okumura, and T Fujinaga. Chondrogenic differentiation of bovine bone marrow mesenchymal stem cells (MSCs) in different hydrogels: Influence of collagen type II extracellular matrix on MSC chondrogenesis. *Biotechnology and Bioengineering*, 93:1152–1163, 2006.

[10] Rowena McBeath, Dana M. Pirone, Celeste M. Nelson, Kiran Bhadriraju, and Christopher S. Chen. Cell shape, cytoskeletal tension, and RhoA regulate stem cell lineage commitment. *Developmental Cell*, 6:483–495, 2004.

[11] Hemanth Akkiraju and Anja Nohe. Role of chondrocytes in cartilage formation, progression of osteoarthritis and cartilage regeneration. *Journal of Developmental Biology*, 3:177–192, 2015.

[12] K Kuhn. The classical collagens: Types I, II, and III. In Mayne, R.; Curgeson, R. E, editor, *Structure and function of collagen types*, pages 1–37. Academic Press, New York, 1987.

[13] T J Wess. Collagen fibril form and function. *Advances in protein chemistry*, 70:341–374, 2005.

[14] Laura Calderon, Estelle Collin, Diego Velasco-Bayon, Mary Murphy, Damien O'Halloran, and Abhay Pandit. Type II collagen-hyaluronan hydrogel: a step towards a scaffold for intervertebral disc tissue engineering. *European cells & materials*, 20:134–148, 2010.

[15] Kate Stuart and Alyssa Panitch. Characterization of gels composed of blends of collagen l, collagen III, and chondroitin sulfate. *Biomacromolecules*, 10:25–31, 2009.

[16] Kate Stuart and Alyssa Panitch. Influence of chondroitin sulfate on collagen gel structure and mechanical properties at physiologically relevant levels. *Biopolymers*, 89:841–851, 2008.

[17] Syam P. Nukavarapu and Deborah L. Dorcemus. Osteochondral tissue engineering: Current strategies and challenges. *Biotechnology Advances*, 31:706–721, 2013.

[18] Shaili Sharma, Alyssa Panitch, and Corey P Neu. Incorporation of an aggrecan mimic prevents proteolytic degradation of anisotropic cartilage analogs. *Acta Biomaterialia*, 9:4618–4625, 2013.

[19] Jonathan C. Bernhard and Alyssa Panitch. Synthesis and characterization of an aggrecan mimic. *Acta Biomaterialia*, 8:1543–1550, 2012.

[20] Timothy Douglas, Sascha Heinemann, Carolin Mietrach, Ute Hempel, Susanne Bierbaum, Dieter Scharnweber, and Hartmut Worch. Interactions of collagen types I and II with chondroitin sulfates A-C and their effect on osteoblast adhesion. *Biomacromolecules*, 8:1085–1092, 2007.

[21] M Keech. The formation of fibrils from collagen solutions. IV. Effect of mucopolysaccharides and nucleic acids: an electron microscope study. *The Journal of biophysical and biochemical cytology*, 9:193–209, 1961.

[22] M Honya and H Misunuma. Collagen fibrillogenesis in vitro: An accelerative effect of surfactants on collagen fibril formation. *Journal of biochemistry*, 75:113–121, 1974.

[23] M B Mathews. The interaction of collagen and acid mucopolysaccharides. A model for connective tissue. *The Biochemical journal*, 96:710–716, 1965.

[24] B Obrink and A Wasteson. Nature of the interaction of chondroitin 4-sulphate and chondroitin sulphate-proteoglycan with collagen. *Biochemistry Journal*, 121:227–233, 1971.

[25] J. S. Pieper, P. M. Van Der Kraan, T. Hafmans, J. Kamp, P. Buma, J. L C Van Susante, W. B. Van Den Berg, J. H. Veerkamp, and T. H. Van Kuppevelt. Crosslinked type II collagen matrices: Preparation, characterization, and potential for cartilage engineering. *Biomaterials*, 23:3183–3192, 2002.

[26] A Borzacchiello, L Ambrosio, P Netti, and L Nicolais. Rheology of biological fluids and their substitutes. In Michael J. Yaszemski, Debra J. Trantolo, Kai-Uwe Lewandrowski, Vasif Hasirci, David E. Altobelli, and Donald L. Wise, editors, *Tissue Engineering And Novel Delivery Systems*, pages 268–283. CRC Press, Boca Raton, 1st edition, 2003.

[27] Y Kato, Y Mukudai, A Okimura, A Shimazu, and S Nakamura. Effects of hyaluronic acid on the release of cartilage matrix proteoglycan and fibronectin from the cell matrix layer of chondrocyte cultures: Interactions between hyaluronic acid and chondroitin sulfate glycosaminoglycan. *Journal of Rheumatology*, 22:158–159, 1995.

[28] A. O. Brightman, B. P. Rajwa, J. E. Sturgis, M. E. McCallister, J. P. Robinson, and S. L. Voytik-Harbin. Time-lapse confocal reflection microscopy of collagen fibrillogenesis and extracellular matrix assembly in vitro. *Biopolymers*, 54:222–234, 2000.

[29] Dimitar Stamov, Milauscha Grimmer, Katrin Salchert, Tilo Pompe, and Carsten Werner. Heparin intercalation into reconstituted collagen I fibrils: Impact on growth kinetics and morphology. *Biomaterials*, 29:1–14, 2008.

[30] Sylvie Lélu and Alain Pluen. Characterization of composite networks made of type I collagen, hyaluronic acid and decorin. *Macromolecular Symposia*, 256:175–188, 2007.

[31] H Notbohm, S Mosler, P K Müller, and J Brinckmann. In vitro formation and aggregation of heterotypic collagen I and III fibrils. *International journal of biological macromolecules*, 15:299–304, 1993.

[32] S.T. Kreger, B.J. Bell, J. Bailey, E. Stites, J. Kuske, B. Waisner, and S. L. Voytik-Harbin. Polymerization and matrix physical properties as important design considerations for soluble collagen formulations. *Biopolymers*, 93:690–707, 2010.

[33] Elizabeth E Antoine, Pavlos Vlachos, and Marissa Nichole Rylander. Review of collagen I hydrogels for bioengineered tissue microenvironments: Characterization of mechanics, structure, and transport. *Tissue engineering: Part B*, 20(6):683–696, 2014.

[34] Lalitha Sivakumar and Gunjan Agarwal. The influence of discoidin domain receptor 2 on the persistence length of collagen type I fibers. *Biomaterials*, 31:4802–4808, 2010.

[35] Spencer P. Lake and Victor H. Barocas. Mechanical and structural contribution of non-fibrillar matrix in uniaxial tension: A collagen-agarose co-gel model. *Annals of Biomedical Engineering*, 39:1891–1903, 2011.

[36] J. E. Lee, J. C. Park, Y. S. Hwang, J. K. Kim, J. G. Kim, and H. Suh. Characterization of UV-irradiated dense/porous collagen membranes: morphology, enzymatic degradation, and mechanical properties. *Yonsei Medical Journal*, 42:172–179, 2001.

[37] Marjan Shayegan and Nancy R. Forde. Microrheological characterization of collagen systems: From molecular solutions to fibrillar gels. *PLoS ONE*, 8:1–12, 2013.

[38] Damien O. Halloran, Sibylle Grad, Martin Stoddart, Peter Dockery, Mauro Alini, and Abhay S. Pandit. An injectable cross-linked scaffold for nucleus pulposus regeneration. *Biomaterials*, 29:438–447, 2008.

[39] Bin Xu, Yanhang Zhang, and Ming Jay Chow. Experimental and modeling study of collagen scaffolds with the effects of crosslinking and fiber alignment. *International Journal of Biomaterials*, 2011:1–12, 2011.

[40] Ming Thau Sheu, Ju Chun Huang, Geng Chang Yeh, and Hsiu O. Ho. Characterization of collagen gel solutions and collagen matrices for cell culture. *Biomaterials*, 22:1713–1719, 2001.

[41] C. R. Lee, A. J. Grodzinsky, H. P. Hsu, and M. Spector. Effects of a cultured autologous chondrocyte-seeded type II collagen scaffold on the healing of a chondral defect in a canine model. *Journal of Orthopaedic Research*, 21:272–281, 2003.

[42] Anne-Marie Freyria, Marie-Claire Ronzière, Delphine Cortial, Laurent Galois, Daniel Hartmann, Daniel Herbage, and Frédéric Mallein-Gerin. Comparative phenotypic analysis of articular chondrocytes cultured within type I or type II collagen scaffolds. *Tissue Engineering Part A*, 15:1233–1245, 2009.

[43] S. Nehrer, H.A. Breinan, A. Ramappa, H-P. Hsu, T. Minas, S. Shortkroff, C.B. Sledge, I.V. Yannas, and M. Spector. Chondrocyte-seeded collagen matrices implanted in a chondral defect in a canine model. *Biomaterials*, 19:2313–2328, 1998.

[44] Jenny W. Reboredo, Tobias Weigel, Andre Steinert, Lars Rackwitz, Maximilian Rudert, and Heike Walles. Investigation of migration and differentiation of human mesenchymal stem cells on five-layered collagenous electrospun scaffold mimicking native cartilage structure. *Advanced Healthcare Materials*, 5:2191–2198, 2016.

[45] Lu Yuan, Bao Li, Jirong Yang, Yilu Ni, Yingying Teng, Likun Guo, Hongsong Fan, Yujiang Fan, and Xingdong Zhang. Effects of composition and mechanical property of injectable collagen I/II composite hydrogels on chondrocyte behaviors. *Tissue Engineering Part A*, 22:899–906, 2016.

3. INCORPORATION OF AGGRECAN MIMETIC MOLECULES IN COLLAGEN HYDROGELS

The supporting information in this chapter consists of parts of a manuscript by Sharma S, Vazquez-Portalatin N, Calve S, and Panitch A, published in ACS Biomaterials Science & Engineering, Volume 2, Issue 2, 2016.

3.1 Abstract

Articular cartilage tissue engineering efforts aim towards the development of cartilage repair strategies that mimic healthy articular cartilage. In this work, we studied whether an aggrecan mimic, CS-GAH$_b$, composed of chondroitin sulfate (CS) and hyaluronic acid (HA) binding peptides, GAH, and not its separate components, is able to prevent GAG and collagen degradation when incorporated into chondrocyte-embedded collagen gels. Previously, the aggrecan mimic was synthesized using a crosslinker and was named CS-BMPH-GAH. Here, we introduce a new chemistry to synthesize CS-GAH$_b$ without the crosslinker. Bovine chondrocytes were cultured and embedded in collagen type I scaffolds with CS, GAH, CS and GAH, or CS-GAH$_b$ molecules. Gels composed of 3:1 collagen type I and II with CS or CS-GAH$_b$ were also studied. Gels were cultured for 8 days and the media and gels were collected throughout the culture period. GAG and collagen degradation, GAG retention in the gels, and cytokine production were investigated. A preliminary set of gels were used to perform LC-MS/MS and detect the proteins produced by the chondrocytes in the collagen scaffolds. The results obtained showed CS-GAH$_b$ is able to decrease GAG and collagen release and increase GAG retention in the gels. CS-GAH$_b$ also stimulated cytokine production during the initial days of scaffold culture. However, the addition of CS-GAH$_b$ into the chondrocyte embedded collagen scaffolds did not

affect ECM protein expression in the gels. The incorporation of collagen type II into the collagen type I scaffolds did not significantly affect GAG and cytokine production and ECM protein synthesis, but did increase collagen release. The results suggest the complex interaction between CS-GAH$_b$, the chondrocytes, and the gel matrix make these scaffolds promising constructs for articular cartilage repair.

3.2 Introduction

Collagen type I has been extensively studied and used to develop scaffolds for articular cartilage tissue engineering [1–18]. Collagen type I is an attractive material because of its abundant availability [19], biocompatibility [20], wide clinical approval [20–22], and its contribution to chondrocyte proliferation [10, 22, 23]. Collagen type I has, however, a limited chondrogenic ability [4, 20, 22, 24, 25]. Recent constructs have been designed incorporating collagen type II [1, 2, 4, 17, 25–47]. This interest in collagen type II stems from the fact that collagen type II is the major component of the articular cartilage extracellular matrix (ECM) and forms the network of fibrils that contain the ECM proteoglycans [48, 49]. Collagen type II is able to stabilize chondrocyte morphology [1,22,26,28], as well as stimulate chondrogenic differentiation of mesenchymal stem cells (MSCs) and collagen type II synthesis [4, 25, 32, 34, 35, 39, 42, 44, 46]. Similar to collagen type I, collagen type II use in tissue constructs also has drawbacks. Collagen type II is potentially arthritogenic [22, 50, 51] and has limited clinical approval [10, 22].

Proteoglycans are glycoconjugates that have glycosaminoglycan (GAG) side chains attached to a central core protein and contribute 4-7% wet weight of the ECM in articular cartilage [52]. Aggrecan is the largest aggregating proteoglycan present in the ECM and contains CS side chains attached to an HA core protein [53, 54]. All of these components anchor aggrecan within the ECM and, due to their negative charge, provide cartilage with its osmotic properties and resistance to compression confering cartilage some of its mechanical properties [55, 56]. Aggrecan has also been

shown to protect collagen type II from degradation [57, 58]. However, aggrecan contains proteolytic cleavage sequences that are attacked by proteinases such as matrix metalloproteinases (MMPs) and aggrecanases during cartilage degradation present in osteoarthritis (OA) [53, 59].

Articular cartilage tissue engineering efforts aim towards the development of cartilage repair strategies that mimic articular cartilage. Past works have studied GAG interaction [6,7,17,26,28,60–62] and incorporation into collagen type I gels [6,7,16,17, 26, 28, 61–64] as well as GAG effects on chondrocyte cultures [16, 26, 28, 64, 65]. GAG incorporation and production in scaffolds containing collagen type II have also been studied [17, 26, 28, 29, 36, 40]. Several groups have constructed chondrocyte seeded collagen type II scaffolds with CS and demonstrated their superior ability to stimulate GAG synthesis and preserve chondrocyte morphology in comparison to collagen type I gels [26, 28]. We previously prepared 3:1 collagen type I and II collagen gels and demostrated their ability to retain GAGs [17].

Previously, our lab designed and synthesized an aggrecan mimic (CS-BMPH-GAH) composed of HA binding peptides attached to a CS backbone [66] via a heterobifunctional crosslinker N- (β-Maleimidopropionic acid) hydrazide, trifluoroacetic acid salt (BMPH). This molecule was able to bind to HA in solution and significantly increase the storage modulus when compared to CS and HA solutions [66]. When incorporated in collagen type I constructs with HA, these molecules also showed an increase in compressive strength in contrast to collagen type I only gels and collagen type I gels with HA and CS [12, 66]. Additionally, these gels with CS-BMPH-GAH were shown to significantly reduce collagen and HA degradation in the presence of hyaluronidase and MMP-1 [66]. Sharma *et al* further examined the efficacy of these aggrecan mimics in *ex vivo* and *in vivo* OA models [67]. In an OA environment, these molecules were able to prevent CS degradation and lower cytokine IL-1β production in human OA synovial fluid *ex vivo* models. In *in vivo* rat models, the aggrecan mimic was able to preserve GAG and cartilage in articular cartilage tissue sections

from rat knee joints [67]. These results suggest CS-BMPH-GAH molecules are able to functionally mimic aggrecan [12, 66].

Even though Sharma *et al* studied these molecules in collage type I gels and their effects on chondrocytes, the effects of the separate components and the assembled molecule were not compared. In the work described herein, we synthesized the CS-BMPH-GAH molecule using a new chemistry that does not require the BMPH crosslinker and labeled the new molecule as CS-GAH$_b$. We further studied the effects of the CS-GAH$_b$ molecule and its separate components on chondrocytes embedded in collagen type I constructs. Furthermore, we also studied the effects of the addition of collagen type II to the chondrocyte embedded collagen type I gels with CS or CS-GAH$_b$.

3.3 Materials and Methods

3.3.1 Peptide Synthesis

A hyaluronic acid (HA) binding peptide sequence (GAHWQFNALTVR) [68] was modified to include a GSG spacer and a hydrazide group at the C terminus resulting in a modified peptide with a GAHWQFNALTVRGSG-$NHNH_2$ sequence (Figure 3.1). The modified HA binding peptide was obtained from InnoPep (San Diego, CA). The synthesis of a biotinylated version of the modified HA-binding peptide was loosely based on the method described by Zheng *et al* (Figure 3.1A) [69]. The non-biotinylated and the biotinylated HA-binding peptides were labeled GAH (Figure 3.1B) and GAH$_b$, respectively, for the rest of the work discussed herein.

Resin Modification

Resin was modified with a hydrazide group according to previous work [69]. Briefly, 1 g of 2-Chlorotrityl chloride (2-ClTrt) resin with a 1.52 mmol/g loading was washed and allowed to swell in 50% (v/v) dichloromethane (DCM)/ dimethyl-

formamide (DMF) for 1 h. The resin was then modified with 10 mL of 10.8% (v/v) hydrazine hydrate and 100 μL of N,N-diisopropylethylamine (DIPEA) and left to react for 2 h at room temperature. The resin was drained and left to react for another hour with 10 mL of 10.8% (v/v) hydrazine hydrate and 100 μL of DIPEA to ensure hydrazine hydrate coupling. After modifying the resin with a hydrazide group, 10 mL of 10% (v/v) methanol and DMF were added to the resin and allowed to shake for 30 min. Glycine, the first amino acid, along with ethyl(hydroxyimino)cyanoacetate (Oxyma Pure) were dissolved in DMF and added to the modified resin. DIPEA and N,N'-diisopropylcarbodiimide (DIC) were also added to the resin with a 4 M excess. After coupling the glycine to the resin overnight, more glycine with Oxyma Pure, DIC, and DIPEA were added to the resin to ensure full coupling of the first amino acid. The modified resin was washed, dried with DCM, and stored at $-80\,^{\circ}$C until further use.

GAH Automated Peptide Synthesis

A 0.1 mmol of the modified glycine-$NHNH_2$ 2-ClTrt resin was weighed and placed into the reaction vessel of a Liberty Blue peptide synthesizer (CEM Corportation, Matthews, NC). Next, 0.1 mmol of the necessary amino acids were weighed, dissolved in DMF to a 0.2 M final concentration, and placed in their corresponding positions on the instrument. The resin was allowed to swell in DMF and was then deprotected with 20% piperidine using 30 W microwave power at 60 °C for 3 min. The resin was washed with DMF three times before adding 2.5 mL of the amino acid, 1 mL of the activator (DIC), and 0.5 mL of the activator base (Oxyma Pure). The first five amino acids were coupled at 50 °C for 40 min, except for arginine. The other nine amino acids were coupled at 50 °C for 1 h. Due to arginine-arginine interactions, the amino acid was double coupled at 50 °C for 1 h for each coupling step. After each amino acid coupling, the resin was washed with DMF and deprotected with piperidine. Finally, the resin was washed with DMF and the peptide sequence was deprotected one last

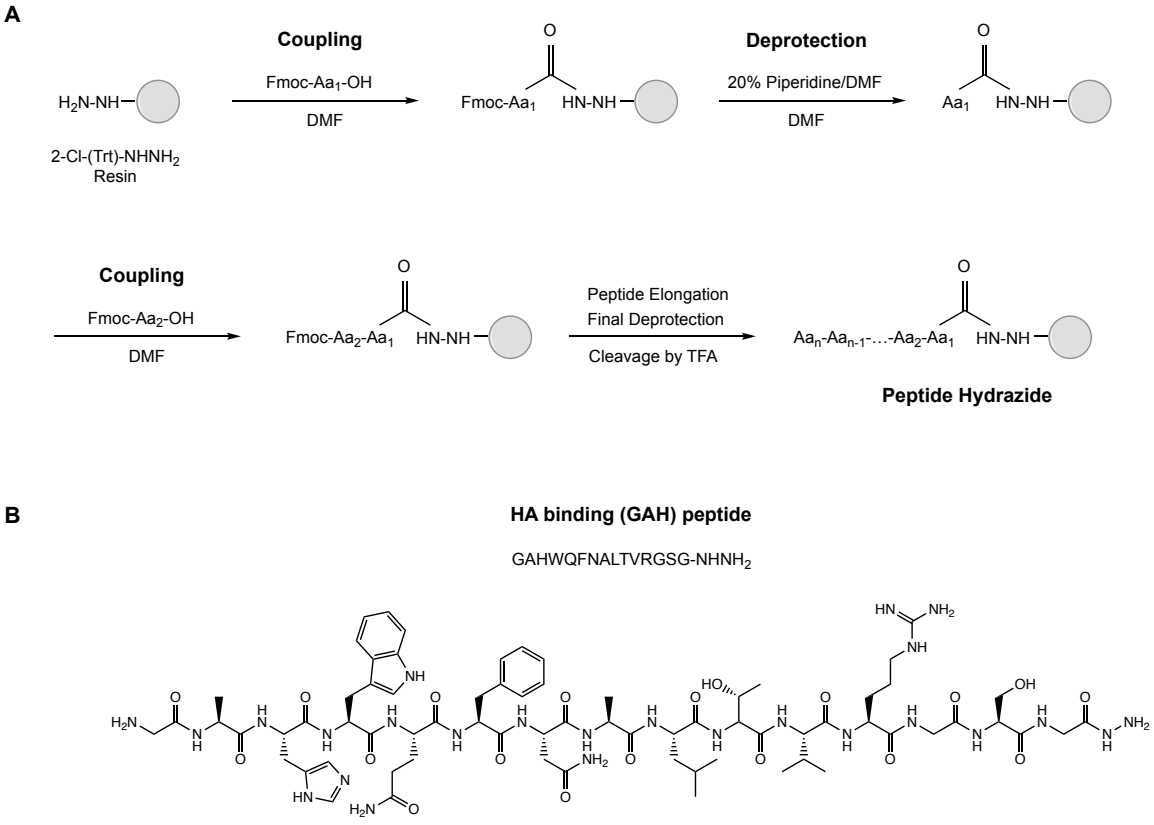

Figure 3.1.: Illustrations of (A) the peptide synthesis process with a hydrazide-modified resin and (B) the synthesized HA binding peptide with a hydrazide group. Modified from Zheng *et al* [69].

time (Figure 3.1A). Once the synthesis was done, the resin with the attached peptide was collected into a 10 mL disposable polypropylene column, washed with DMF and DCM, and dried.

Peptide Biotinylation

After synthesis, the GAH peptide 3.1B) and resin were washed with DMF. Biotin was dissolved to 1 mM in 5 mL of a 1:1 DMF to dimethyl sulfoxide (DMSO) solution. Once dissolved, 2.1 mL of a 0.45 M (2-(1H-benzotriazol-1-yl)-1,1,3,3- tetramethyluronium hexafluorophosphate (HBTU)/hydroxybenzotriazole (HOBt) solution and 0.3

mL of DIPEA were added to the biotin solution. The activated biotin solution was added to the resin and allowed to couple to the peptide overnight. A ninhydrin test was performed to ensure the coupling was complete. The resin was washed three times with 1:1 DMF:DMSO to remove the uncoupled biotin. Afterwards, the resin was washed twice with DMF and two more times with DCM. Finally, the resin was allowed to dry prior to cleavage.

Peptide Cleavage

The biotinylated peptide with the hydrazide group was cleaved from the resin by reacting it for 2 h while shaking with 3 mL of a trifluoroacetic acid (TFA) cocktail consisting of 88% (v/v) TFA, 5% (w/v) phenol, 5% (v/v) H_2O, and 2% (v/v) triisopropylsilane (TIPS) [69]. The cleaved peptide was filtered and collected into a 50 mL conical tube. The resin was washed two more times with the TFA cocktail and the filtrate was collected into the tube. Cold diethyl ether was added to the filtrate to precipitate the crude peptide. The peptide was then centrifuged at 3,000g for 5 min at room temperature. The supernatant was decanted and the crude peptide, with diethyl ether, was centrifuged two more times. The crude petide was allowed to air dry before purification.

Peptide Purification

The crude GAH_b peptide was dissolved in 10% acetonitrile (ACN) in H_2O and purified on an ÄKTA Pure FPLC (GE Healthcare Bio-Sciences, Pittsburgh, PA) with a C18 prep protein column packed with 5μm silica particles (AAPTEC, Louisville, KY) and an ACN gradient with 0.1% TFA. Peptide molecular weight was confirmed by matrix-assisted laser desorption ionization time-of-flight (MALDI TOF) mass spectrometry with a Bruker UltraFlextreme analyzer (Bruker Daltonics Inc., Billerica, MA).

3.3.2 Peptidoglycan Synthesis

The synthesis of the CS-GAH$_b$ molecules was modified from the one described by Bernhard *et al* [66]. The peptides were conjugated to a chondroitin sulfate (CS) (Seikagaku, Tokyo, Japan) backbone via an amide bond using a new DMTMM (4-(4,6-dimethoxy-1,3,5-triazin-2-yl)-4-methyl-morpholinium chloride) chemistry (Figure 3.2) [70]. Briefly, the CS was dissolved in 0.1 M 2-(N-morpholino)ethanesulfonic acid (MES) buffer (pH 4.5). To activate the carboxyl groups in the backbone, 184.48 μL of 0.27 M DMTMM were used to react the CS for 5 min at room temperature. After the CS solution was activated, 1 mole of the GAH$_b$ peptide per 1 mole of CS were dissolved to 10 mg/mL in 0.1 M MES buffer and added to the activated CS to functionalize it. The solution was allowed to react in a shaker for 12 h at room temperature. Once the biotinylated peptide had been conjugated to the CS backbone, an average of 10.5 moles of the GAH peptide per 1 mole of CS were added to the molecule solution and allowed to react in a shaker for 60 h at room temperature. The solution was filtered via a KR2i KrosFlo tangential flow filtration system (Repligen, Waltham, MA) with a modified polyethersulfone (mPES) hollow fiber filter with a 10kD MWCO. Our lab had previously described these peptide conjugated sugar backbone molecules as peptidoglycans. The CS-GAH$_b$ peptidoglycans were frozen, lyophilized, and stored at $-80\,^{\circ}$C for later use.

3.3.3 Peptide Quantification

The final concentration of peptides attached to the CS backbone was quantified using a Pierce Quantitative Colorimetric Peptide Assay (Thermo Scientific, Waltham, MA) in a SpectraMax M5 Multimode Microplate Reader (Molecular Devices, Sunnyvale, CA). This assay was used to quantify the GAH peptide concentration attached to the CS backbone via colorimetric absorbance of a copper complex reduced by the amide bonds present in the sample. Briefly, 20 μL of the CS-GAH$_b$ molecule and 180 μL of the working reagent were combined into a 96-well plate and left shaking

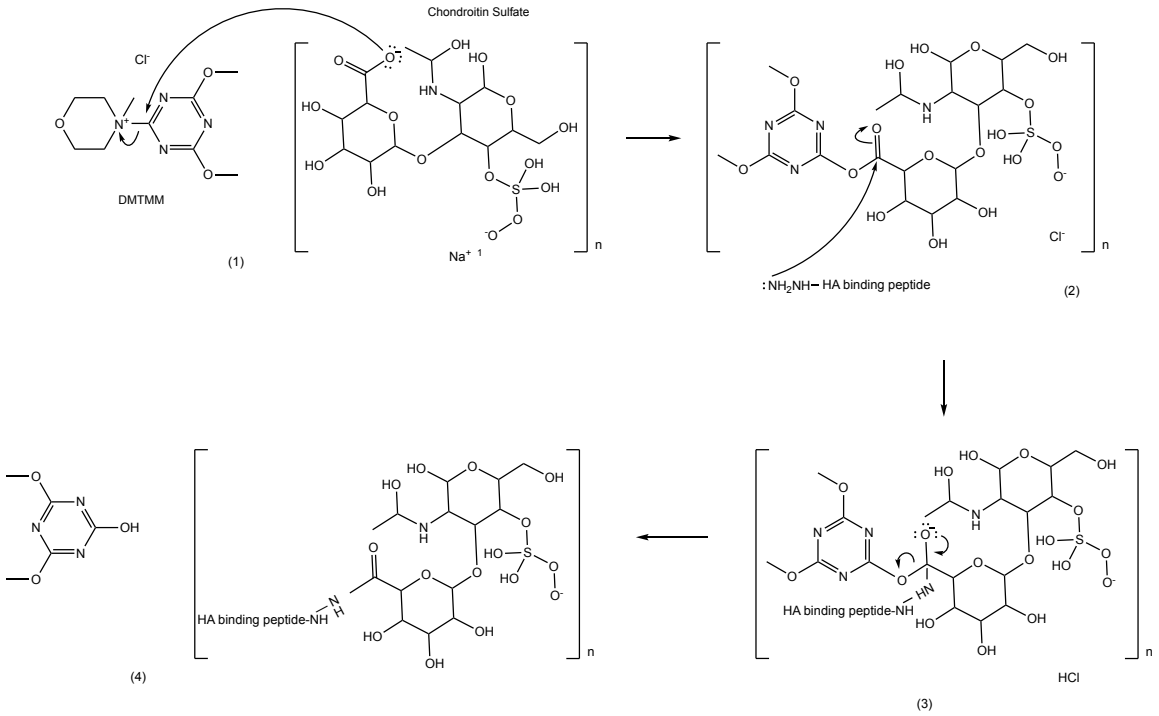

Figure 3.2.: Peptidoglycan synthesis via DMTMM chemistry. The molecule synthesis starts with a (1) nucleophilic attack of the carboxylic group in CS on the triazine part of DMTMM. This attack forms (2) an ester bond between the CS and DMTMM. The nucleophilic amine on the HA binding peptide then attacks the ester's carboxylic carbon to form (3) an amide bond. This reaction results in the (4) attachment of HA binding peptides to the CS backbone.

for a minute. The plate was then incubated at 37 °C for 15 min. The absorbance of the samples was measured at 480 nm. A GAH peptide standard curve was used to calculate the peptide concentration in the samples.

3.3.4 Chondrocyte Isolation and Culture

Fetal bovine chondrocytes were isolated from bovine knees obtained from an abattoir (Animal Technologies, Tyler, TX) as described by Sharma [12]. Cartilage was harvested from the knees using a scalpel and washed with 1x PBS three times before slicing it into smaller pieces. The cartilage was then added to 50 mL conical tubes with 25 mL of DMEM/F12 medium containing 0.1% bovine serum albumin (BSA), 0.2% (w/v) collagenase P, 100 units/mL penicillin, 100 μg/mL streptomycin, and 3% fetal bovine serum (FBS). The cartilage was degraded by incubating the tubes in a shaker at 37 °C and 230 rpm for 2 h. Afterwards, 10 mL of 10% FBS DMEM/F12 containing 0.1% BSA, 25 mM HEPES, 100 units/mL penicillin, 100 μg/mL streptomycin, and 50 μg/mL ascorbic acid 2-phosphate were added to the degraded cartilage. The samples were then filtered using a sterile 70 μm cell strainer to release the chondrocytes in the solution. The chondrocytes were washed by centrifuging them at 1,000 rpm for 5 min. The supernatant was decanted and the pellet was resuspended in 10 mL of 10% FBS DMEM/F12. The chondrocytes were washed two more times before counting them with 0.4% (w/v) Trypan Blue and resuspending them in chondrocyte growth medium supplemented with growth medium supplement mix (PromoCell GmbH, Heidelberg, Germany), 100 units/mL penicillin, and 100 μg/mL streptomycin. The cells were then cultured in flasks with an initial seeding density of 10,000 cells/cm^2, and incubated at 37 °C and 5% CO_2 in a humidified incubator. The medium was changed 24 h after the inital plating and then every 2 days.

3.3.5 Chondrocyte-embedded Collagen Gels Preparation

Collagen gels were prepared similarly to work previously done in our lab [17]. Stock solutions of rat tail collagen type I (BD Biosciences, Franklin Lakes, NJ) and chicken sternal collagen type II (Millipore Sigma, Saint Louis, MO) were prepared in 20 mM acetic acid at a concentration of 5 mg/mL. The pH of the collagen solutions was raised to 7.4 with the addition of 10x PBS and 1 M NaOH. The final concentrations of the collagen solutions were brought to 4 mg/mL with the addition of HA and the corresponding glycosaminoglycan (GAG) in 1x PBS. The gels prepared consisted of 1:0 or 3:1 collagen type I to collagen type II ratio with 0.2 mg/mL of added hyaluronic acid (HA). HA (1.5 - 1.8 x 10^6 Da) (Millipore Sigma, Saint Louis, MO) was dissolved in 1x PBS to 10 mg/mL. The GAG (e.g. CS or CS-GAH_b) and GAH peptide stock solutions were dissolved in 1x PBS to a final concentration of 65 mg/mL. Gels were made with CS, GAH, both CS and GAH, or CS-GAH_b at a final concentration of 47 μM of added CS or peptidoglycan.

Controls were prepared without GAGs or peptide. The isolated fetal bovine chondrocytes were added to stock solutions of either 1:0 or 3:1 collagen type I to collagen type II at a final concentration of 5 x 10^5 cells/mL. These components were gently mixed to avoid bubbles in the solutions. Gels with a final volume of 100 μL were allowed to polymerize in a 96-well plate for 2 h at 37 °C in a 5% CO_2 humidified incubator [71]. After polymerization, 150 μL of chondrocyte growth medium were added to each gel and gels were allowed to equilibrate for 3 days. The experimental design for this study is shown in Table 3.1. The culture medium was collected two days after gel polymerization and was labeled as day -1. The third and last day of equilibration was termed as day 0. The culture medium containing the GAGs, collagen, and proteins released from the gels was collected and replaced every 2 days for 8 days. Gels for GAG retention were collected at days 0, 4, and 8 and stored in 150 μL of RNA later at -80 °C until further testing.

Gels for preliminary proteomic analysis were synthesized with or without CS-GAH_b. These constructs were prepared with 3:1 collagen type I to collagen type II blends, except for the control samples. These gels were also cultured for 21 days and were collected at days 0, 7, and 21. The gels prepared and collected were: Control Day 0, 3:1 Control Day 0, Control Day 7, 3:1 CS-GAH_b Day 7, and 3:1 CS-GAH_b Day 21. Once collected, the gels were stored in 150 μL of RNA later at $-80\,^{\circ}$C until testing.

Table 3.1.: Experimental design for the chondrocyte-embedded collagen gels.

	Collagen (mg/mL)		HA	Molecules (mg/mL)		
Samples	Type I	Type II	(mg/mL)	CS	GAH	CS-GAH_b
Control	4	-	0.2	-	-	-
CS	4	-	0.2	1.88	-	-
GAH	4	-	0.2	-	0.07	-
CS, GAH	4	-	0.2	1.88	0.07	-
CS-GAH_b	4	-	0.2	-	-	2.60
3:1 CS	3	1	0.2	1.88	-	-
3:1 CS-GAH_b	3	1	0.2	-	-	2.60

3.3.6 Gel Digestion

Gels needed for GAG retention analysis were digested in a papain solution as described previously [72]. A papain digestion buffer was prepared with 125 μg/mL papain, 5 mM L-cysteine, 100 mM sodium phosphate monobasic (NaH_2PO_4), and 5 mM ethylenediaminetetraacetic acid (EDTA) and pH at 6.5. The lyophilized gels were placed in microcentrifuge tubes and 110 μL of the papain digestion buffer were added to each sample. The gels were incubated at $60\,^{\circ}$C for 24 h followed by $100\,^{\circ}$C for 10 min. Afterwards, the gels were centrifuged, frozen at $-80\,^{\circ}$C, and lyophilized. The gels were then resuspended in 110 μL of ultrapure water for further analysis.

3.3.7 Glycosaminoglycan Retention and Release

GAG release was detected by measuring the amount of CS and CS-GAH$_b$ released into the cell culture media as previously described [73]. Briefly, 20 μL of sample were added to a well in a 96-well plate and 180 μL of dimethylmethylene blue (DMMB) dye solution were added to each sample. The absorbance was measured at 525 nm. CS and CS-GAH$_b$ standard curves were used to obtain the GAG concentrations in the samples. GAG release is reported as day to day release from days -1 and 0. Data presented at days 4 and 8 is reported as cumulative release from days 2 and 4 and days 6 and 8, respectively. GAG retention in the gels was detected by measuring the amount of CS and CS-GAH$_b$ present in the digested gel samples collected at days 0, 4, and 8.

3.3.8 Collagen Release

The amount of collagen released into the cell culture medium was measured with a Sircol Collagen Assay (Biocolor, Carrickfergus, United Kingdom). Briefly, 50 μL of medium sample were combined with 50 μL of chondrocyte growth medium and 1 mL of Sircol dye reagent to fully saturate the collagen molecules. The samples were placed in a mechanical shaker for 30 min to allow the collagen-dye complex to precipitate out of the solution. The samples were then centrifuged and the supernatants were removed. The unbound dye was removed by adding 750 μL of an acid-salt wash reagent to each sample followed by centrifugation and supernatant removal. For each sample, the collagen bound dye was dissolved in 250 μL of alkali reagent. 200 μL of the samples were transferred to a 96-well plate and the absorbance was measured at 555 nm. A collagen standard curve was used to obtain the collagen concentrations in the samples. Collagen release was measured from media collected at days -1 and 0. Measurements for days 4 and 8 is reported as cumulative release from days 2 and 4 and days 6 and 8, respectively.

3.3.9 Cytokine Release

Culture medium obtained from the chondrocyte embedded collagen gels were used to analyze interleukin-6 (IL-6) and tumor necrosis factor α (TNF-α) release. The cytokines were measured with DuoSet ELISA kits (R&D Systems, Minneapolis, MN) according to manufacturer's instructions. Briefly, 96-well plates were incubated overnight with 100 μL/well of diluted capture antibody at room temperature. The wells were washed three times with 0.05% Tween 20 in PBS and were blocked with 300 μL of 5% Tween 20 in PBS for 1 h. The plates were washed once again before 100 μL per sample were added. The samples were incubated for 2 h at room temperature and washed before 100 μL/well of the detection antibody were added. The plates were incubated for another 2 h before washing and adding 100 μL/well of the Streptavidin-HRP solution. The samples were incubated in the dark for 20 min. The plates were washed once again and 100 μL/well of the Substrate Solution were added. The plates were then incubated in the dark for 20 min. Afterwards, 50 μL/well of the 2N H_2SO_4 stop solution were added. Finally, the optical density of these samples were measured at 450 nm and 540 nm. The values with wavelength correction were obtained by substracting the 540 nm readings from the readings at 450 nm. Standard curves were prepared with bovine IL-6 and TNF-α. Cytokine release is reported as day to day release from days -1 and 0. Data presented at days 4 and 8 is reported as cumulative release from days 2 and 4 and days 6 and 8, respectively.

3.3.10 Proteomics Analysis

The frozen chondrocyte-embedded collagen gels stored in RNA later for proteomic analysis were reduced, alkylated and extracted following a modified protocol based on previous work done by Savaliev *et al* [74]. Briefly, the gels were cut into $\sim$1 mm^3 bands and placed into microcentrifuge tubes. The gels were washed three times with 150 μL of 50 mM ammonium bicarbonate (AMBIC) and dehydrated by washing them three more times with ACN while shaking. The ACN was discarded and the gels

were rehydrated in 10 mM dithiothreitol (DTT) in 50 mM AMBIC and incubated for 30 min at 56 °C to reduce the disulfide bonds in the protein. The gel pieces were dehydrated in ACN three times. The ACN was replaced with 150 μL 55 mM iodoacetamide (IAA) in 50 mM AMBIC and incubated for 20 min in the dark at room temperature. The gels were washed twice with 200 μL of 50 mM AMBIC and then dehydrated with four ACN washes. The dehhydrated gels were rehydrated in 150 μL of 6.2 mg/mL trypsin in 50 mM AMBIC and digested overnight at 37 °C.

After digestion, the supernatants were collected into new microcentrifuge tubes. Peptides were extracted from the gel pieces by sonicating them in a water bath for 10 min in a 60% ACN and 0.1% TFA solution and centrifuging them for 10 min. The supernatants were collected and combined with the supernatants collected previously. The mixture was dried in a speed vac until there were 10 μL of liquid left.

The digested gels were analyzed by liquid chromatography-mass spectrometry (LC-MS/MS) on a Thermo Scientific Q Exactive Plus Orbitrap mass spectrometer as previously described [75]. The spectral data obtained from the MS/MS were searched with Uniprot Bovine Proteome database, a database of common laboratory contaminants (www.thegpm.org/ crap) and an equal number of reverse decoy sequences, employing X! Tandem (The GPM, thegpm.org; version X! Tandem Alanine). Scaffold (version Scaffold_4.8.9, Proteome Software Inc., Portland) was used to corroborate the peptide and proteins identified. An overall peptide decoy FDR of 1.0% and a protein decoy FDR of 0.12% were used as thresholds. Proteins that contained similar peptides and were not differentiated based on MS/MS analysis were clustered.

3.3.11 Statistics

The data are represented as a mean with error bars corresponding to standard deviation. Statistical significance was analyzed with two way analysis of variance (ANOVA) and Tukey's *post hoc* tests with α=0.05. Each experiment was repeated twice with $n \geq 3$ in each data set, except for the proteomics analysis. Data presented

here were obtained from one of the experiment runs. Preliminary proteomics analysis were performed once with n=2.

3.4 Results

3.4.1 Peptidoglycan synthesis and peptide quantification

The GAH and GAH$_b$ peptides, along with CS, were used to synthesize CS-GAH$_b$, an HA binding molecule that mimics aggrecan. Previously, Bernhard *et al* [66] designed and synthesized this molecule through oxidation chemistry using N-(β-Maleimidopropionic acid) hydrazide, trifluoroacetic acid salt (BMPH) as a heterobifunctional crosslinker to attach the GAH peptides to the CS backbone. In this work, DMTMM chemistry was used to synthesize the molecules because it is inexpensive, does not require a crosslinker addition, and requires less steps than the BMPH chemistry [70]. Molecules synthesized with this new chemistry appear to behave similarly to those made through oxidation chemistry. With DMTMM chemistry (Figure 3.2), an average of 9.6 moles of the GAH peptide were attached per 1 mole of the CS backbone.

3.4.2 CS-GAH$_b$ decreases GAG release into media and increases GAG retention in the gels

We previously diffused HA binding (CS-BMPH-GAH) and collagen II binding (CS-BMPH-WYRGRL) molecules through normal and aggrecan depleted bovine cartilage explants as described in Section 3.8 [76]. They showed the amount of CS released into cell culture media decreased considerably over the course of the 21 day culture period and used the cumulative amount of CS seen in culture media over a period of 7 days for assessment (Figure S 3.9A). The amount of CS released from the ECM into the culture was significantly lower for explants that were treated with CS-BMPH-GAH as compared to explants that were aggrecan depleted and left untreated ($p < 0.01$).

No significant difference was seen for explants treated with CS-BMPH-WYRGRL or CS-BMPH-GAH+CS-BMPH-WYRGRL (Figure S3.9B). Based on these results, we further studied the effects of the CS-GAH molecule and its separate components on chondrocytes embedded in collagen type I constructs. Furthermore, we also studied the effects of the addition of collagen type II to the chondrocyte embedded collagen type I gels.

The amount of GAGs released from the collagen type I gels into the culture decreased over the course of the 8 day culture period (Figure 3.3A). At day -1, the amount of GAGs released from the gels into the culture was significantly higher for gels with only CS when compared to the rest of the gels (Figure 3.3C). The gels containing CS-GAH$_b$ had an initial significantly lower GAG release than the other gels containing CS. Control and GAH peptide gels had a significantly lower GAG release than the gels initially prepared with CS-GAH$_b$ or CS. No significant difference was observed among the gels at days 4 and 8.

GAGs released from the collagen I and 3:1 collagen I and II gels with added CS or CS-GAH$_b$ decreased over the course of the 8 day culture period as well (Figure 3.3B). At days -1 and 0, the amount of GAGs released from the CS-GAH$_b$ and 3:1 CS-GAH$_b$ gels were significantly lower than those released by gels containing CS (Figure 3.3D). However, the amount of GAGs released from the CS-GAH$_b$ gels was not significantly different from the amount released by the 3:1 CS-GAH$_b$ gels. No significant difference was observed among the gels at days 4 and 8. The GAG release differences observed were between gels containing CS or CS-GAH$_b$. The addition of collagen type II into the gels did not seem to make a difference when compared to the collagen type I only gels.

The amount of GAGs retained in the collagen type I gels remained constant for the control gels and the gels containing GAH peptide only (Figure 3.4A). However, the amount of GAGs retained in the gels decreased for the rest of the gels over the course of the 8 day culture period. While the initial GAG concentration retained was similar among the CS, CS and GAH, and CS-GAH$_b$ gels, the CS-GAH$_b$ gels were

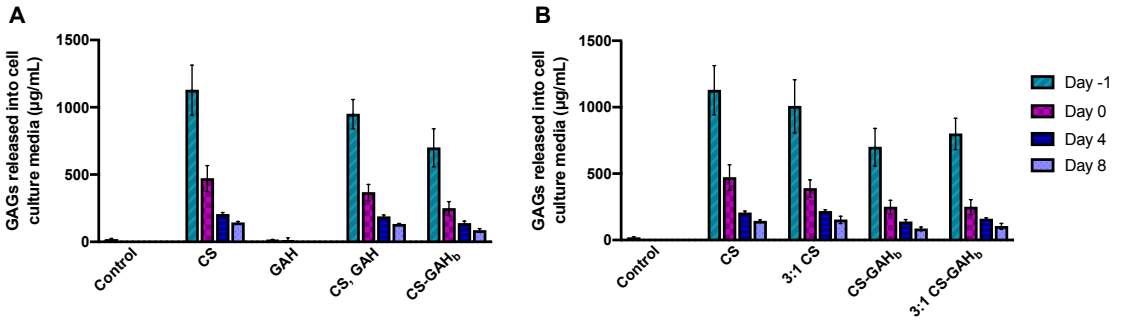

C

		Day -1					Day 0					Day 4					Day 8				
		Control	CS	GAH	CS,GAH	CS-GAH$_b$	Control	CS	GAH	CS,GAH	CS-GAH$_b$	Control	CS	GAH	CS,GAH	CS-GAH$_b$	Control	CS	GAH	CS,GAH	CS-GAH$_b$
Day -1	Control	-	*<0.0001*	>0.9999	*<0.0001*	*<0.0001*	>0.9999	*<0.0001*	>0.9999	*<0.0001*	*0.0332*	>0.9999	0.7663	>0.9999	0.8940	0.9988	>0.9999	0.9976	>0.9999	0.9995	>0.9999
	CS		-	*<0.0001*	*0.0022*	*<0.0001*		*<0.0001*	*<0.0001*	*<0.0001*	*<0.0001*		*<0.0001*	*<0.0001*	*<0.0001*	*<0.0001*		*<0.0001*	*<0.0001*	*<0.0001*	*<0.0001*
	GAH			-	*<0.0001*	*<0.0001*			>0.9999	*0.0017*	0.2917			>0.9999	0.9763	0.9999			>0.9999	>0.9999	>0.9999
	CS,GAH				-	*<0.0001*				*<0.0001*	*<0.0001*				*<0.0001*	*<0.0001*				*<0.0001*	*<0.0001*
	CS-GAH$_b$					-					*<0.0001*					*<0.0001*					*<0.0001*
Day 0	Control		*<0.0001*	>0.9999	*<0.0001*	*<0.0001*	-	*<0.0001*	>0.9999	*<0.0001*	0.0640	>0.9999	0.7512	>0.9999	0.8757	0.9971	>0.9999	0.9949	>0.9999	0.9985	>0.9999
	CS			*<0.0001*	*<0.0001*	*0.0126*		-	*<0.0001*	0.9991	0.1755		0.2129	*<0.0001*	0.1248	*0.0186*		*0.0232*	*<0.0001*	*0.0143*	*0.0016*
	GAH				*<0.0001*	*<0.0001*			-	*0.0001*	0.1025			>0.9999	0.9291	0.9992			>0.9999	0.9997	>0.9999
	CS,GAH					*<0.0001*				-	0.9920				0.9084	0.5041				0.4475	0.1297
	CS-GAH$_b$										-					>0.9999					0.9679
Day 4	Control		*<0.0001*	>0.9999	*<0.0001*	*<0.0001*		*<0.0001*	>0.9999	*0.0042*	0.3516	-	0.9255	>0.9999	0.9716	0.9997	>0.9999	0.9995	>0.9999	0.9999	>0.9999
	CS			0.9312	*<0.0001*	*<0.0001*			0.8343	0.9684	>0.9999		-	0.9255	>0.9999	>0.9999		>0.9999	0.9255	>0.9999	>0.9999
	GAH				*<0.0001*	*<0.0001*				*0.0042*	0.3516			-	0.9716	0.9997			>0.9999	0.9999	>0.9999
	CS,GAH					*<0.0001*					>0.9999				-	>0.9999				>0.9999	>0.9999
	CS-GAH$_b$															-					>0.9999
Day 8	Control		*<0.0001*	>0.9999	*<0.0001*	*<0.0001*		*<0.0001*	>0.9999	*0.0042*	0.3516		0.9255	>0.9999	0.9716	0.9997	-	0.9995	>0.9999	0.9999	>0.9999
	CS			0.9997	*<0.0001*	*<0.0001*			0.9985	0.5541	>0.9999			0.9995	>0.9999	>0.9999		-	0.9995	>0.9999	>0.9999
	GAH				*<0.0001*	*<0.0001*				*0.0042*	0.3516				0.9716	0.9997			-	0.9999	>0.9999
	CS,GAH					*<0.0001*					0.9998					>0.9999				-	>0.9999
	CS-GAH$_b$																				-

D

		Day -1					Day 0					Day 4					Day 8				
		Control	CS	3:1 CS	CS-GAH$_b$	3:1 CS-GAH$_b$	Control	CS	3:1 CS	CS-GAH$_b$	3:1 CS-GAH$_b$	Control	CS	3:1 CS	CS-GAH$_b$	3:1 CS-GAH$_b$	Control	CS	3:1 CS	CS-GAH$_b$	3:1 CS-GAH$_b$
Day -1	Control	-	*<0.0001*	*<0.0001*	*<0.0001*	*<0.0001*	>0.9999	*<0.0001*	*<0.0001*	*0.0332*	*0.0332*	>0.9999	0.7663	0.6562	0.998	0.9857	>0.9999	0.9976	0.9927	>0.9999	>0.9999
	CS		-	0.2782	*<0.0001*	*<0.0001*		*<0.0001*	*<0.0001*	*<0.0001*	*<0.0001*		*<0.0001*	*<0.0001*	*<0.0001*	*<0.0001*		*<0.0001*	*<0.0001*	*<0.0001*	*<0.0001*
	3:1 CS			-	*<0.0001*	*<0.0001*			*<0.0001*	*<0.0001*	*<0.0001*			*<0.0001*	*<0.0001*	*<0.0001*			*<0.0001*	*<0.0001*	*<0.0001*
	CS-GAH$_b$				-	0.6884				*<0.0001*	*<0.0001*				*<0.0001*	*<0.0001*				*<0.0001*	*<0.0001*
	3:1 CS-GAH$_b$					-					*<0.0001*					>0.9999					*<0.0001*
Day 0	Control		*<0.0001*	*<0.0001*	*<0.0001*	*<0.0001*	-	*<0.0001*	*<0.0001*	0.0640	0.0639	>0.9999	0.7512	0.6484	0.9971	0.9774	>0.9999	0.9949	0.9871	>0.9999	>0.999
	CS			*<0.0001*	*0.0126*	*<0.0001*		-	>0.9999	0.1755	0.1755		0.2129	0.2913	*0.0186*	*0.0457*		*0.0232*	*0.0348*	*0.0016*	*0.0041*
	3:1 CS				*<0.0001*	*<0.0001*			-	0.9405	0.9405			0.9392	0.3143	0.5095			0.4445	0.0611	0.1182
	CS-GAH$_b$					*<0.0001*				-	>0.9999				>0.9999	>0.9999				0.9679	0.9932
	3:1 CS-GAH$_b$										-					>0.9999					0.9932
Day 4	Control		*<0.0001*	*<0.0001*	*<0.0001*	*<0.0001*		*<0.0001*	*0.0015*	0.3516	0.3515	-	0.9255	0.8757	0.9997	0.9968	>0.9999	0.9995	0.9984	>0.9999	>0.9999
	CS			*<0.0001*	*<0.0001*	*<0.0001*			0.8868	>0.9999	>0.9999		-	>0.9999	>0.9999	>0.9999		>0.9999	>0.9999	>0.9999	>0.9999
	3:1 CS				*<0.0001*	*<0.0001*				>0.9999	>0.9999			-	>0.9999	>0.9999			>0.9999	0.9999	>0.9999
	CS-GAH$_b$					*<0.0001*					>0.9999				-	>0.9999				>0.9999	>0.9999
	3:1 CS-GAH$_b$															-					>0.9999
Day 8	Control		*<0.0001*	*<0.0001*	*<0.0001*	*<0.0001*		*<0.0001*	*0.0015*	0.3516	0.3515		0.9255	0.8757	0.9997	0.9968	-	0.9995	0.9984	>0.9999	>0.9999
	CS			*<0.0001*	*<0.0001*	*<0.0001*			0.3567	>0.9999	>0.9999			>0.9999	>0.9999	>0.9999		-	>0.9999	>0.9999	>0.9999
	3:1 CS				*<0.0001*	*<0.0001*				>0.9999	>0.9999				>0.9999	>0.9999			-	>0.9999	>0.9999
	CS-GAH$_b$					*<0.0001*					0.9678					>0.9999				-	>0.9999
	3:1 CS-GAH$_b$																				-

Figure 3.3.: GAGs released from collagen gels into cell culture media over an eight day culture period. GAG release was measured every 2 days and is shown as day to day measurements for days -1 and 0. For days 4 and 8, data is reported as cumulative measurements from days 2 and 4 and days 6 and 8, respectively. GAG loss was measured by a DMMB assay. GAGs released from chondrocyte embedded (A) collagen I gels with added CS, GAH, CS and GAH, or CS-GAH$_b$ and (B) collagen I and 3:1 collagen I and collagen II gels with added CS or CS-GAH$_b$ were analyzed. P-values obtained from Tukey's *post hoc* tests denote statistical significance (red) between the (C) collagen I gels and (D) collagen I and II blend gels (α=0.05). Bars represent average $\pm$ standard deviation ($n \geq 3$).

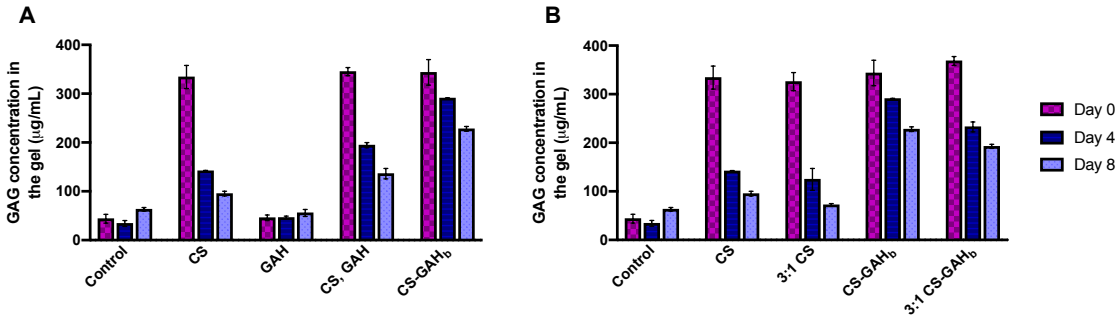

C

		Day 0					Day 4					Day 8				
		Control	CS	GAH	CS,GAH	CS-GAH$_b$	Control	CS	GAH	CS,GAH	CS-GAH$_b$	Control	CS	GAH	CS,GAH	CS-GAH$_b$
Day 0	Control	-	*<0.0001*	>0.9999	*<0.0001*	*<0.0001*	>0.9999	*<0.0001*	>0.9999	*<0.0001*	*<0.0001*	0.8838	*0.0001*	0.9994	*<0.0001*	*<0.0001*
	CS		-	*<0.0001*	0.9971	0.9996		*<0.0001*	*<0.0001*	*<0.0001*	*0.0031*		*<0.0001*	*<0.0001*	*<0.0001*	*<0.0001*
	GAH			-	*<0.0001*	*<0.0001*			>0.9999	*<0.0001*	*<0.0001*			>0.9999	*<0.0001*	*<0.0001*
	CS,GAH				-	>0.9999				*<0.0001*	*<0.0001*				*<0.0001*	*<0.0001*
	CS-GAH$_b$					-					*<0.0001*					*<0.0001*
Day 4	Control		*<0.0001*	0.9996	*<0.0001*	*<0.0001*	-	*<0.0001*	>0.9999	*<0.0001*	*<0.0001*	0.4954	*<0.0001*	0.9105	*<0.0001*	*<0.0001*
	CS			*<0.0001*	*<0.0001*	*<0.0001*		-	*<0.0001*	*0.0013*	*<0.0001*		*0.0092*	*<0.0001*	>0.9999	*<0.0001*
	GAH				*<0.0001*	*<0.0001*			-	*<0.0001*	*<0.0001*			>0.9999	*<0.0001*	*<0.0001*
	CS,GAH					*<0.0001*				-	*<0.0001*				*0.0002*	0.2441
	CS-GAH$_b$										-					*<0.0001*
Day 8	Control		*<0.0001*	0.9517	*<0.0001*	*<0.0001*		*<0.0001*	0.9919	*<0.0001*	*<0.0001*	-	0.2939	>0.9999	*<0.0001*	*<0.0001*
	CS			*0.0003*	*<0.0001*	*<0.0001*			*0.0043*	*<0.0001*	*<0.0001*		-	0.0608	*0.0447*	*<0.0001*
	GAH				*<0.0001*	*<0.0001*				*<0.0001*	*<0.0001*			-	*<0.0001*	*<0.0001*
	CS,GAH					*<0.0001*					*<0.0001*				-	*<0.0001*
	CS-GAH$_b$															-

D

		Day 0					Day 4					Day 8				
		Control	CS	3:1 CS	CS-GAH$_b$	3:1 CS-GAH$_b$	Control	CS	3:1 CS	CS-GAH$_b$	3:1 CS-GAH$_b$	Control	CS	3:1 CS	CS-GAH$_b$	3:1 CS-GAH$_b$
Day 0	Control	-	*<0.0001*	*<0.0001*	*<0.0001*	*<0.0001*	>0.9999	*<0.0001*	*<0.0001*	*<0.0001*	*<0.0001*	0.8838	*0.0001*	0.2738	*<0.0001*	*<0.0001*
	CS		-	>0.9999	0.9996	*0.0051*		*<0.0001*	*<0.0001*	*0.0031*	*<0.0001*		*<0.0001*	*<0.0001*	*<0.0001*	*<0.0001*
	3:1 CS			-	0.7346	*0.0001*			*<0.0001*	*0.0488*	*<0.0001*			*<0.0001*	*<0.0001*	*<0.0001*
	CS-GAH$_b$				-	0.1693				*<0.0001*	*<0.0001*				*<0.0001*	*<0.0001*
	3:1 CS-GAH$_b$					-					*<0.0001*					*<0.0001*
Day 4	Control		*<0.0001*	*<0.0001*	*<0.0001*	*<0.0001*	-	*<0.0001*	*<0.0001*	*<0.0001*	*<0.0001*	0.4954	*<0.0001*	0.0922	*<0.0001*	*<0.0001*
	CS			*<0.0001*	*<0.0001*	*<0.0001*		-	0.9896	*<0.0001*	*<0.0001*		*0.0092*	*<0.0001*	*<0.0001*	*0.0026*
	3:1 CS				*<0.0001*	*<0.0001*			-	*<0.0001*	*<0.0001*			*0.0014*	*<0.0001*	*<0.0001*
	CS-GAH$_b$					*<0.0001*				-	*0.0002*				*<0.0001*	*<0.0001*
	3:1 CS-GAH$_b$										-					0.0526
Day 8	Control		*<0.0001*	*<0.0001*	*<0.0001*	*<0.0001*		*<0.0001*	*<0.0001*	*<0.0001*	*<0.0001*	-	0.2939	>0.9999	*<0.0001*	*<0.0001*
	CS			*<0.0001*	*<0.0001*	*<0.0001*			0.4622	*<0.0001*	*<0.0001*		-	0.8403	*<0.0001*	*<0.0001*
	3:1 CS				*<0.0001*	*<0.0001*				*<0.0001*	*<0.0001*			-	*<0.0001*	*<0.0001*
	CS-GAH$_b$					*<0.0001*					>0.9999				-	0.1627
	3:1 CS-GAH$_b$															-

Figure 3.4.: GAGs retained in collagen gels over an eight day culture period. GAGs retained were measured from gels cultured up to days 0, 4, and 8 by performing a DMMB assay. GAGs retained in chondrocyte embedded (A) collagen I gels with added CS, GAH, CS and GAH, or CS-GAH$_b$ and (B) collagen I and 3:1 collagen I and II gels with added CS or CS-GAH$_b$ were analyzed. P-values obtained from Tukey's *post hoc* tests denote statistical significance (red) between the (C) collagen I gels and (D) collagen I and II blend gels (α=0.05). Bars represent average $\pm$ standard deviation ($n \geq 3$).

able to retain a significantly higher concentration of GAGs at the end of the 8 days (Figures 3.4A and 3.4C).

The concentration of GAGs retained from the collagen I and 3:1 collagen I and II gels with added CS or CS-GAH$_b$ decreased over the course of the 8 day culture period (Figure 3.4B). At day -1, the amount of GAGs retained in the 3:1 CS-GAH$_b$ gels was significantly higher than those retained by gels containing CS (Figure 3.4D). However, the amount of GAGs retained from the CS-GAH$_b$ gels was not significantly different to the amount retained by the 3:1 CS-GAH$_b$ gels. At the end of the 8 days, the CS-GAH$_b$ gels were able to retain a significantly higher concentration of GAGs than the rest of the gels. The largest GAG retained differences observed were between CS or CS-GAH$_b$ incorporation in the gels. Nevertheless, the addition of collagen type II into the gels seemed to decrease the amount of GAG retained when comparing the CS-GAH$_b$ and 3:1 CS-GAH$_b$ gels.

3.4.3 GAGs decrease collagen release into cell culture media while addition of collagen type II increases it

Although the collagen type I gels started to release collagen into the cell culture media at day 4 (Figure 3.5A), the control gels were the only ones to show a significant increase in collagen release over the 8 day period (Figure 3.5C). At day -1, the 3:1 collagen I and II gels with added CS or CS-GAH$_b$ showed a significant amount of collagen released into the media (Figures 3.5B and 3.5D). Meanwhile, the rest of the gels did not show any collagen release until day 4. At day 4, the 3:1 CS-GAH$_b$ gels released a significantly higher amount of collagen than the rest of the gels, except for the control. Moreover, at day 8, the 3:1 CS and 3:1 CS-GAH$_b$ gels released a significantly higher amount of collagen than the rest of the gels, except for the control. The control gels and the gels containing collagen type II released higher amounts of collagen than the rest. Incorporation of GAGs (CS or CS-GAH$_b$) decreased collagen

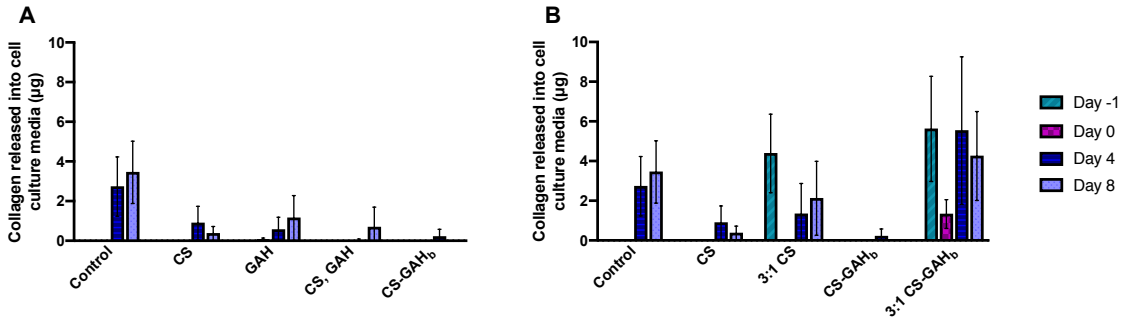

C

		Day -1					Day 0					Day 4					Day 8				
		Control	CS	GAH	CS,GAH	CS-GAH$_b$	Control	CS	GAH	CS,GAH	CS-GAH$_b$	Control	CS	GAH	CS,GAH	CS-GAH$_b$	Control	CS	GAH	CS,GAH	CS-GAH$_b$
Day -1	Control	-	>0.9999	>0.9999	>0.9999	>0.9999	>0.9999	>0.9999	>0.9999	>0.9999	>0.9999	0.0822	>0.9999	>0.9999	>0.9999	>0.9999	*0.0029*	>0.9999	0.9993	>0.9999	>0.9999
	CS		-	>0.9999	>0.9999	>0.9999		>0.9999	>0.9999	>0.9999	>0.9999		>0.9999	>0.9999	>0.9999	>0.9999		>0.9999	0.9993	>0.9999	>0.9999
	GAH			-	>0.9999	>0.9999			>0.9999	>0.9999	>0.9999			>0.9999	>0.9999	>0.9999			0.9992	>0.9999	>0.9999
	CS,GAH				-	>0.9999				>0.9999	>0.9999				>0.9999	>0.9999				>0.9999	>0.9999
	CS-GAH$_b$					-					>0.9999					>0.9999					>0.9999
Day 0	Control		>0.9999	>0.9999	>0.9999	>0.9999	-	>0.9999	>0.9999	>0.9999	>0.9999	0.2921	>0.9999	>0.9999	>0.9999	>0.9999	*0.0304*	>0.9999	>0.9999	>0.9999	>0.9999
	CS		>0.9999	>0.9999	>0.9999	>0.9999		-	>0.9999	>0.9999	>0.9999		>0.9999	>0.9999	>0.9999	>0.9999		>0.9999	>0.9999	>0.9999	>0.9999
	GAH			>0.9999	>0.9999	>0.9999			-	>0.9999	>0.9999			>0.9999	>0.9999	>0.9999			>0.9999	>0.9999	>0.9999
	CS,GAH				>0.9999	>0.9999				-	>0.9999				>0.9999	>0.9999				>0.9999	>0.9999
	CS-GAH$_b$					-					>0.9999					>0.9999					>0.9999
Day 4	Control		0.0782	0.0747	0.0782	0.0747		0.2332	0.2643	0.2921	0.2332	-	0.9851	0.9058	0.5555	0.6955	>0.9999	0.8074	0.9983	0.9490	0.5287
	CS			>0.9999	>0.9999	>0.9999			>0.9999	>0.9999	>0.9999		-	>0.9999	>0.9999	>0.9999			>0.9999	>0.9999	>0.9999
	GAH				>0.9999	>0.9999				>0.9999	>0.9999			-	>0.9999	>0.9999				>0.9999	>0.9999
	CS,GAH					>0.9999					>0.9999				-	>0.9999				>0.9999	>0.9999
	CS-GAH$_b$															-					>0.9999
Day 8	Control		*0.0027*	*0.0025*	*0.0027*	*0.0025*		*0.0196*	*0.0238*	*0.0304*	*0.0196*		0.6683	0.4077	0.1195	0.1907	-	0.2781	0.8444	0.5072	0.1088
	CS			>0.9999	>0.9999	>0.9999			>0.9999	>0.9999	>0.9999			>0.9999	>0.9999	>0.9999		-	>0.9999	>0.9999	>0.9999
	GAH				0.9993	0.9992				>0.9999	>0.9999				>0.9999	>0.9999			-	>0.9999	>0.9999
	CS,GAH					>0.9999					>0.9999					>0.9999				-	>0.9999
	CS-GAH$_b$																				-

D

		Day -1					Day 0					Day 4					Day 8				
		Control	CS	3:1 CS	CS-GAH$_b$	3:1 CS-GAH$_b$	Control	CS	3:1 CS	CS-GAH$_b$	3:1 CS-GAH$_b$	Control	CS	3:1 CS	CS-GAH$_b$	3:1 CS-GAH$_b$	Control	CS	3:1 CS	CS-GAH$_b$	3:1 CS-GAH$_b$
Day -1	Control	-	>0.9999	*<0.0001*	>0.9999	*<0.0001*	>0.9999	>0.9999	>0.9999	>0.9999	0.8611	0.0822	>0.9999	0.9932	>0.9999	*<0.0001*	*0.0029*	>0.9999	0.5104	>0.9999	*<0.0001*
	CS		-	*<0.0001*	>0.9999	*<0.0001*		>0.9999	>0.9999	>0.9999	0.8514		>0.9999	0.9928	>0.9999	*<0.0001*		>0.9999	0.5001	>0.9999	*<0.0001*
	3:1 CS			-	*<0.0001*	0.3061			*<0.0001*	*<0.0001*	*<0.0001*			*0.0192*	*<0.0001*	0.9992			0.3556	*<0.0001*	>0.9999
	CS-GAH$_b$				-	*<0.0001*				>0.9999	0.8421				>0.9999	*<0.0001*				>0.9999	*<0.0001*
	3:1 CS-GAH$_b$					-					*<0.0001*					>0.9999					0.9894
Day 0	Control		>0.9999	*<0.0001*	>0.9999	*<0.0001*	-	>0.9999	>0.9999	>0.9999	0.9895	0.2921	>0.9999	0.9993	>0.9999	*<0.0001*	*0.0304*	>0.9999	0.7991	>0.9999	*0.0009*
	CS			*<0.0001*	>0.9999	*<0.0001*		-	>0.9999	>0.9999	0.9805		>0.9999	0.9988	>0.9999	*<0.0001*		>0.9999	0.7467	>0.9999	*0.0005*
	3:1 CS				>0.9999	*<0.0001*			-	>0.9999	0.9805			0.9988	>0.9999	*<0.0001*			0.7467	>0.9999	*0.0005*
	CS-GAH$_b$					*<0.0001*				-	0.9805				>0.9999	*<0.0001*				>0.9999	*0.0005*
	3:1 CS-GAH$_b$										-					*0.0006*					0.1335
Day 4	Control		0.0782	0.9094	0.0747	*0.0390*		0.2332	0.2332	0.2332	0.9975	-	0.9851	0.9998	0.6955	0.4721	>0.9999	0.8074	>0.9999	0.5287	0.9991
	CS			*0.0020*	>0.9999	*<0.0001*			>0.9999	>0.9999	>0.9999		-	>0.9999	>0.9999	*0.0015*		>0.9999	>0.9999	>0.9999	0.1393
	3:1 CS				0.9923	*<0.0001*				0.9988	>0.9999			-	>0.9999	*0.0088*			>0.9999	>0.9999	0.3875
	CS-GAH$_b$					*<0.0001*					>0.9999				-	*<0.0001*				>0.9999	*0.0159*
	3:1 CS-GAH$_b$															-					>0.9999
Day 8	Control		*0.0027*	>0.9999	*0.0025*	0.4407		*0.0196*	*0.0196*	*0.0196*	0.7488		0.6683	0.9278	0.1907	0.9361	-	0.2781	>0.9999	0.1088	>0.9999
	CS			*<0.0001*	>0.9999	*<0.0001*			>0.9999	>0.9999	>0.9999			>0.9999	>0.9999	*0.0001*		-	0.9923	>0.9999	*0.0281*
	3:1 CS				0.4909	*0.0019*				0.7467	>0.9999				0.9759	0.1205			-	0.9240	0.9218
	CS-GAH$_b$					*<0.0001*					0.9989					*<0.0001*				-	*0.0072*
	3:1 CS-GAH$_b$																				-

Figure 3.5.: Collagen released into cell culture media over an eight day culture period. Collagen released was measured every 2 days and is shown as as day to day measurements for days -1 and 0. For days 4 and 8, data is reported as cumulative measurements from days 2 and 4 and days 6 and 8, respectively. Collagen loss was measured by a Sircol assay. Collagen released from chondrocyte embedded (A) collagen I gels with added CS, GAH, CS and GAH, or CS-GAH$_b$ and (B) collagen I and 3:1 collagen I and II gels with added CS or CS-GAH$_b$ were analyzed. P-values obtained from Tukey's *post hoc* tests denote statistical significance (red) between the (C) collagen I gels and (D) collagen I and II blend gels (α=0.05). Bars represent average $\pm$ standard deviation ($n \geq 3$).

release into cell culture media. However, in the presence of GAGs, the addition of collagen type II in the gels increases collagen release.

3.4.4 CS-GAH$_b$ increases cytokine release into cell culture media

IL-6 and TNF-α production were studied to determine whether the addition of the molecules or their separate components stimulates the production of proinflammatory cytokines. IL-6 production released into cell culture media was only detected for the CS-GAH$_b$ collagen gels (Figure 3.6A). The IL-6 production in the rest of the collagen type I gels was too low to detect. There was an initial spike in IL-6 production at day -1, followed by a decrease in production at day 0 and another significant spike at day 4 (Figures 3.6A and 3.6C). IL-6 release into the culture media was also observed for the 3:1 CS-GAH$_b$ gels (Figure 3.6B). While the CS-GAH$_b$ collagen I gels showed spikes in IL-6 release, the 3:1 CS-GAH$_b$ gels presented a significant release at day -1 followed by a decrease over the course of the 8 day culture period (Figures 3.6B and 3.6D). The IL-6 production in the rest of the 3:1 collagen I and II gels was too low to detect.

Similar to IL-6, TNF-α release into cell culture media was observed for the CS-GAH$_b$ collagen gels only (Figure 3.7A). The TNF-α release for the rest of the gels was too low to detect. Significant increases in TNF-α release for the CS-GAH$_b$ collagen gels were detected for days -1 and 4 (Figure 3.7C). TNF-α release was also observed for the 3:1 CS-GAH$_b$ gels (Figure 3.7B). Both the CS-GAH$_b$ and the 3:1 CS-GAH$_b$ gels showed spikes in TNF-α release at days -1 and 4 (Figure 3.7D). The TNF-α collected in the media for the rest of the 3:1 collagen I and II gels was too low to detect.

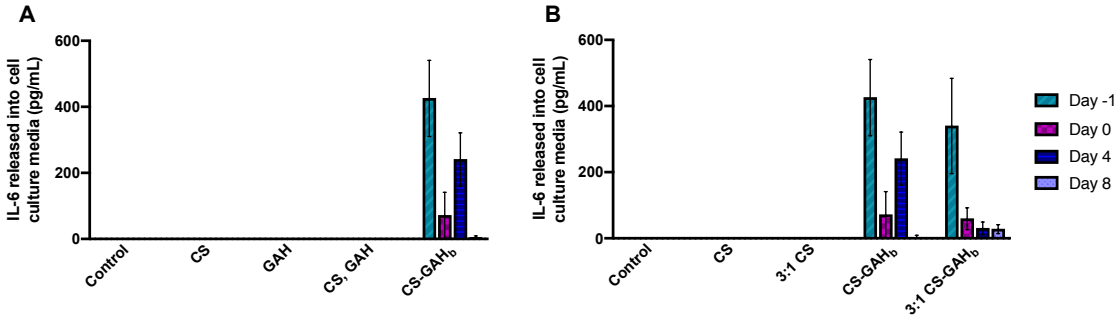

C

		Day -1					Day 0					Day 4					Day 8				
		Control	CS	GAH	CS,GAH	CS-GAH$_b$	Control	CS	GAH	CS,GAH	CS-GAH$_b$	Control	CS	GAH	CS,GAH	CS-GAH$_b$	Control	CS	GAH	CS,GAH	CS-GAH$_b$
Day -1	Control	-	>0.9999	>0.9999	>0.9999	<0.0001	>0.9999	>0.9999	>0.9999	>0.9999	0.6806	>0.9999	>0.9999	>0.9999	>0.9999	<0.0001	>0.9999	>0.9999	>0.9999	>0.9999	>0.9999
	CS		-	>0.9999	>0.9999	<0.0001		>0.9999	>0.9999	>0.9999	0.6806		>0.9999	>0.9999	>0.9999	<0.0001		>0.9999	>0.9999	>0.9999	>0.9999
	GAH			-	>0.9999	<0.0001			>0.9999	>0.9999	0.6806			>0.9999	>0.9999	<0.0001			>0.9999	>0.9999	>0.9999
	CS,GAH				-	<0.0001				>0.9999	0.6806				>0.9999	<0.0001				>0.9999	>0.9999
	CS-GAH$_b$					-					<0.0001					0.0003					<0.0001
Day 0	Control		>0.9999	>0.9999	>0.9999	<0.0001	-	>0.9999	>0.9999	>0.9999	0.9400	>0.9999	>0.9999	>0.9999	>0.9999	<0.0001	>0.9999	>0.9999	>0.9999	>0.9999	>0.9999
	CS			>0.9999	>0.9999	<0.0001		-	>0.9999	>0.9999	0.9400		>0.9999	>0.9999	>0.9999	<0.0001		>0.9999	>0.9999	>0.9999	>0.9999
	GAH				>0.9999	<0.0001			-	>0.9999	0.9400			>0.9999	>0.9999	<0.0001			>0.9999	>0.9999	>0.9999
	CS,GAH					<0.0001				-	0.9400				>0.9999	<0.0001				>0.9999	>0.9999
	CS-GAH$_b$										-					0.0169					0.9976
Day 4	Control		>0.9999	>0.9999	>0.9999	<0.0001		>0.9999	>0.9999	>0.9999	0.9952	-	>0.9999	>0.9999	>0.9999	0.0004	>0.9999	>0.9999	>0.9999	>0.9999	>0.9999
	CS			>0.9999	>0.9999	<0.0001			>0.9999	>0.9999	0.9952		-	>0.9999	>0.9999	0.0004		>0.9999	>0.9999	>0.9999	>0.9999
	GAH				>0.9999	<0.0001				>0.9999	0.9952			-	>0.9999	0.0004			>0.9999	>0.9999	>0.9999
	CS,GAH					<0.0001					0.9952				-	0.0004				>0.9999	>0.9999
	CS-GAH$_b$															-					0.0005
Day 8	Control		>0.9999	>0.9999	>0.9999	<0.0001		>0.9999	>0.9999	>0.9999	0.9952		>0.9999	>0.9999	>0.9999	0.0004	-	>0.9999	>0.9999	>0.9999	>0.9999
	CS			>0.9999	>0.9999	<0.0001			>0.9999	>0.9999	0.9952			>0.9999	>0.9999	0.0004		-	>0.9999	>0.9999	>0.9999
	GAH				>0.9999	<0.0001				>0.9999	0.9952				>0.9999	0.0004			-	>0.9999	>0.9999
	CS,GAH					<0.0001					0.9952					0.0004				-	>0.9999
	CS-GAH$_b$																				-

D

		Day -1					Day 0					Day 4					Day 8				
		Control	CS	3:1 CS	CS-GAH$_b$	3:1 CS-GAH$_b$	Control	CS	3:1 CS	CS-GAH$_b$	3:1 CS-GAH$_b$	Control	CS	3:1 CS	CS-GAH$_b$	3:1 CS-GAH$_b$	Control	CS	3:1 CS	CS-GAH$_b$	3:1 CS-GAH$_b$
Day -1	Control	-	>0.9999	>0.9999	<0.0001	<0.0001	>0.9999	>0.9999	>0.9999	0.6806	0.9295	>0.9999	>0.9999	>0.9999	<0.0001	>0.9999	>0.9999	>0.9999	>0.9999	>0.9999	>0.9999
	CS		-	>0.9999	<0.0001	<0.0001		>0.9999	>0.9999	0.6806	0.9295		>0.9999	>0.9999	<0.0001	>0.9999		>0.9999	>0.9999	>0.9999	>0.9999
	3:1 CS			-	<0.0001	<0.0001			>0.9999	0.6806	0.9295			>0.9999	<0.0001	>0.9999			>0.9999	>0.9999	>0.9999
	CS-GAH$_b$				-	0.0056				<0.0001	<0.0001				0.0003	<0.0001				<0.0001	<0.0001
	3:1 CS-GAH$_b$					-					<0.0001					<0.0001					<0.0001
Day 0	Control		>0.9999	>0.9999	<0.0001	<0.0001	-	>0.9999	>0.9999	0.9400	0.9940	>0.9999	>0.9999	>0.9999	<0.0001	>0.9999	>0.9999	>0.9999	>0.9999	>0.9999	>0.9999
	CS			>0.9999	<0.0001	<0.0001		-	>0.9999	0.9400	0.9940		>0.9999	>0.9999	<0.0001	>0.9999		>0.9999	>0.9999	>0.9999	>0.9999
	3:1 CS				<0.0001	<0.0001			-	0.9400	0.9940			>0.9999	<0.0001	>0.9999			>0.9999	>0.9999	>0.9999
	CS-GAH$_b$					<0.0001				-	>0.9999				0.0169	>0.9999				0.9976	>0.9999
	3:1 CS-GAH$_b$										-					>0.9999					>0.9999
Day 4	Control		>0.9999	>0.9999	<0.0001	<0.0001		>0.9999	>0.9999	0.9952	0.9998	-	>0.9999	>0.9999	0.0004	>0.9999	>0.9999	>0.9999	>0.9999	>0.9999	>0.9999
	CS			>0.9999	<0.0001	<0.0001			>0.9999	0.9952	0.9998		-	>0.9999	0.0004	>0.9999		>0.9999	>0.9999	>0.9999	>0.9999
	3:1 CS				<0.0001	<0.0001				0.9952	0.9998			-	0.0004	>0.9999			>0.9999	>0.9999	>0.9999
	CS-GAH$_b$					0.5878					0.0057				-	0.0053				>0.9999	0.0043
	3:1 CS-GAH$_b$															-					>0.9999
Day 8	Control		>0.9999	>0.9999	<0.0001	<0.0001		>0.9999	>0.9999	0.9952	0.9998		>0.9999	>0.9999	0.0004	>0.9999	-	>0.9999	>0.9999	>0.9999	>0.9999
	CS			>0.9999	<0.0001	<0.0001			>0.9999	0.9952	0.9998			>0.9999	0.0004	>0.9999		-	>0.9999	>0.9999	>0.9999
	3:1 CS				<0.0001	<0.0001				0.9952	0.9998				0.0004	>0.9999			-	>0.9999	>0.9999
	CS-GAH$_b$					<0.0001					>0.9999					>0.9999				-	>0.9999
	3:1 CS-GAH$_b$																				-

Figure 3.6.: IL-6 released from collagen gels into cell culture media over eight days. IL-6 release was measured with an ELISA and is shown as day to day measurements for days -1 and 0. For days 4 and 8, data is reported as cumulative measurements from days 2 and 4 and days 6 and 8, respectively. IL-6 produced in chondrocyte embedded (A) collagen I gels with added CS, GAH, CS and GAH, or CS-GAH$_b$ and (B) collagen I and 3:1 collagen I and II gels with added CS or CS-GAH$_b$ were analyzed. P-values obtained from Tukey's *post hoc* tests denote statistical significance (red) between the (C) collagen I gels and (D) collagen I and II blend gels (α=0.05). Bars represent average $\pm$ standard deviation ($n \geq 3$).

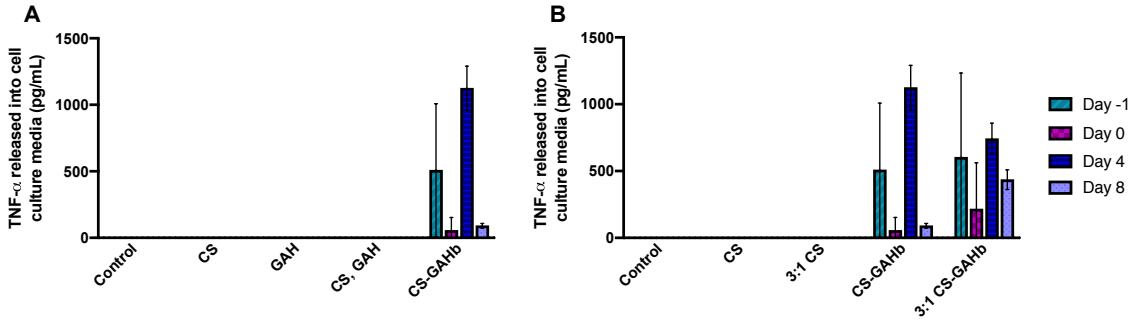

C

		Day -1					Day 0					Day 4					Day 8				
		Control	CS	GAH	CS,GAH	CS-GAH$_b$	Control	CS	GAH	CS,GAH	CS-GAH$_b$	Control	CS	GAH	CS,GAH	CS-GAH$_b$	Control	CS	GAH	CS,GAH	CS-GAH$_b$
Day -1	Control	-	>0.9999	>0.9999	>0.9999	*<0.0001*	>0.9999	>0.9999	>0.9999	>0.9999	>0.9999	>0.9999	>0.9999	>0.9999	>0.9999	*<0.0001*	>0.9999	>0.9999	>0.9999	>0.9999	>0.9999
	CS		-	>0.9999	>0.9999	*<0.0001*		>0.9999	>0.9999	>0.9999	>0.9999		>0.9999	>0.9999	>0.9999	*<0.0001*		>0.9999	>0.9999	>0.9999	>0.9999
	GAH			-	>0.9999	*<0.0001*			>0.9999	>0.9999	>0.9999			>0.9999	>0.9999	*<0.0001*			>0.9999	>0.9999	>0.9999
	CS,GAH				-	*<0.0001*				>0.9999	>0.9999				>0.9999	*<0.0001*				>0.9999	>0.9999
	CS-GAH$_b$					-					0.0520					*0.0355*					0.6514
Day 0	Control		>0.9999	>0.9999	>0.9999	*0.0106*	-	>0.9999	>0.9999	>0.9999	>0.9999	>0.9999	>0.9999	>0.9999	>0.9999	*<0.0001*	>0.9999	>0.9999	>0.9999	>0.9999	>0.9999
	CS			>0.9999	>0.9999	*0.0106*		-	>0.9999	>0.9999	>0.9999		>0.9999	>0.9999	>0.9999	*<0.0001*		>0.9999	>0.9999	>0.9999	>0.9999
	GAH				>0.9999	*0.0106*			-	>0.9999	>0.9999			>0.9999	>0.9999	*<0.0001*			>0.9999	>0.9999	>0.9999
	CS,GAH					*0.0106*				-	>0.9999				>0.9999	*<0.0001*				>0.9999	>0.9999
	CS-GAH$_b$										-					*<0.0001*					>0.9999
Day 4	Control		>0.9999	>0.9999	>0.9999	0.2433		>0.9999	>0.9999	>0.9999	>0.9999	-	>0.9999	>0.9999	>0.9999	*<0.0001*	>0.9999	>0.9999	>0.9999	>0.9999	>0.9999
	CS			>0.9999	>0.9999	0.2433			>0.9999	>0.9999	>0.9999		-	>0.9999	>0.9999	*<0.0001*		>0.9999	>0.9999	>0.9999	>0.9999
	GAH				>0.9999	0.2433				>0.9999	>0.9999			-	>0.9999	*<0.0001*			>0.9999	>0.9999	>0.9999
	CS,GAH					0.2433					>0.9999				-	*<0.0001*				>0.9999	>0.9999
	CS-GAH$_b$															-					*0.0005*
Day 8	Control		>0.9999	>0.9999	>0.9999	0.2433		>0.9999	>0.9999	>0.9999	>0.9999		>0.9999	>0.9999	>0.9999	*<0.0001*	-	>0.9999	>0.9999	>0.9999	>0.9999
	CS			>0.9999	>0.9999	0.2433			>0.9999	>0.9999	>0.9999			>0.9999	>0.9999	*<0.0001*		-	>0.9999	>0.9999	>0.9999
	GAH				>0.9999	0.2433				>0.9999	>0.9999				>0.9999	*<0.0001*			-	>0.9999	>0.9999
	CS,GAH					0.2433					>0.9999					*<0.0001*				-	>0.9999
	CS-GAH$_b$																				-

D

		Day -1					Day 0					Day 4					Day 8				
		Control	CS	3:1 CS	CS-GAH$_b$	3:1 CS-GAH$_b$	Control	CS	3:1 CS	CS-GAH$_b$	3:1 CS-GAH$_b$	Control	CS	3:1 CS	CS-GAH$_b$	3:1 CS-GAH$_b$	Control	CS	3:1 CS	CS-GAH$_b$	3:1 CS-GAH$_b$
Day -1	Control	-	>0.9999	>0.9999	*<0.0001*	*<0.0001*	>0.9999	>0.9999	>0.9999	>0.9999	0.9923	>0.9999	>0.9999	>0.9999	*<0.0001*	*0.0020*	>0.9999	>0.9999	>0.9999	>0.9999	0.5720
	CS		-	>0.9999	*<0.0001*	*<0.0001*		>0.9999	>0.9999	>0.9999	0.9915		>0.9999	>0.9999	*<0.0001*	*0.0019*		>0.9999	>0.9999	>0.9999	0.5630
	3:1 CS			-	*<0.0001*	*<0.0001*			>0.9999	>0.9999	0.9915			>0.9999	*<0.0001*	*0.0019*			>0.9999	>0.9999	0.5630
	CS-GAH$_b$				-	>0.9999				0.0520	0.7930				*0.0355*	0.9996				0.6514	>0.9999
	3:1 CS-GAH$_b$					-					0.2286					>0.9999					>0.9999
Day 0	Control		>0.9999	>0.9999	*0.0106*	*0.0004*	-	>0.9999	>0.9999	>0.9999	0.9996	>0.9999	>0.9999	>0.9999	*<0.0001*	*0.0158*	>0.9999	>0.9999	>0.9999	>0.9999	0.8003
	CS			>0.9999	*0.0106*	*0.0004*		-	>0.9999	>0.9999	0.9996		>0.9999	>0.9999	*<0.0001*	*0.0158*		>0.9999	>0.9999	>0.9999	0.8003
	3:1 CS				*0.0106*	*0.0004*			-	>0.9999	0.9996			>0.9999	*<0.0001*	*0.0158*			>0.9999	>0.9999	0.8003
	CS-GAH$_b$					*0.0030*				-	>0.9999				*<0.0001*	*0.0452*				>0.9999	0.9420
	3:1 CS-GAH$_b$					-					-					0.4260					>0.9999
Day 4	Control		>0.9999	>0.9999	0.2433	*0.0468*		>0.9999	>0.9999	>0.9999	>0.9999	-	>0.9999	>0.9999	*<0.0001*	0.0941	>0.9999	>0.9999	>0.9999	>0.9999	0.9459
	CS			>0.9999	0.2433	*0.0468*			>0.9999	>0.9999	>0.9999		-	>0.9999	*<0.0001*	0.0941		>0.9999	>0.9999	>0.9999	0.9459
	3:1 CS				0.2433	*0.0468*				>0.9999	>0.9999			-	*<0.0001*	0.0941			>0.9999	>0.9999	0.9459
	CS-GAH$_b$					0.1992					*0.0004*				-	0.9884				*0.0005*	0.1847
	3:1 CS-GAH$_b$															-					0.9996
Day 8	Control		>0.9999	>0.9999	0.2433	*0.0468*		>0.9999	>0.9999	>0.9999	>0.9999		>0.9999	>0.9999	*<0.0001*	0.0941	-	>0.9999	>0.9999	>0.9999	0.9459
	CS			>0.9999	0.2433	*0.0468*			>0.9999	>0.9999	>0.9999			>0.9999	*<0.0001*	0.0941		-	>0.9999	>0.9999	0.9459
	3:1 CS				0.2433	*0.0468*				>0.9999	>0.9999				*<0.0001*	0.0941			-	>0.9999	0.9459
	CS-GAH$_b$					0.2258					>0.9999					0.2805				-	0.9973
	3:1 CS-GAH$_b$															-					-

Figure 3.7.: TNF-α released from collagen gels into cell culture media over eight days. TNF-α release was measured with an ELISA and is shown as day to day measurements for days -1 and 0. For days 4 and 8, data is reported as cumulative measurements from days 2 and 4 and days 6 and 8, respectively. TNF-α produced in chondrocyte embedded (A) collagen I gels with added CS, GAH, CS and GAH, or CS-GAH$_b$ and (B) collagen I and 3:1 collagen I and II gels with added CS or CS-GAH$_b$ were analyzed. P-values obtained from Tukey's *post hoc* tests denote statistical significance (red) between the (C) collagen I gels and (D) collagen I and II blend gels (α=0.05). Bars represent average $\pm$ standard deviation ($n \geq 3$).

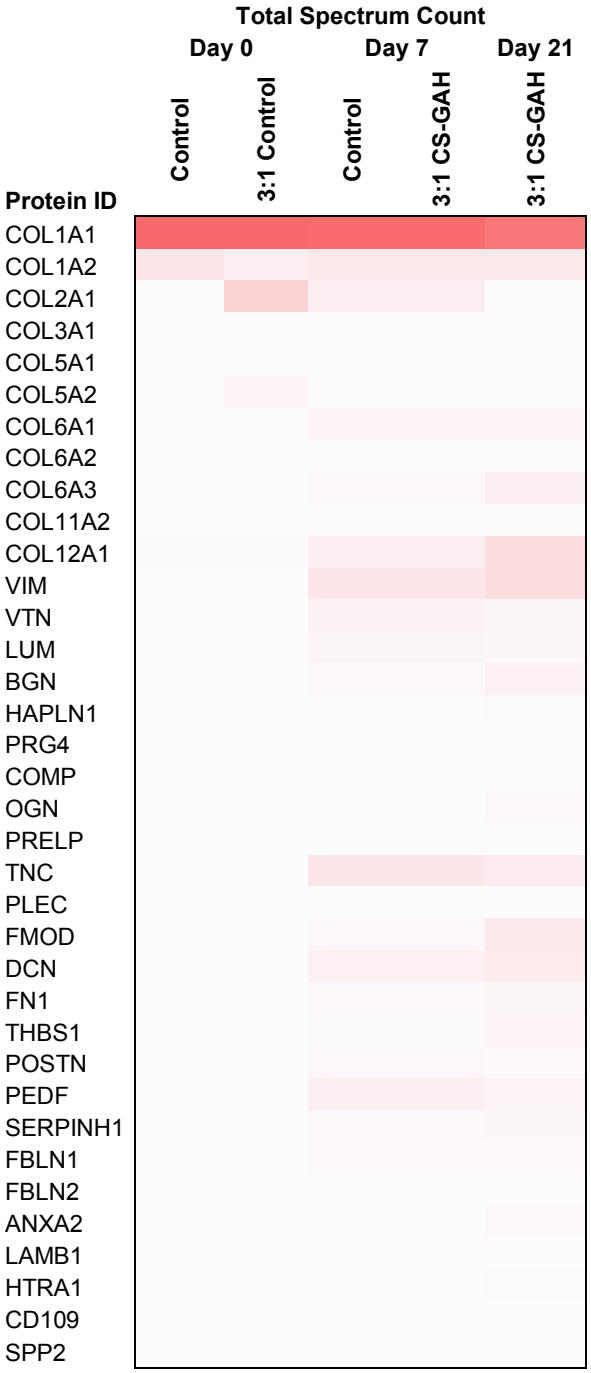

Figure 3.8.: Heat map showing the preliminary expression of proteins involved in cartilage synthesis, degradation, and homeostasis produced by the chondrocytes in the different collagen scaffolds (n=2). Increasing red gradient indicates an increase in the protein expression remaining in the gels.

3.4.5 Encapsulated chondrocytes produce ECM proteins involved in cartilage synthesis, degradation, and homeostasis

A preliminary set of chondrocyte embedded collagen gels collected at days 0, 7, and 21 were reduced, alkylated, and trypsin digested to perform LC MS/MS and detect the proteins produced by the chondrocytes that still remained in the collagen scaffolds. Figure 3.8 shows the proteins detected in the collagen scaffolds and Table 3.2 describes their roles in cartilage synthesis, degradation, and homeostasis. The results obtained show an increase in COL6A1, COL6A3, COL12A1, VIM, VTN, LUM, BGN, HAPLN1, OGN, TNC, FMOD, DCN, FN1, THBS1, POSTN, PEDF, SERPINH1, FBLN1, ANXA2, and HTRA1 production during the 21 day incubation period. In contrast, there was a decrease in COL2A1 and COL5A2 production.

Table 3.2.: Proteins detected in the chondrocyte embedded collagen gels.

Protein	**ID**	**Function**
Collagen type I	COL1A1 COL1A2	Confers tensile strength to the ECM [77].
Collagen type II	COL2A1	Makes up 90-95% of all the collagen in articular cartilage and forms the network of fibrils that contain the ECM proteoglycans [48, 49, 78]. Fragments induce pro-inflammatory cytokines and MMPs [50].
Collagen type III	COL3A1	Synthesized as a modifier of existing fibril networks in response to tissue and matrix damage [79].
Collagen type V	COL5A1 COL5A2	Regulator of collagen fibril formation, structure, and matrix organization [80].

continued on next page

Table 3.2.: *continued*

Protein	**ID**	**Function**
Collagen type VI	COL6A1 COL6A2 COL6A3	Forms a network that anchors the chondrocyte to the PCM in articular cartilage [81]. Mediates cell-matrix interactions and intermolecular interactions [82]. Transmits mechanical and osmotic stresses from the ECM to the chondrocytes [83].
Collagen type XI	COL11A2	Involved in PCM organization by interacting with cartilage proteoglycans [81, 84]. First cartilage collagen produced by MSCs during chondrogenic differentiation [85].
Collagen type XII	COL12A1	Protects tissue integrity [81, 86]. Mediates interactions between fibrils and matrix macromolecules and cells [81, 86, 87].
Vimentin	VIM	Contributes to chondrocyte stiffness [88].
Vitronectin	VTN	Mediates the attachment and spreading of cells to the ECM [89]. Binds collagen and GAGs [89].
Lumican	LUM	Mediator of TLR-4 activation of inflammation, cartilage degradation and macrophage polarization [90].

continued on next page

Table 3.2.: *continued*

Protein	**ID**	**Function**
Biglycan	BGN	Binds fribrillar collagens [91]. Activates chondrocytes via TLR-4 resulting in net loss of cartilage [92]. Possesses pro-inflammatory properties [92]. Plays a role in bone mineralization [93].
Hyaluronan and proteoglycan link protein 1	HAPLN1	Strengthens and stabilizes proteoglycan aggregates with HA in the ECM [94].
Lubricin (Proteoglycan 4)	PRG4	Plays a role in joint lubrication and synovial homeostasis [95–97].
Cartilage oligomeric matrix protein	COMP	Stimulates chondrocyte proliferation and MSC chondrogenesis [98–100]. Catalyzes collagen fibrillogenesis [101]. Enhances osteogenesis [102]. COMP fragments serve as biomarkers of OA [103].
Osteoglycin (Mimecan)	OGN	Induces bone formation in conjunction with BMPs and may regulate osteoblast differentiation [104, 105].
Prolargin	PRELP	Anchors basement membranes (perlecan) to the underlying connective tissue (collagen I and II) [106].

continued on next page

Table 3.2.: *continued*

Protein	**ID**	**Function**
Tenascin	TNC	Protects articular cartilage from proteoglycan depletion [107]. Promotes chondrocyte proliferation and increases proteoglycan content [108]. TNC fragments might induce cartilage matrix degradation [109].
Plectin	PLEC	Links the cytoskeleton to junctions found in the plasma membrane that connect different cells [110]. Acts as a link between actin microfilaments, microtubules, and intermediate filaments [110, 111].
Fibromodulin	FMOD	Regulates collagen fibril assembly [112].
Decorin	DCN	Binds to collagen type I fibrils [113–115] and plays a role in fibrillogenesis [115–117] and matrix assembly [115, 117, 118].
Cumulus cell specific fibronectin 1 transcript variant	FN1	Contributes to protease-mediated damage to cartilage [119, 120].
Thrombospondin-1	THBS1	Mediates cell-to-cell and cell-to-matrix interactions [121, 122]. Binds to ECM ligands [123].

continued on next page

Table 3.2.: *continued*

Protein	**ID**	**Function**
Periostin	POSTN	Promotes cartilage degradation in OA by upregulating MMP-13 and ADAMTS4 through the canonical Wnt pathway [124, 125]. Contributes to the maturation and shape retention of tissue engineered cartilage [126]. Involved in osteoblast recruitment, attachment, and spreading [127].
Pigment epithelium-derived factor	PEDF	Heightens cartilage degeneration in an inflamed environment [128].
Serpin H1	SERPINH1	Binds specifically to collagen [129]. Plays a role in cartilage and endochondral bone formation [130].
Fibulin	FBLN1 FBLN2	Involved in the structural integrity of basement membranes and elastic fibers [131–133]. Mediates cellular processes and tissue remodeling [131].
Annexin A2	ANXA2	Increases osteoclast formation [134].
Laminin subunit β1	LAMB1	Binds to basement membrane proteins [135]. May guide or maintain chondrocyte differentiation [135].
Serine protease HTRA1	HTRA1	Damages the PCM network and alters chondrocyte metabolism [136].

continued on next page

Table 3.2.: *continued*

Protein	**ID**	**Function**
CD109 molecule	CD109	Regulates TGF-β signaling [137, 138] and ECM protein production. May maintain cartilage function and integrity [138].
Secreted phosphoprotein 24	SPP24	Affects BMP activity and regulates bone formation [139, 140].

ECM: extracellular matrix; MMPs: matrix metalloproteinases; PCM: pericellular matrix; GAGs: glycosaminoglycans; TLR-4: toll-like receptor 4; HA: hyaluronic acid; MSC: mesenchymal stem cells; OA: osteoarthritis; BMPs: bone morphogenetic proteins; ADAMTS4: a disintegrin and metalloproteinase with thrombospondin motifs-4; TGF-β: tranforming growth factor-β

3.5 Discussion

In this work, we studied the effects of the CS-GAH$_b$ molecule and its separate components on chondrocytes embedded in collagen type I constructs. Furthermore, we also studied the effects of the addition of collagen type II to the chondrocyte-embedded collagen type I gels with CS or CS-GAH$_b$.

First, we measured the amount of GAGs and collagen released into cell culture media and the amount of GAGs retained in the gels to determine whether the CS-GAH$_b$ molecules and the separate components stimulated or prevented GAG and collagen degradation. The results suggest CS-GAH$_b$ gels are able to decrease GAG release into cell culture media (Figure 3.3) and increase GAG retention in the gels (Figure 3.4) in comparison to other gels with added CS. The addition of CS or CS-GAH$_b$ into the gels decreased collagen release from the gels (Figure 3.5). These results are consistent with Sharma *et al* where they saw a decrease in CS and collagen release

from chondrocyte-embedded collagen type I gels that incorporated CS-BMPH-GAH when compared to gels with CS and HA [12]. Similarly, we previously observed a decrease in CS released from bovine cartilage explants treated with CS-BMPH-GAH when compared to untreated explants (Figure S 3.9) [76]. These observations could be attributed to the CS-GAH$_b$ molecules binding to HA and forming denser and more stable gel networks that are able to limit the amount of CS and collagen being released. These results could also be due to the mimetic molecule's ability to protect from collagen and CS degradation, hence, decreasing GAG and collagen release into cell culture media and increasing GAG retention in the gels as observed previously [12, 66, 67, 76].

The collagen type II addition to the 3:1 collagen type I to II gels did not affect GAG retention and release (Figures 3.3B, 3.3D, 3.4B, and 3.4D). Similarly, Rutgers *et al* observed no significant differences in GAG release and retention between chondrocyte seeded collagen type I gels and chondrocyte seeded collagen type II gels [38]. Additionally, Pulkkinen *et al* compared chondrocytes in culture medium and chondrocytes seeded in recombinant human collagen type II gels injected into nude mice and did not observe significant differences in GAG content between these samples [36]. In contrast, Kontturi *et al* and Pieper *et al* have observed significant increases in GAG production in collagen type II gels [28,40]. Even though collagen type II did not affect GAG retention and release, collagen type II addition increased the amount of collagen released into cell culture media when compared to collagen type I only gels. Collagen type II gels have been known to be difficult to synthesize due to collagen type II's lesser ability to form fibrils [17, 66] and incorporate into hydrogels [17] which could result in more collagen being released than incorporated into the gels. Future work should focus on studying the collagen content in the gels to determine the amount of collagen incorporated and the amount released.

In OA, chondrocytes produce proinflammatory cytokines involved in the degradation of the ECM and its components [141–145]. For this reason, we studied whether the incorporation of the CS-GAH$_b$ molecule and collagen type II in the chondrocyte

embedded gels affects the production and release of cytokines IL-6 and TNF-α. In OA, IL-6 enhances MMP-13 production stimulating proteoglycan degradation [145–147]. Meanwhile, TNF-α increases production of MMPs and a disintegrin and metalloproteinase with thrombospondin motifs (ADAMTS) [145,148–151], inhibits proteoglycan and collagen type II synthesis [145, 152, 153], and stimulates synthesis of proinflammatory cytokines such as IL-6 [145, 154] and IL-8 [145, 155]. Our results showed an inital increase in IL-6 and TNF-α production and release followed by a decrease in cytokine production at day 8 in gels containing CS-GAH$_b$ (Figures 3.6 and 3.7). Even though proinflammatory cytokine presence is largely associated with catabolic activities in the ECM, the relationship between cytokines and cartilage degradation and repair is a more complex system [145, 156–161]. Previous work has revealed IL-6 to have anabolic effects on chondrocytes *in vitro* [156, 157]. IL-6 has shown abilities to increase tissue inhibitor of metalloproteinases-1 (TIMP-1), transforming growth factor-1 (TGF-1), interleukin-1 receptor antagonist (IL-1ra), and collagen type II synthesis [156, 162–165]. Moreover, chondrocytes, isolated from defects and OA cartilage, with an increase in inflammatory cytokine release were able to produce cartilaginous tissue *in vitro* similar to the tissue produced by healthy chondrocytes with respect to GAG production [157]. In previous studies, Sharma *et al* showed that CS-BMPH-GAH molecules incorporated in choncrocyte embedded collagen gels were able to increase compressive stiffness, decrease collagen and GAG release, and enhance aggrecan and collagen type II expression [67]. Similarly, the aggrecan mimic was able to reduce catabolic gene expression in a simulated OA environment [76]. These results coupled with our GAG retention and release, collagen release, and the initial spike in cytokine production observed in our experiments could be attributed to an early attempt at repair and could be a signal of anabolic activities in the ECM.

Finally, we identified the proteins expressed by the chondrocytes into the gels to determine whether the CS-GAH$_b$ molecules stimulated ECM protein production. Our peliminary results showed that 36 of the proteins expressed are involved in cartilage synthesis, degradation, and homeostasis (Figure 3.8 and Table 3.2) [166]. The

presence of collagen types I [77], II [48, 49], III [79], V [80], VI [81–83], XI [81, 84], and XII [81, 86, 87] are indicative of pericellular matrix (PCM) and ECM synthesis. Other proteins expressed that are involved in network synthesis, structure, stiffness, and maturation are periostin [126], CD109 molecule [138], hyaluronan and proteoglycan link protein 1 [94], decorin [113–118], fibromodulin [112], cartilage oligomeric matrix protein (COMP) [101,167], lubricin [95–97], prolargin [106], biglycan [91], vitronectin [89], Serpin H1 [129], and fibulin [131–133]. Proteins involved in cell attachment, stiffness, proliferation, and interaction detected in the gels are vimentin [88], vitronectin [89], plectin [110, 111], COMP [98–100], thrombospondin-1 [121–123], laminin subunit $\beta 1$ [135], and tenascin [108]. The identification of tenascin [108], vitronectin [89], and hyaluronan and proteoglycan link protein [94] also indicated the presence of proteins associated with increased proteoglycan content and proteoglycan binding. Proteins related to ECM degradation and homeostasis such as lumican [90], COMP [103], biglycan [92], periostin [124, 125], fibronectin [119, 120], pigment epithelium-derived factor [128], and serine protease HTRA1 [136] were also identified. Additionally, molecules associated with osteoclast and osteogenesis like biglycan [93], COMP [102], osteoglycin [104, 105], annexin A2 [134], and secreted phosphoprotein 24 [139, 140] were detected. The presence and interactions of all of these elements suggest the development and homeostasis of PCM and ECM and cell-matrix interfaces in the gels as previously observed by Wilson *et al* in femoral head cartilage obtained from mice at post-natal days 3 and 21 [168] and in 3-week neocartilage and 3-day post-natal mouse cartilage [169].

Based on all of the results obtained in the work presented, collagen type II did not significantly affect GAG retention and release, cytokine production, and protein expression in the gels. Collagen type II did increase collagen release which could be attributed to collagen type II not being fully incorporated in the gels. These results are consistent with previous work [36, 38]. However, collagen type II incorporation in gels has been known to stimulate a cartilaginous tissue synthesis [22, 33, 36] and

chondrocyte morphology [1,22,26,28]. These contrasting results suggest collagen type II interactions with chondrocytes need to be further elucidated.

3.6 Conclusion

The work discussed herein has shown that the incorporation of CS-GAH$_b$ in chondrocyte embedded collagen gels with HA, and not its separate comoponents, is able to prevent GAG and collagen release. CS-GAH$_b$ also stimulated cytokine production during the initial days of scaffold culture. CS-GAH$_b$, however, did not affect the chondrocytes' ECM protein expression in the gels. The incorporation of collagen type II into the collagen type I scaffolds did not significantly affect GAG and cytokine production and ECM protein synthesis, but did increase collagen release. Thus, these results suggest CS-GAH$_b$ incorporation into chondrocyte embedded collagen type I gels are promising constructs for articular cartilage repair. Addition of collagen type II to these gels could help maintain chondrocyte morphology and stimulate cartilaginous tissue synthesis, but needs to be further studied. Future work will focus on studying the effects of CS-GAH$_b$ and its separate components on the proteome of chondrocytes embedded in collagen gels over a 7 day period.

3.7 Acknowledgements

This work was supported by the National Institutes of Health (NIAMS R21AR065644 and R21AR065398). The authors thank Dr. Brett Phinney and Michelle Salemi from the University of California Davis Proteomics Core Facility for performing LC MS/MS and obtaining the spectral data used for proteomic analysis.

3.8 Supporting Information

The supporting information consists of parts of a manuscript by Sharma S, Vazquez-Portalatin N, Calve S, and Panitch A, published in ACS Biomaterials Science & Engineering, Volume 2, Issue 2, 2016.

3.8.1 Materials and Methods

Peptide GAHWQFNALTVRGGGC (GAH) and WYRGRLGC (WYRGRL) were purchased from Genscript (Piscataway, NJ).

Synthesis of molecules

Synthesis of collagen type I and HA binding peptidoglycans has been previously described by our laboratory [66, 170]. Utilizing the same methods, CS augmented with collagen type II and HA binding peptides were synthesized. Briefly, 2μM chondroitin-6 sulfate was oxidized by reacting with 30 mM sodium periodate for 48 h to form reactive aldehyde functional groups. A heterobifunctional crosslinker N-(β-Maleimidopropionic acid) hydrazide, trifluoroacetic acid salt (BMPH) and sodium cyanoborohydride were added to the oxidized CS and reacted for 4 h. A glycine-cysteine spacer was added by the manufacturer to the C terminus of the respective binding peptides to yield GAHWQFNALTVRGGGC (HA binding peptide, referred to as GAH) and WYRGRLGC (collagen type II binding peptide, referred to as WYRGRL). Ten binding peptides of either GAH or WYRGRL were conjugated to the CS-BMPH molecule by allowing the thiol group on the peptides to react with the maleimide group of BMPH for 2 h. Peptides were added at a 1:1 molar ratio of peptide:CS. The end product of the functionalized molecules yielded CS-BMPH-WYRGRL (type II-binding molecule) and CS-BMPH-GAH (HA-binding molecule). Molecules were separated using size exclusion chromatography with an ÄKTA Purifier FPLC (GE Healthcare) and a column packed with polyacrylamide beads (Bio-Rad

Labs). After synthesis, molecules were lyophilized and stored at −80 °C until further testing.

Tissue harvest

Cartilage explants were obtained from three month old bovine knee joints obtained from an abattoir within 24 h of slaughter (Dutch Valley Veal, South Holland, IL). The explants were removed using a 3 mm diameter cork borer from the load bearing region of the femoral condoyle and washed three times in serum free DMEM medium with 50 μg/mL ascorbic acid 2-phosphate, 100 μg/mL sodium pyruvate, 0.1% BSA, 100 units/mL penicillin, 100 μg/mL streptomycin and 25 mM HEPES. Explants required for *ex vivo* inflammatory model were weighed in a sterile hood and cultured for three days in 5% FBS supplemented media prior to testing.

Ex vivo inflammatory model

Aggrecan Removal

An *ex vivo* model stimulating early OA like conditions was designed by removing aggrecan from cartilage explants. Freshly harvested explants were cultured for three days in DMEM/F-12 media (50 μg/mL ascorbic acid 2-phosphate, 100 μg/mL sodium pyruvate, 0.1% BSA, 100 units/mL penicillin, 100 μg/mL streptomycin and 25 mM HEPES) supplemented with 5% FBS [171]. Native aggrecan was removed from harvested cartilage explants using a previously described protocol [172]. Briefly, plugs were treated with 0.5% (w/v) trypsin in Hank's Balanced Salt Solution (HBSS) for 3 h at 37 °C. After trypsin treatment, explants were washed three times in HBSS and incubated with 20% FBS to inactivate residual trypsin activity.

Diffusion of molecules through cartilage explant

Following trypsin treatment, molecules were diffused through aggrecan depleted cartilage explants. Molecules dissolved in distilled water at 10 μM concentration

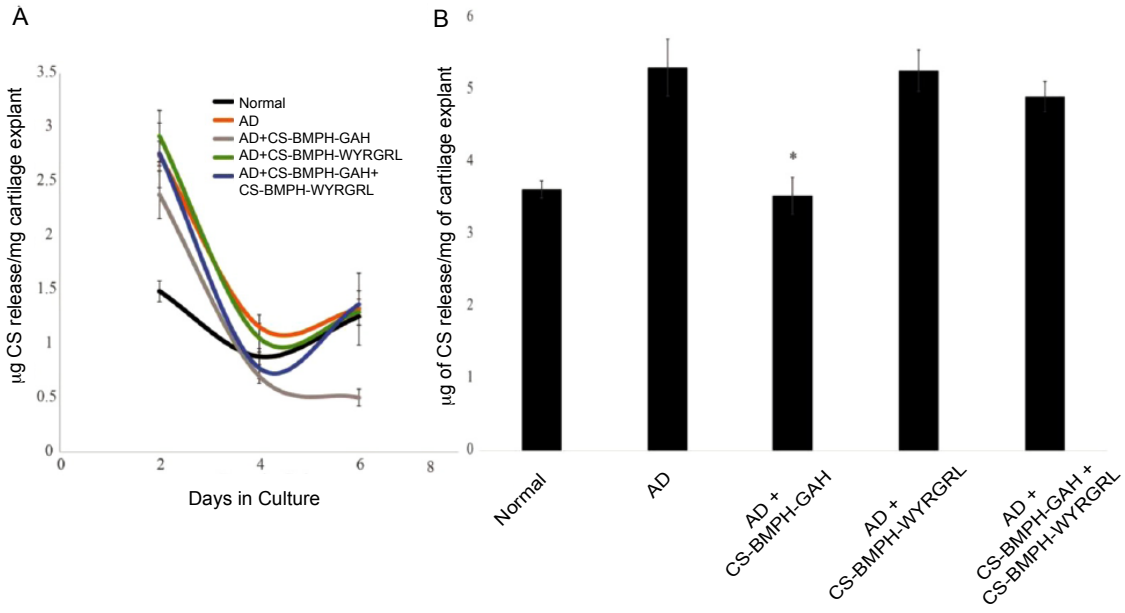

Figure S 3.9.: CS released into cell culture media over a seven day culture period. CS release was (A) measured every 2 days and (B) measured as a culmination of seven day culture period. CS loss was measured by a DMMB assay. The addition of CS-BMPH-GAH, has a significant effect on preventing loss of CS from the aggrecan-depleted (AD) scaffolds ($p < 0.01$). * denotes statistical significance between explants treated with CS-BMPH-GAH after aggrecan depletion and explants left untreated. Bars represent average ± SEM (n=9).

were diffused through the articular surface of cartilage explants by placing 10 μL of the solution on the surface every ten minutes for one hour at room temperature. The molecules diffused included: 1) CS-BMPH-GAH, 2) CS-BMPH-WYRGRL, and 3) CS-BMPH-GAH+CS-BMPH-WYRGRL. Normal cartilage and aggrecan depleted cartilage were treated with 1x PBS as positive and negative controls, respectively. The explants were cultured for three weeks. Experimental conditions were: 1) Normal cartilage, 2) aggrecan depleted cartilage (AD), 3) AD+CS-BMPH-GAH, 4) AD+CS-BMPH-WYRGRL and 5) AD+CS-BMPH-GAH+CS-BMPH-WYRGRL. Culture medium was replaced every two days for 21 days. Media aliquots collected were stored at $-80\,^{\circ}$C for fragmentation assessment.

3.9 References

[1] Stefan Nehrer, Howard A. Breinan, Arun Ramappa, Sonya Shortkroff, Gretchen Young, Tom Minas, Clement B. Sledge, Ioannis V. Yannas, and Myron Spector. Canine chondrocytes seeded in type I and type II collagen implants investigated in vitro. *Journal of Biomedical Materials Research*, 1997.

[2] Stefan Nehrer, Howard A Breinan+, Arun Ramappa, Gretchen Young, Sonya Shortkroff, Libby K Louie+, Clement B Sledge, Ioannis V Yannas+, and Myron Spector. Matrix collagen type and pore size influence behaviour of seeded canine chondrocytes. *Biomaterials*, 18:769–776, 1997.

[3] M. Ochi, Y. Uchio, K. Kawasaki, S. Wakitani, and J. Iwasa. Transplantation of cartilage-like tissue made by tissue engineering in the treatment of cartilage defects of the knee. *The Journal of Bone and Joint Surgery*, 2002.

[4] C. W. Chen, Y. H. Tsai, W. P. Deng, S. N. Shih, C. L. Fang, J. G. Burch, W. H. Chen, and W. F. Lai. Type I and II collagen regulation of chondrogenic differentiation by mesenchymal progenitor cells. *Journal of Orthopaedic Research*, 23(2):446–453, 2005.

[5] Laurent Galois, Sandrine Hutasse, Delphine Cortial, Cécile F. Rousseau, Laurent Grossin, Marie Clarie Ronziere, Daniel Herbage, and Anne Marie Freyria. Bovine chondrocyte behaviour in three-dimensional type I collagen gel in terms of gel contraction, proliferation and gene expression. *Biomaterials*, 2006.

[6] Kate Stuart and Alyssa Panitch. Influence of chondroitin sulfate on collagen gel structure and mechanical properties at physiologically relevant levels. *Biopolymers*, 89:841–851, 2008.

[7] Kate Stuart and Alyssa Panitch. Characterization of gels composed of blends of collagen l, collagen III, and chondroitin sulfate. *Biomacromolecules*, 10:25–31, 2009.

[8] C. Albrecht, B. Tichy, S. Nürnberger, S. Hosiner, L. Zak, S. Aldrian, and S. Marlovits. Gene expression and cell differentiation in matrix-associated chondrocyte transplantation grafts: A comparative study. *Osteoarthritis and Cartilage*, 2011.

[9] Dennis C. Crawford, Thomas M. DeBerardino, and Riley J. Williams. NeoCart, an autologous cartilage tissue implant, compared with microfracture for treatment of distal femoral cartilage lesions: An FDA phase-II prospective, randomized clinical trial after two years. *Journal of Bone and Joint Surgery - Series A*, 2012.

[10] Akon Higuchi, Qing Dong Ling, Shih Tien Hsu, and Akihiro Umezawa. Biomimetic cell culture proteins as extracellular matrices for stem cell differentiation, 2012.

[11] Turgay Efe, Christina Theisen, Susanne Fuchs-Winkelmann, Thomas Stein, Alan Getgood, Marga B. Rominger, Jürgen R.J. Paletta, and Markus D. Schofer. Cell-free collagen type I matrix for repair of cartilage defects-clinical and magnetic resonance imaging results. *Knee Surgery, Sports Traumatology, Arthroscopy*, pages 1915–1922, 2012.

[12] Shaili Sharma, Alyssa Panitch, and Corey P. Neu. *Acta Biomaterialia*.

[13] Maximilian Petri, Maximilian Broese, Annika Simon, Emmanouil Liodakis, Max Ettinger, Daniel Guenther, Johannes Zeichen, Christian Krettek, Michael Jagodzinski, and Carl Haasper. CaReS® (MACT) versus microfracture in treating symptomatic patellofemoral cartilage defects: A retrospective matched-pair analysis. *Journal of Orthopaedic Science*, 2013.

[14] D Saris, A Price, Widuchowski W, and Bertrand-Marchand M. Matrix-Applied Characterized Autologous Cultured Chondrocytes Versus Microfracture: Two-Year Follow-up of a Prospective Randomized Trial. *Am J Sports Med*, 42(6):1384–1394, 2014.

[15] Lukas Zak, Christian Albrecht, Barbara Wondrasch, Harald Widhalm, György Vekszler, Siegfried Trattnig, Stefan Marlovits, and Silke Aldrian. Results 2 years after matrix-associated autologous chondrocyte transplantation using the Novocart 3D scaffold: An analysis of clinical and radiological data. *American Journal of Sports Medicine*, 2014.

[16] Tyler Novak, Sherry L Voytik-Harbin, and Corey P Neu. Cell encapsulation in a magnetically aligned collagen GAG copolymer microenvironment. *Acta Biomaterialia*, 11:274–282, 2015.

[17] Nelda Vazquez-Portalatín, Claire E Kilmer, Alyssa Panitch, and Julie C Liu. Characterization of Collagen Type I and II Blended Hydrogels for Articular Cartilage Tissue Engineering. *Biomacromolecules*, 17:3145–3152, 2016.

[18] Guang Zhen Jin and Hae Won Kim. Effects of Type I Collagen Concentration in Hydrogel on the Growth and Phenotypic Expression of Rat Chondrocytes. *Tissue Engineering and Regenerative Medicine*, 2017.

[19] K Gelse, E Pöschl, and T Aigner. Collagens-structure, function, and biosynthesis.

[20] Brian J Huang, Jerry C Hu, and Kyriacos A Athanasiou. Cell-based tissue engineering strategies used in the clinical repair of articular cartilage. *Biomaterials*, 98:1–22, 2016.

[21] E. B. Hunziker. Articular cartilage repair: Basic science and clinical progress. A review of the current status and prospects. *Osteoarthritis and Cartilage*, 2002.

[22] Vincent Irawan, Tzu-Cheng Sung, Akon Higuchi, and Ikoma Toshiyuki. Collagen Scaffolds in Cartilage Tissue Engineering and Relevant Approaches for Future Development. *Tissue Engineering and Regenerative Medicine*, 15(6):673–697, 2018.

[23] Tsuguharu Takahashi, Toru Ogasawara, Yukiyo Asawa, Yoshiyuki Mori, Eiju Uchinuma, Tsuyoshi Takato, and Kazuto Hoshi. Three-Dimensional Microenvironments Retain Chondrocyte Phenotypes During Proliferation Culture. *Tissue Engineering*, 2007.

[24] J. Farjanel, G. Schürmann, and P. Bruckner. Contacts with fibrils containing collagen I, but not collagens II, IX, and XI, can destabilize the cartilage phenotype of chondrocytes. *Osteoarthritis and Cartilage*, 2001.

[25] Z. F. Lu, B. Zandieh Doulabi, P. I. Wuisman, R. A. Bank, and M. N. Helder. Influence of collagen type II and nucleus pulposus cells on aggregation and differentiation of adipose tissue-derived stem cells. *Journal of Cellular and Molecular Medicine*, 2008.

[26] S. Nehrer, H.A. Breinan, A. Ramappa, H-P. Hsu, T. Minas, S. Shortkroff, C.B. Sledge, I.V. Yannas, and M. Spector. Chondrocyte-seeded collagen matrices implanted in a chondral defect in a canine model. *Biomaterials*, 19:2313–2328, 1998.

[27] Howard A Breinan, Scott D Martin, Hu-Ping Hsu, and Myron Spector. Healing of Canine Articular Cartilage Defects Treated with Microfracture, a Type-I1 Collagen Matrix, or Cultured Autologous Chondrocytes. *Journal of Orthopaedic Research*, 18:781–789, 2000.

[28] J. S. Pieper, P. M. Van Der Kraan, T. Hafmans, J. Kamp, P. Buma, J. L C Van Susante, W. B. Van Den Berg, J. H. Veerkamp, and T. H. Van Kuppevelt. Crosslinked type II collagen matrices: Preparation, characterization, and potential for cartilage engineering. *Biomaterials*, 23:3183–3192, 2002.

[29] Pieter Buma, Jeroen S Pieper, Tony Van Tienen, Job L C Van Susante, Peter M Van Der Kraan, Jacques H Veerkamp, Wim B Van Den Berg, Rene P H Veth, and Toin H Van Kuppevelt. Cross-linked type I and type II collagenous matrices for the repair of full-thickness articular cartilage defects-A study in rabbits. *Biomaterials*, 24:3255–3263, 2003.

[30] C. R. Lee, A. J. Grodzinsky, H. P. Hsu, and M. Spector. Effects of a cultured autologous chondrocyte-seeded type II collagen scaffold on the healing of a chondral defect in a canine model. *Journal of Orthopaedic Research*, 21:272–281, 2003.

[31] Takahiro Ohno, Keizo Tanisaka, Yosuke Hiraoka, Takashi Ushida, Tamotsu Tamaki, and Tetsuya Tateishi. Effect of type I and type II collagen sponges as 3D scaffolds for hyaline cartilage-like tissue regeneration on phenotypic control of seeded chondrocytes in vitro. *Materials Science and Engineering C*, 2004.

[32] D Bosnakovski, M Mizuno, G Kim, S Takagi, M Okumura, and T Fujinaga. Chondrogenic differentiation of bovine bone marrow mesenchymal stem cells (MSCs) in different hydrogels: Influence of collagen type II extracellular matrix on MSC chondrogenesis. *Biotechnology and Bioengineering*, 93:1152–1163, 2006.

[33] H J Pulkkinen, V Tiitu, P Valonen, E.-R Hämäläinen, M J Lammi, and I Kiviranta. Recombinant human type II collagen as a material for cartilage tissue engineering. *The International Journal of Artificial Organs*, 31(11):960–969, 2008.

[34] Elise Duval, Sylvain Leclercq, Jean Marc Elissalde, Magali Demoor, Philippe Galéra, and Karim Boumédiene. Hypoxia-inducible factor 1α inhibits the fibroblast-like markers type I and type III collagen during hypoxia-induced chondrocyte redifferentiation: Hypoxia not only induces type II collagen and aggrecan, but it also inhibits type I and type III collagen i. *Arthritis and Rheumatism*, 2009.

[35] Anne-Marie Freyria, Marie-Claire Ronzière, Delphine Cortial, Laurent Galois, Daniel Hartmann, Daniel Herbage, and Frédéric Mallein-Gerin. Comparative phenotypic analysis of articular chondrocytes cultured within type I or type II collagen scaffolds. *Tissue Engineering Part A*, 15:1233–1245, 2009.

[36] H J Pulkkinen, V Tiitu, P Valonen, J S Jurvelin, M J Lammi, and I Kiviranta. Engineering of cartilage in recombinant human type II collagen gel in nude mouse model in vivo. *Osteoarthritis and Cartilage*, 18:1077–1087, 2010.

[37] ZuFu Lu, Behrouz Zandieh Doulabi, ChunLing Huang, Ruud A Bank, and Marco N Helder. Collagen type II enhances chondrogenesis in adipose tissue-derived stem cells by affecting cell shape. *Tissue engineering. Part A*, 16:81–90, 2010.

[38] Marijn Rutgers, Daniel B Saris, Lucienne A Vonk, Mattie H Van Rijen, Vanessa Akrum, Danielle Langeveld, Antonette Van Boxtel, Wouter J Dhert, and Laura B Creemers. Effect of Collagen Type I or Type II on Chondrogenesis by Cultured Human Articular Chondrocytes. *Tissue Engineering Part A*, 19(1-2):59–65, 2013.

[39] Amos Matsiko, John P. Gleeson, and Fergal J. O'Brien. Scaffold Mean Pore Size Influences Mesenchymal Stem Cell Chondrogenic Differentiation and Matrix Deposition. *Tissue Engineering Part A*, 2014.

[40] Leena-Stiina Kontturi, Elina Järvinen, Virpi Muhonen, Estelle C Collin, Abhay S Pandit, Ilkka Kiviranta, Marjo Yliperttula, and Arto Urtti. An injectable, in situ forming type II collagen/hyaluronic acid hydrogel vehicle for chondrocyte delivery in cartilage tissue engineering. *Drug Deliv. and Transl. Res.*, 4:149–158, 2014.

[41] Lu Yuan, Bao Li, Jirong Yang, Yilu Ni, Yingying Teng, Likun Guo, Hongsong Fan, Yujiang Fan, and Xingdong Zhang. Effects of composition and mechanical property of injectable collagen I/II composite hydrogels on chondrocyte behaviors. *Tissue Engineering Part A*, 22:899–906, 2016.

[42] Henrique V. Almeida, Binulal N. Sathy, Ivan Dudurych, Conor T. Buckley, Fergal J. O'Brien, and Daniel J. Kelly. Anisotropic Shape-Memory Alginate Scaffolds Functionalized with Either Type I or Type II Collagen for Cartilage Tissue Engineering. *Tissue Engineering Part A*, 23:55–68, 2017.

[43] Mariana Lazarini, Pedro Bordeaux-Rego, Renata Giardini-Rosa, Adriana S. S. Duarte, Mariana Ozello Baratti, Alessandro Rozim Zorzi, João Batista de Miranda, Carlos Lenz Cesar, Ângela Luzo, and Sara Teresinha Olalla Saad. Natural Type II Collagen Hydrogel, Fibrin Sealant, and Adipose-Derived Stem Cells as a Promising Combination for Articular Cartilage Repair. *CARTILAGE*, 8(4):439–443, 2017.

[44] M. Tamaddon, M. Burrows, S. A. Ferreira, F. Dazzi, J. F. Apperley, A. Bradshaw, D. D. Brand, J. Czernuszka, and E. Gentleman. Monomeric, porous type II collagen scaffolds promote chondrogenic differentiation of human bone marrow mesenchymal stem cells in vitro. *Scientific Reports*, 2017.

[45] Yongli Gao, Bao Li, Weili Kong, Lu Yuan, Likun Guo, Chuan Li, Hongsong Fan, Yujiang Fan, and Xingdong Zhang. Injectable and self-crosslinkable hydrogels based on collagen type II and activated chondroitin sulfate for cell delivery. *International journal of biological macromolecules*, 118:2014–2020, 2018.

[46] Claire E Kilmer. *Collagen Type I and II Blend Hydrogels for Articular Cartilage Tissue Engineering*. PhD thesis, Purdue University, 2019.

[47] H J Pulkkinen, V Tiitu, P Valonen, J S Jurvelin, L Rieppo, J Töyräs, T S Silvast, M J Lammi, and I Kiviranta. Repair of osteochondral defects with recombinant human type II collagen gel and autologous chondrocytes in rabbit.

[48] Richard Mayne. Cartilage Collagens: What Is Their Function, and Are They Involved in Articular Disease? *Arthritis & Rheumatism*, 32(3):241–246, 1989.

[49] A R Poole, M Kobayashi, T Yasuda, S Laverty, F Mwale, T Kojima, T Sakai, C Wahl, S El-Maadawy, G Webb, E Tchetina, and W Wu. Type II collagen degradation and its regulation in articular cartilage in osteoarthritis. *Annals of the Rheumatic Diseases*, 61(Suppl 2):ii78–ii81, nov 2002.

[50] Andreas R. Klatt, Brigitte Paul-Klausch, Gabriele Klinger, Getrud Kühn, Joerg H. Renno, Marc Banerjee, Gebhart Malchau, and Klaus Wielckens. *Journal of Orthopaedic Research*.

[51] Mary B. Goldring. Chondrogenesis, chondrocyte differentiation, and articular cartilage metabolism in health and osteoarthritis. *Therapeutic Advances in Musculoskeletal Disease*, 2012.

[52] Van C. Mow, Anthony Ratcliffe, and A. R. Poole. *Biomaterials*.

[53] Chris Kiani, Liwen Chen, Yao Jiong Wu, Albert J Yee, and Burton B Yang. *Cell Research*.

[54] H Muir. The chondrocyte, architect of cartilage. Biomechanics, structure, function and molecular biology of cartilage matrix macromolecules. *BioEssays : news and reviews in molecular, cellular and developmental biology*, 17(12):1039–1048, 1995.

[55] T.E. Hardingham, S Tew, and A Murdoch. Tissue engineering and cartilage. *Arthritis Research*, 4:63–68, 2002.

[56] Mohit Kapoor and Nizar N. Mahomed. *Osteoarthritis: Pathogenesis, diagnosis, available treatments, drug safety, regenerative and precision medicine*. Springer International Publishing, 2015.

[57] Michael A Pratta, Wenqing Yao, Carl Decicco, Micky D Tortorella, Riu-Qin Liu, Robert A Copeland, Ronald Magolda, Robert C Newton, James M Trzaskos, and Elizabeth C Arner. *The Journal of Biological Chemistry*.

[58] Christopher B. Little, Clare T. Meeker, Suzanne B. Golub, Kate E. Lawlor, Pamela J. Farmer, Susan M. Smith, and Amanda J. Fosang. Blocking aggrecanase cleavage in the aggrecan interglobular domain abrogates cartilage erosion and promotes cartilage repair. *Journal of Clinical Investigation*, 117:1627–1636, 2007.

[59] T. Aigner and L. McKenna. Molecular pathology and pathobiology of osteoarthritic cartilage. *Cellular and Molecular Life Sciences*, 59(1):5–18, 2002.

[60] B Obrink and A Wasteson. Nature of the interaction of chondroitin 4-sulphate and chondroitin sulphate-proteoglycan with collagen. *Biochemistry Journal*, 121:227–233, 1971.

[61] J. E. Lee, J. C. Park, Y. S. Hwang, J. K. Kim, J. G. Kim, and H. Suh. Characterization of UV-irradiated dense/porous collagen membranes: morphology, enzymatic degradation, and mechanical properties. *Yonsei Medical Journal*, 42:172–179, 2001.

[62] Timothy Douglas, Sascha Heinemann, Carolin Mietrach, Ute Hempel, Susanne Bierbaum, Dieter Scharnweber, and Hartmut Worch. Interactions of collagen types I and II with chondroitin sulfates A-C and their effect on osteoblast adhesion. *Biomacromolecules*, 8:1085–1092, 2007.

[63] J. S. Pieper, T. Hafmans, J. H. Veerkamp, and T. H. Van Kuppevelt. Development of tailor-made collagen-glycosaminoglycan matrices: EDC/NHS crosslinking, and ultrastructural aspects. *Biomaterials*, 21(6):581–593, 2000.

[64] Job L.C. Van Susante, Jeroen Pieper, Pieter Buma, Toin H. Van Kuppevelt, Henk Van Beuningen, Peter M. Van Der Kraan, Jacques H. Veerkamp, Wim B. Van Den Berg, and René P.H. Veth. Linkage of chondroitin-sulfate to type I collagen scaffolds stimulates the bioactivity of seeded chondrocytes in vitro. *Biomaterials*, 2001.

[65] a Shimazu, a Jikko, M Iwamoto, T Koike, W Yan, Y Okada, M Shinmei, S Nakamura, and Y Kato. Effects of hyaluronic acid on the release of proteoglycan from the cell matrix in rabbit chondrocyte cultures in the presence and absence of cytokines. *Arthritis and rheumatism*, 36:247–53, 1993.

[66] Jonathan C. Bernhard and Alyssa Panitch. Synthesis and characterization of an aggrecan mimic. *Acta Biomaterialia*, 8:1543–1550, 2012.

[67] Shaili Sharma, Aeju Lee, Kuiwon Choi, Kwangmeyung Kim, Inchan Youn, Stephen B. Trippel, and Alyssa Panitch. *Macromolecular Bioscience*.

[68] M E Mummert, M Mohamadzadeh, D I Mummert, N Mizumoto, and A Takashima. *The Journal of Experimental Medicine*.

[69] Ji-Shen Zheng, Shan Tang, Yun-Kun Qi, Zhi-Peng Wang, and Lei Liu. Chemical synthesis of proteins using peptide hydrazides as thioester surrogates. *Nature Protocols*, 8(12):2483–2495, dec 2013.

[70] Sara Rydergren. *Chemical Modifications of Hyaluronan using DMTMM-Activated Amidation*. PhD thesis, Uppsala Universitet, 2013.

[71] Ulrich Nöth, Lars Rackwitz, Andrea Heymer, Meike Weber, Bernd Baumann, Andre Steinert, Norbert Schütze, Franz Jakob, and Jochen Eulert. Chondrogenic differentiation of human mesenchymal stem cells in collagen type I hydrogels. *Journal of Biomedical Materials Research Part A*, 83A(3):626–635, dec 2007.

[72] Julie N. Renner, Yeji Kim, and Julie C. Liu. Bone Morphogenetic Protein-Derived Peptide Promotes Chondrogenic Differentiation of Human Mesenchymal Stem Cells. *Tissue Engineering Part A*, 18(23-24):2581–2589, dec 2012.

[73] Richard W. Farndale, David J. Buttle, and Alan J. Barrett. *Biochimica et Biophysica Acta (BBA) - General Subjects*.

[74] Sergei V Saveliev, Carolyn C Woodroofe, Grzegorz Sabat, Christopher M Adams, Dieter Klaubert, Keith Wood, and Marjeta Urh. Mass Spectrometry Compatible Surfactant for Optimized In-Gel Protein Digestion. *Analytical Chemistry*, 85:907–914, 2013.

[75] Robert H Rice, Blythe P Durbin-Johnson, Michelle Salemi, Mary E Schwartz, David M Rocke, and Brett S Phinney. Proteomic profiling of Pachyonychia congenita plantar callus. *Journal of Proteomics*, 165:132–137, 2017.

[76] Shaili Sharma, Nelda Vazquez-Portalatin, Sarah Calve, and Alyssa Panitch. Biomimetic Molecules Lower Catabolic Expression and Prevent Chondroitin Sulfate Degradation in an Osteoarthritic ex Vivo Model. *ACS Biomaterials Science & Engineering*, 2(2):241–250, feb 2016.

[77] Laura E. Niklason. Understanding the Extracellular Matrix to Enhance Stem Cell-Based Tissue Regeneration. *Cell Stem Cell*, 22(3):302–305, mar 2018.

[78] Hemanth Akkiraju and Anja Nohe. Role of chondrocytes in cartilage formation, progression of osteoarthritis and cartilage regeneration. *Journal of Developmental Biology*, 3:177–192, 2015.

[79] Jiann-Jiu Wu, Mary Ann Weis, Lammy S Kim, and David R Eyre. Type III Collagen, a Fibril Network Modifier in Articular Cartilage *. *The Journal of Biological Chemistry*, 285(24):18537–18544, 2010.

[80] Richard J. Wenstrup, Jane B. Florer, Eric W. Brunskill, Sheila M. Bell, Inna Chervoneva, and David E. Birk. Type V Collagen Controls the Initiation of Collagen Fibril Assembly. *The Journal of Biological Chemistry*, 279(51):53331–53337, dec 2004.

[81] Yunyun Luo, Dovile Sinkeviciute, Yi He, Morten Karsdal, Yves Henrotin, Ali Mobasheri, Patrik Önnerfjord, and Anne Bay-Jensen. The minor collagens in articular cartilage. *Protein & Cell*, 8(8):560–572, aug 2017.

[82] Martin Pfaff, Monique Aumailley, Ulrich Specks, Joachim Knolle, Hans Günter Zerwes, and Rupert Timpl. Integrin and Arg-Gly-Asp Dependence of Cell Adhesion to the Native and Unfolded Triple Helix of Collagen Type VI. *Experimental Cell Research*, 206(1):167–176, may 1993.

[83] Nicole A Zelenski, Holly A Leddy, Johannah Sanchez-Adams, Jinzi Zhang, Paolo Bonaldo, Wolfgang Liedtke, and Farshid Guilak. Type VI Collagen Regulates Pericellular Matrix Properties, Chondrocyte Swelling, and Mechanotransduction in Mouse Articular Cartilage. *Arthritis & rheumatology*, 67(5):1286–1294, may 2015.

[84] Gerald N. Smith Jr., Karen A. Hasty, and Kenneth D. Brandt. Type XI Collagen is Associated with the Chondrocyte Surface in Suspension Culture. *Matrix*, 9(3):186–192, jun 1989.

[85] Jinping Xu, Wei Wang, Matt Ludeman, Kevin Cheng, Takayuki Hayami, Jeffrey C Lotz, and Sunil Kapila. Chondrogenic differentiation of human mesenchymal stem cells in three-dimensional alginate gels. *Tissue engineering. Part A*, 14(5):667–680, may 2008.

[86] Katsuhiko Arai, Yuko Nagashima, Taeko Takemoto, and Toshio Nishiyama. Mechanical Strain Increases Expression of Type XII Collagen in Murine Osteoblastic MC3T3-E1 Cells. *Cell Structure and Function*, 33(2):203–210, 2008.

[87] Drew W. Taylor, Nazish Ahmed, Justin Parreno, Gregory P. Lunstrum, Allan E. Gross, Eleftherios P. Diamandis, and Rita A. Kandel. Collagen Type XII and Versican Are Present in the Early Stages of Cartilage Tissue Formation by Both Redifferentating Passaged and Primary Chondrocytes. *Tissue Engineering Part A*, 21(3-4):683–693, feb 2015.

[88] Dominik R Haudenschild, Jianfen Chen, Nina Pang, Nikolai Steklov, Shawn P Grogan, Martin K Lotz, and Darryl D D'Lima. Vimentin contributes to changes in chondrocyte stiffness in osteoarthritis. *Journal of Orthopaedic Research*, 29(1):20–25, jan 2011.

[89] Iris Schvartz, Dalia Seger, and Shmuel Shaltiel. Molecules in focus: Vitronectin. *The International Journal of Biochemistry & Cell Biology*, 31:539–544, 1999.

[90] G. Barreto, B. Senturk, L. Colombo, P. Neidenbach, G. Salzmann, M. Rottmar, and M. Zenobi-Wong. Lumican regulation of toll-like receptor 4- mediated inflammation in osteoarthritis. *Osteoarthritis and Cartilage*, 26:S123–S124, apr 2018.

[91] Anders Aspberg. Cartilage Proteoglycans. In S Grässel and A Aszódi, editors, *Cartilage: Volume 1: Physiology and Development*, pages 1–22. Springer International Publishing, Cham, 2016.

[92] Goncalo Barreto, Antti Soininen, Pekka Ylinen, Jerker Sandelin, Yrjö T. Konttinen, Dan C. Nordström, and Kari K. Eklund. Soluble biglycan: a potential mediator of cartilage degradation in osteoarthritis. *Arthritis Research & Therapy*, 17:1–15, 2015.

[93] Adele L. Boskey and Pamela Gehron Robey. The Regulatory Role of Matrix Proteins in Mineralization of Bone. In Robert Marcus, David W. Dempster, Jane A. Cauley, David Feldman, and Marjorie Luckey, editors, *Osteoporosis*, chapter 11, pages 235–255. Academic Press, 4th edition, jan 2013.

[94] Andrew P Spicer, Adriane Joo, and Rodney A Bowling. A hyaluronan binding link protein gene family whose members are physically linked adjacent to chondroitin sulfate proteoglycan core protein genes: the missing links. *The Journal of Biological Chemistry*, 278(23):21083–21091, jun 2003.

[95] David A Swann and Eric L Radin. The Molecular Basis of Articular Lubrication I. Purification and properties of a lubricating fraction from the bovine synovial fluid *. *The Journal of Biological Chemistry*, 247(24):8069–8073, 1972.

[96] Gregory D Jay. Lubricin and surfacing of articular joints. *Current Opinion in Orthopaedics*, 15(5):355–359, oct 2004.

[97] David K Rhee, Jose Marcelino, MacArthur Baker, Yaoqin Gong, Patrick Smits, Véronique Lefebvre, Gregory D Jay, Matthew Stewart, Hongwei Wang, Matthew L Warman, and John D Carpten. The secreted glycoprotein lubricin protects cartilage surfaces and inhibits synovial cell overgrowth. *The Journal of Clinical Investigation*, 115(3):622–631, mar 2005.

[98] Ke Xu, Yan Zhang, Kirill Ilalov, Cathy S Carlson, Jian Q Feng, Paul E Di Cesare, and Chuan-Ju Liu. Cartilage Oligomeric Matrix Protein Associates with Granulin-Epithelin Precursor (GEP) and Potentiates GEP-stimulated Chondrocyte Proliferation. *The Journal of Biological Chemistry*, 282(15):11347–11355, 2007.

[99] J Kipnes, A.L Carlberg, G.A Loredo, J Lawler, R.S Tuan, and D.J Hall. Effect of cartilage oligomeric matrix protein on mesenchymal chondrogenesis in vitro. *Osteoarthritis and Cartilage*, 11(6):442–454, jun 2003.

[100] Karen L Posey, Francoise Coustry, and Jacqueline T Hecht. Cartilage oligomeric matrix protein: COMPopathies and beyond. *Matrix Biology*, 71-72:161–173, 2018.

[101] Krisztina Halász, Anja Kassner, Matthias Mörgelin, and Dick Heinegård. COMP Acts as a Catalyst in Collagen Fibrillogenesis. *The Journal of Biological Chemistry*, 282(43):31166–31173, 2007.

[102] Kazunari Ishida, Chitrangada Acharya, Blaine A Christiansen, Jasper H N Yik, Paul E Dicesare, and Dominik R Haudenschild. Cartilage oligomeric matrix protein enhances osteogenesis by directly binding and activating bone morphogenetic protein-2. *Bone*, 55:23–35, 2013.

[103] A.C. Bay-Jensen, D. Reker, C.F. Kjelgaard-Petersen, A. Mobasheri, M.A. Karsdal, C. Ladel, Y. Henrotin, and C.S. Thudium. Osteoarthritis year in review 2015: soluble biomarkers and the BIPED criteria. *Osteoarthritis and Cartilage*, 24(1):9–20, jan 2016.

[104] Aki Osawa, Masaki Kato, Eriko Matsumoto, Katsuro Iwase, Takashi Sugimoto, Tsutomu Matsui, Hiroshi Ishikura, Sumio Sugano, Hisashi Kurosawa, Masaki Takiguchi, and Naohiko Seki. Activation of genes for growth factor and cytokine pathways late in chondrogenic differentiation of ATDC5 cells. *Genomics*, 88(1):52–64, jul 2006.

[105] Eva Balint, David Lapointe, Hicham Drissi, Caroline Van Der Meijden, Daniel W Young, Andre J van Wijnen, Janet L Stein, Gary S Stein, and Jane B Lian. Phenotype Discovery by Gene Expression Profiling: Mapping of Biological Processes Linked to BMP-2-Mediated Osteoblast Differentiation. *Journal of Cellular Biochemistry*, 89:401–426, 2003.

[106] Eva Bengtsson, Matthias Mörgelin, Takako Sasaki, Rupert Timpl, Dick Heinegård, and Anders Aspberg. The Leucine-rich Repeat Protein PRELP Binds Perlecan and Collagens and May Function as a Basement Membrane Anchor. *The Journal of Biological Chemistry*, 277(17):15061–15068, 2002.

[107] Yuriyo Matsui, Masahiro Hasegawa, Takahiro Iino, Kyoko Imanaka-Yoshida, Toshimichi Yoshida, and Akihiro Sudo. Tenascin-C Prevents Articular Cartilage Degeneration in Murine Osteoarthritis Models. *CARTILAGE*, 9(1):80–88, jan 2018.

[108] Yutaka Nakoshi, Masahiro Hasegawa, Koji Akeda, Takahiro Iino, Akihiro Sudo, Toshimichi Yoshida, and Atsumasa Uchida. Distribution and role of tenascin-C in human osteoarthritic cartilage. *Journal of Orthopaedic Science*, 15(5):666–673, sep 2010.

[109] Masahiro Hasegawa, Toshimichi Yoshida, and Akihiro Sudo. Role of tenascin-C in articular cartilage. *Modern Rheumatology*, 28(2):215–220, mar 2018.

[110] Maria D Mayan, Raquel Gago-Fuentes, Paula Carpintero-Fernandez, Patricia Fernandez-Puente, Purificacion Filgueira-Fernandez, Noa Goyanes, Virginijus Valiunas, Peter R Brink, Gary S Goldberg, and Francisco J Blanco. Articular chondrocyte network mediated by gap junctions: role in metabolic cartilage homeostasis. *Annals of the rheumatic diseases*, 74(1):275–84, jan 2015.

[111] Tatyana M Svitkina, Alexander B Verkhovsky, and Gary G Borisy. Plectin Sidearms Mediate Interaction of Intermediate Filaments with Microtubules and Other Components of the Cytoskeleton. *The Journal of Cell Biology*, 135(4):991–1007, 1996.

[112] Arif T Jan, Eun J Lee, and Inho Choi. Fibromodulin: A regulatory molecule maintaining cellular architecture for normal cellular function. *The International Journal of Biochemistry & Cell Biology*, 80:66–70, 2016.

[113] Douglas R Keene, James D San Antonio, Richard Mayne, David J McQuillan, George Sarris, Samuel A Santoro, and Renato V Iozzo. Decorin Binds Near the C Terminus of Type I Collagen. *The Journal of Biological Chemistry*, 275(29):21801–21804, 2000.

[114] K G Vogel, M Paulsson, and D Heinegård. Specific inhibition of type I and type II collagen fibrillogenesis by the small proteoglycan of tendon. *The Biochemical journal*, 223(3):587–597, nov 1984.

[115] Renato V Iozzo and Liliana Schaefer. Proteoglycan form and function: A comprehensive nomenclature of proteoglycans. *Matrix Biology*, 42:11–55, 2015.

[116] Claus Rühland, Elke Schönherr, Horst Robenek, Uwe Hansen, Renato V. Iozzo, Peter Bruckner, and Daniela G. Seidler. The glycosaminoglycan chain of decorin plays an important role in collagen fibril formation at the early stages of fibrillogenesis. *FEBS Journal*, 274(16):4246–4255, aug 2007.

[117] Charles C. Reed and Renato V. Iozzo. The role of decorin in collagen fibrillogenesis and skin homeostasis. *Glycoconjugate Journal*, 19:249–255, may 2003.

[118] Joseph P. R. O. Orgel, Aya Eid, Olga Antipova, Jordi Bella, and John E. Scott. Decorin Core Protein (Decoron) Shape Complements Collagen Fibril Surface Structure and Mediates Its Binding. *PLoS ONE*, 4(9):e7028, sep 2009.

[119] Gene A Homandberg, Ross Meyers, and Dong-Lin Xie. Fibronectin Fragments Cause Chondrolysis of Bovine Articular Cartilage Slices in Culture. *The Journal of Biological Chemistry*, 267(6):3597–3604, 1992.

[120] Gene A. Homandberg, Catherine Wen, and Francis Hui. Cartilage damaging activities of fibronectin fragments derived from cartilage and synovial fluid. *Osteoarthritis and Cartilage*, 6:231–244, jul 1998.

[121] Jack Lawler. The functions of thrombospondin-1 and-2. *Current Opinion in Cell Biology*, 12(5):634–640, oct 2000.

[122] Paul E DiCesare, Matthias Mörgelin, Karlheinz Mann, and Mats Paulsson. Cartilage oligomeric matrix protein and thrombospondin 1. *European Journal of Biochemistry*, 223(3):927–937, 1994.

[123] Josephine C. Adams. Thrombospondins: Multifunctional Regulators of Cell Interactions. *Annual Review of Cell and Developmental Biology*, 17(1):25–51, nov 2001.

[124] Mukundan Attur, Qing Yang, Kohei Shimada, Yuki Tachida, Hiroyuki Nagase, Paolo Mignatti, Lauren Statman, Glyn Palmer, Thorsten Kirsch, Frank Beier, and Steven B. Abramson. Elevated expression of periostin in human osteoarthritic cartilage and its potential role in matrix degradation via matrix metalloproteinase-13. *The FASEB Journal*, 29(10):4107–4121, oct 2015.

[125] Ryota Chijimatsu, Yasuo Kunugiza, Yoshiaki Taniyama, Norimasa Nakamura, Tetsuya Tomita, and Hideki Yoshikawa. Expression and pathological effects of periostin in human osteoarthritis cartilage. *BMC Musculoskeletal Disorders*, 16(1):1–12, dec 2015.

[126] Ryoko Inaki, Yuko Fujihara, Akira Kudo, Masaki Misawa, Atsuhiko Hikita, Tsuyoshi Takato, and Kazuto Hoshi. Periostin contributes to the maturation and shape retention of tissue-engineered cartilage. *Scientific Reports*, 8(1):1–13, dec 2018.

[127] Lei Cai, RobertH. Brophy, EricD. Tycksen, Xin Duan, RyanM. Nunley, and MuhammadFarooq Rai. Distinct expression pattern of periostin splice variants in chondrocytes and ligament progenitor cells. *The FASEB Journal*, 33(7):8386–8405, 2019.

[128] Daisy S Nakamura, Judith M Hollander, Tomoya Uchimura, Heber C Nielsen, and Li Zeng. Pigment Epithelium-Derived Factor (PEDF) mediates cartilage matrix loss in an age-dependent manner under inflammatory conditions. *BMC Musculoskeletal Disorders*, 18(39):1–12, 2017.

[129] Christine Widmer, Jan M Gebauer, Elena Brunstein, Sabrina Rosenbaum, Frank Zaucke, Cord Drögemüller, Tosso Leeb, and Ulrich Baumann. Molecular basis for the action of the collagen-specific chaperone Hsp47/SERPINH1 and its structure-specific client recognition. *PNAS*, 109(33):13243–13247, aug 2012.

[130] Yusaku Masago, Akihiro Hosoya, Kunito Kawasaki, Shogo Kawano, Akira Nasu, Junya Toguchida, Katsumasa Fujita, Hiroaki Nakamura, Gen Kondoh, and Kazuhiro Nagata. The molecular chaperone Hsp47 is essential for cartilage and endochondral bone formation. *Journal of Cell Science*, 125:1118–1128, mar 2012.

[131] Takeshi Tsuda. Extracellular Interactions between Fibulins and Transforming Growth Factor (TGF)-β in Physiological and Pathological Conditions. *International Journal of Molecular Sciences*, 19(2787):1–18, 2018.

[132] Francois-Xavier Sicot, Takeshi Tsuda, Dessislava Markova, John F Klement, Machiko Arita, Rui-Zhu Zhang, Te-Cheng Pan, Robert P Mecham, David E Birk, and Mon-Li Chu. Fibulin-2 Is Dispensable for Mouse Development and Elastic Fiber Formation. *Molecular and Cellular Biology*, 28(3):1061–1067, 2008.

[133] Rupert Timpl, Takako Sasaki, Günter Kostka, and Mon-Li Chu. Fibulins: a versatile family of extracellular matrix proteins. *Nature Reviews Molecular Cell Biology*, 4(6):479–489, jun 2003.

[134] Cheikh Menaa, Rowena D. Devlin, Sakamuri V. Reddy, Yair Gazitt, Sun Jin Choi, and G. David Roodman. Annexin II increases osteoclast formation by stimulating the proliferation of osteoclast precursors in human marrow cultures. *Journal of Clinical Investigation*, 103(11):1605–1613, jun 1999.

[135] Alexander J Kvist, Alexander Nyström, Kjell Hultenby, Takako Sasaki, Jan F Talts, and Anders Aspberg. The major basement membrane components localize to the chondrocyte pericellular matrix-A cartilage basement membrane equivalent? *Matrix Biology*, 27:22–33, 2008.

[136] Ilona Polur, Peter L Lee, Jacqueline M Servais, Lin Xu, and Yefu Li. Role of HTRA1, a serine protease, in the progression of articular cartilage degeneration. *Histology and histopathology*, 25(5):599–608, 2010.

[137] Gehua Zhen and Xu Cao. Targeting TGFβ signaling in subchondral bone and articular cartilage homeostasis. *Trends in pharmacological sciences*, 35(5):227–236, may 2014.

[138] Y. Chi, J. Antoniou, and A. Philip. CD109 inhibits transforming growth factor-beta signaling and extracellular matrix protein production in human chondrocytes. *Osteoarthritis and Cartilage*, 23:A152, apr 2015.

[139] Haijun Tian, Xiaoda Bi, Chen-Shuang Li, Ke-Wei Zhao, Elsa J Brochmann, Scott R Montgomery, Bayan Aghdasi, Deyu Chen, Michael D Daubs, Jeffrey C Wang, and Samuel S Murray. Secreted phosphoprotein 24 kD (Spp24) and Spp14 affect TGF-β induced bone formation differently. *PloS one*, 8(8):e72645, 2013.

[140] Elsa J. Brochmann, Keyvan Behnam, and Samuel S. Murray. Bone morphogenetic protein2 activity is regulated by secreted phosphoprotein24 kd, an extracellular pseudoreceptor, the gene for which maps to a region of the human genome important for bone quality. *Metabolism*, 58(5):644–650, may 2009.

[141] M J Benito, D J Veale, O FitzGerald, W B van den Berg, and B Bresnihan. Synovial tissue inflammation in early and late osteoarthritis. *Annals of the rheumatic diseases*, 64(9):1263–1267, sep 2005.

[142] Andrew D. Pearle, Russell F. Warren, and Scott A. Rodeo. Basic science of articular cartilage and osteoarthritis, 2005.

[143] Farshid Guilak, Robert J Nims, Amanda Dicks, Chia-Lung Wu, and Ingrid Meulenbelt. Osteoarthritis as a disease of the cartilage pericellular matrix. *Matrix Biology*, 71-72:40–50, 2018.

[144] Alice J Sophia Fox, Asheesh Bedi, and Scott A Rodeo. The Basic Science of Articular Cartilage: Structure, Composition, and Function. *Sports Health*, 1(6):461–468, 2009.

[145] Mohit Kapoor, Johanne Martel-Pelletier, Daniel Lajeunesse, Jean Pierre Pelletier, and Hassan Fahmi. Role of proinflammatory cytokines in the pathophysiology of osteoarthritis. *Nature Reviews Rheumatology*, 7:33–42, 2011.

[146] Benoît Porée, Magdalini Kypriotou, Christos Chadjichristos, Gallic Beauchef, Emmanuelle Renard, Florence Legendre, Martine Melin, Sylviane Gueret, Daniel Jean Hartmann, Frédéric Malléin-Gerin, Jean Pierre Pujol, Karim Boumediene, and Philippe Galéra. Interleukin-6 (IL-6) and/or soluble IL-6 receptor down-regulation of human type II collagen gene expression in articular chondrocytes requires a decrease of Sp1·Sp3 ratio and of the binding activity of both factors to the COL2A1 promoter. *Journal of Biological Chemistry*, 2008.

[147] A. D. Rowan, P. J.T. Koshy, W. D. Shingleton, B. A. Degnan, J. K. Heath, A. B. Vernallis, J. R. Spaull, P. F. Life, K. Hudson, and T. E. Cawston. Synergistic effects of glycoprotein 130 binding cytokines in combination with interleukin-1 on cartilage collagen breakdown. *Arthritis and Rheumatism*, 2001.

[148] John A. Mengshol, Matthew P. Vincenti, Charles I. Coon, Aaron Barchowsky, and Constance E. Brinckerhoff. Interleukin-1 induction of collagenase 3 (matrix metalloproteinase 13) gene expression in chondrocytes requires p38, c-Jun N-terminal kinase, and nuclear factor ??B: Differential regulation of collagenase 1 and collagenase 3. *Arthritis and Rheumatism*, 43(4):801–811, 2000.

[149] Pascal Reboul, Jean Pierre Pelletier, Ginette Tardif, Jean Marie Cloutier, and Johanne Martel-Pelletier. The new collagenase, collagenase-3, is expressed and synthesized by human chondrocytes but not by synoviocytes: A role in osteoarthritis. *Journal of Clinical Investigation*, 97(9):2011–2019, 1996.

[150] Juan Xue, Jianlong Wang, Qiang Liu, and Aijing Luo. Tumor necrosis factor-α induces ADAMTS-4 expression in human osteoarthritis chondrocytes. *Molecular Medicine Reports*, 8(6):1755–1760, 2013.

[151] Veronique Lefebvre, Chantal Peeters-Joris, and Gilbert Vaes. Modulation by interleukin 1 and tumor necrosis factor a of production of collagenase, tissue inhibitor of metalloproteinases and collagen types in differentiated and dedifferentiated articular chondrocytes. *BBA - Molecular Cell Research*, 1052(3):366–378, 1990.

[152] Cheryle A Séguin and Suzanne M Bernier. TNFalpha suppresses link protein and type II collagen expression in chondrocytes: Role of MEK1/2 and NF-kappaB signaling pathways. *Journal of cellular physiology*, 197(3):356–69, 2003.

[153] J Saklatvala. Tumour necrosis factor alpha stimulates resorption and inhibits synthesis of proteoglycan in cartilage. *Nature*, 322:547–549, 1986.

[154] P A Guerne, D A Carson, and M Lotz. IL-6 production by human articular chondrocytes. Modulation of its synthesis by cytokines, growth factors, and hormones in vitro. *Journal of immunology (Baltimore, Md. : 1950)*, 144(2):499–505, jan 1990.

[155] M Lotz, R Terkeltaub, and P M Villiger. Cartilage and joint inflammation. Regulation of IL-8 expression by human articular chondrocytes. *Journal of immunology (Baltimore, Md. : 1950)*, 148(2):466–473, 1992.

[156] Anika I Tsuchida, Michiel Beekhuizen, Marijn Rutgers, Gerjo JVM van Osch, Joris EJ Bekkers, Arjan GJ Bot, Bernd Geurts, Wouter JA Dhert, Daniel BF Saris, and Laura B Creemers. Interleukin-6 is elevated in synovial fluid of patients with focal cartilage defects and stimulates cartilage matrix production in an in vitro regeneration model. *Arthritis research*, 14:1–12, 2012.

[157] Anika I Tsuchida, Michiel Beekhuizen, Marieke Hart, Timothy Radstake, Wouter JA Dhert, Daniel BF Saris, Gerjo van Osch, and Laura B Creemers. Cytokine profiles in the joint depend on pathology, but are different between synovial fluid, cartilage tissue and cultured chondrocytes. *Arthritis research & therapy*, 16:1–15, 2014.

[158] Mary B Goldring. Osteoarthritis and Cartilage: The Role of Cytokines. *Current Rheumatology Reports*, 2:459–465, 2000.

[159] Mary B Goldring, Miguel Otero, Darren A Plumb, Cecilia Dragomir, Marta Favero, Karim El Hachem, Ko Hashimoto, Helmtrud I Roach, Eleonora Olivotto, Rosa Maria Borzì, and Kenneth B Marcu. Roles of inflammatory and anabolic cytokines in cartilage metabolism: signals and multiple effectors converge upon MMP-13 regulation in osteoarthritis. *European Cells and Materials*, 21:202–220, 2014.

[160] Peter M Van Der Kraan. The Interaction between Joint Inflammation and Cartilage Repair. *Tissue Engineering and Regenerative Medicine*, 16(4):327–334, 2019.

[161] Carola Cavallo, Giovanna Desando, Andrea Facchini, and Brunella Grigolo. Chondrocytes from patients with osteoarthritis express typical extracellular matrix molecules once grown onto a three-dimensional hyaluronan-based scaffold. *Journal of Biomedical Materials Research - Part A*, 93(1):86–95, 2010.

[162] Aki Namba, Yukiko Aida, Naoto Suzuki, Yusuke Watanabe, Takayuki Kawato, Masafumi Motohashi, Masao Maeno, Hideo Matsumura, and Mitsuhiko Matsumoto. Effects of IL-6 and Soluble IL-6 Receptor on the Expression of Cartilage Matrix Proteins in Human Chondrocytes. *Connective Tissue Research*, 48(5):263–270, 2007.

[163] M. Lotz and P. A. Guerne. Interleukin-6 induces the synthesis of tissue inhibitor of metalloproteinases-1/erythroid potentiating activity (TIMP-1/EPA). *Journal of Biological Chemistry*, 266(4):2017–2020, 1991.

[164] J Martel-Pelletier, N Alaaeddine, and J P Pelletier. Cytokines and their role in the pathophysiology of osteoarthritis. *Frontiers in bioscience : a journal and virtual library*, 4:D694–703, 1999.

[165] Hans Georg Schaible, G. Segond Von Banchet, M. K. Boettger, R. Bräuer, M. Gajda, F. Richter, S. Hensellek, D. Brenn, and G. Natura. The role of proinflammatory cytokines in the generation and maintenance of joint pain: Annals of the New York Academy of Sciences. *Annals of the New York Academy of Sciences*, 1193:60–69, 2010.

[166] C. Sanchez, A.-C. Bay-Jensen, T. Pap, M. Dvir-Ginzberg, H. Quasnichka, R. Barrett-Jolley, A. Mobasheri, and Y. Henrotin. Chondrocyte secretome: a source of novel insights and exploratory biomarkers of osteoarthritis. *Osteoarthritis and Cartilage*, 25(8):1199–1209, aug 2017.

[167] Ming-Feng Hsueh, Patrik Önnerfjord, and Virginia Byers Kraus. Biomarkers and proteomic analysis of osteoarthritis. *Matrix Biology*, 39:56–66, oct 2014.

[168] Richard Wilson, Emma L Norris, Bent Brachvogel, Constanza Angelucci, Snezana Zivkovic, Lavinia Gordon, Bianca C Bernardo, Jacek Stermann, Kiyotoshi Sekiguchi, Jeffrey J Gorman, and John F Bateman. Changes in the Chondrocyte and Extracellular Matrix Proteome during Post-natal Mouse Cartilage Development. *Molecular & Cellular Proteomics*, 11:1–18, 2012.

[169] Richard Wilson, Anders F Diseberg, Lavinia Gordon, Snezana Zivkovic, Liliana Tatarczuch, Eleanor J Mackie, Jeffrey J Gorman, and John F Bateman. Comprehensive Profiling of Cartilage Extracellular Matrix Formation and Maturation Using Sequential Extraction and Label-free Quantitative Proteomics. *Molecular & Cellular Proteomics*, 9(1296-1313), 2010.

[170] John E. Paderi and Alyssa Panitch. *Biomacromolecules*.

[171] Takahiro Niikura and A. Hari Reddi. *Arthritis & Rheumatism*.

[172] A R Poole, I Pidoux, A Reiner, L H Tang, H Choi, and L Rosenberg. *The journal of histochemistry and cytochemistry : official journal of the Histochemistry Society*.

4. ULTRASOUND-GUIDED INTRA-ARTICULAR INJECTIONS IN GUINEA PIG KNEES

This chapter consists of a manuscript by Vazquez-Portalatin N, Breur GJ, Panitch A, and Goergen CJ, published in Bone and Joint Research, Volume 4, Issue 1, 2015.

4.1 Abstract

Dunkin Hartley guinea pigs, a commonly used animal model of osteoarthritis, were used to determine if high frequency ultrasound can ensure intra-articular injections are accurately positioned in the knee joint. A high-resolution small animal ultrasound system with a 40 MHz transducer was used for image-guided injections. A total of 36 guinea pigs were anaesthetized with isoflurane and placed on a heated stage. Sterile needles were inserted directly into the knee joint medially, while the transducer was placed on the lateral surface, allowing the femur, tibia, and fat pad to be visualized in the images. B-mode cine loops were acquired during 100 μL. We assessed our ability to visualize 1) important anatomical landmarks, 2) the needle and 3) anatomical changes due to the injection. From the ultrasound images, we were able to visualize clearly the movement of anatomical landmarks in 75% of the injections. The majority of these showed separation of the fat pad (67.1%), suggesting the injections were correctly delivered in the joint space. We also observed dorsal joint expansion (23%) and patellar tendon movement (10%) in a smaller subset of injections. The results demonstrate this image-guided technique can be used to visualize the location of an intra-articular injection in the joints of guinea pigs. Future studies using an ultrasound-guided approach could help improve the injection accuracy in a variety of anatomical locations and animal models, in the hopes of developing anti-arthritic therapies.

4.2 Introduction

Osteoarthritis is a chronic joint condition characterized by joint pain, crepitus, reduction of range of movement and variable degrees of inflammation, cartilage erosion and subchondral changes in bone. It is estimated that somewhere between 15% and 20% of the entire US population suffers from some form of arthritis [1]. While osteoarthritis occurs at multiple locations, cartilage breakdown in the knee leads to significant comorbidities since these are weight-bearing joints [2]. The development of locally injected anti-arthritic drugs to limit or even prevent cartilage breakdown is a current area of research [3–6], but it is difficult to ensure that injected material is deposited adjacent to cartilage in the synovial space. These false positives can lead to question of whether a therapy is not working correctly or has simply not been delivered to the right location. Previous clinical studies in humans have demonstrated that ultrasound guidance will improve the accuracy of an intra-articular injection [7–10], but similar studies that focus on animal disease models have not been conducted. Indeed, the small body size of many laboratory animals requires high frequency ultrasound capable of producing images with good image resolution at shallow depths [11–13].

Dunkin Hartley guinea pigs develop spontaneous, age-related osteoarthritis, characterized by cartilage degeneration, osteophyte formation, subchondral bone changes and synovitis, making these animals a popular disease model for the human condition [14]. These albino guinea pigs have histological evidence of osteoarthritis as early as three months old and disease severity continues to increase with age. Previous work has shown that proteoglycan content increases, collagen concentration in cartilage decreases, and radiological changes (including osteophyte formation, sclerosis of subchondral bone, femoral condyle cyst formation and calcification of collateral ligaments) present more in older animals [14]. At the level of the tibial plateau, their knee joints are typically 2 cm to 3 cm in the cranio-caudal direction and 1 cm to 2 cm in the medio-lateral direction. The joint is $<$ 1 cm below the skins surface in

the parapatellar region. These features thus make visualization with high frequency ultrasound possible.

The purpose of this study was to determine if high-frequency ultrasound could be used to ensure intra-articular injections were correctly deposited in the knee joint. While we focused on the knees of Dunkin Hartley guinea pigs, the methods of ultrasound-guided injection described here could be used to improve accuracy of injection in a variety of small animal models. Indeed, joint visualization should be possible as long as the anatomy allows for both needle insertion and placement of the ultrasound transducer head. We did not focus on direct visualization of the needle with ultrasound, but rather the movement and changes within the intra-articular space in order to quantify the location of the injection. Future small animal studies using this ultrasound-guided approach can help confirm intra-articular deposition of injected fluid and aid in the development of anti-arthritic therapies.

4.3 Materials and Methods

4.3.1 Animal Model

A total of 216 injections in 36 Dunkin Hartley guinea pigs were imaged for this study: 12 animals received one injection bilaterally, 12 animals received three injections bilaterally, and 12 animals received five injections bilaterally. The right stifle joints were injected with 100 μL of phosphate-buffered saline and the left joints with 100 μL of a proteoglycan (aggrecan) mimetic. Animals were anaesthetized with 2% to 5% isoflurane in 2 L/min O_2 using a chamber and a mask. The hair covering both knee joints was removed with clippers and the skin was scrubbed with chlorhexidine gluconate (2% dilution) and sterile saline. The rate of respiration was monitored visually and each animal was placed on a heated stage to maintain body temperature. Depth of anaesthesia was assessed with periodic toe pinches. Alcohol swabs were used to clean the transducer and stage between animals.

Figure 4.1.: Photograph of intra-articular injections in the right knee of a guinea pig. Image shows the ultrasound transducer, needle and knee during the injection. The right hand of the operator held the syringe that was inserted in the joint, while the left hand controlled the positioning of the limb of the guinea pig. The ultrasound probe, clamped to an adjustable rail system (not shown), was oriented in a craniolateral-caudomedial oblique direction.

4.3.2 Ultrasound Imaging

A high-resolution small animal ultrasound system was used for the image-guided injections (Vevo2100, FUJIFILM VisualSonics Inc., Toronto, Canada). A 256-element, 40 MHz linear transducer with a 7.0 mm geometric focus (MS550D) was clamped to an adjustable bench-mounted rail system designed for the positioning of a small animal. The axial, lateral and elevation image resolution were 40 μm, 90μm, and 193 μm, respectively. Guinea pigs were positioned in dorsal recumbency on the heated stage such that the knee joint could be easily manipulated (Figure 4.1).

A sterile 28-gauge needle was then inserted approximately halfway between the patella and tibial tuberosity, just medial to the patellar tendon. The needle was inserted into the knee joint until it was in direct contact with the medial condyle of the femur, without the benefit of ultrasound visualization (Figure 4.1). We then applied sterile ultrasound gel over the lateral joint area before lowering the ultrasound

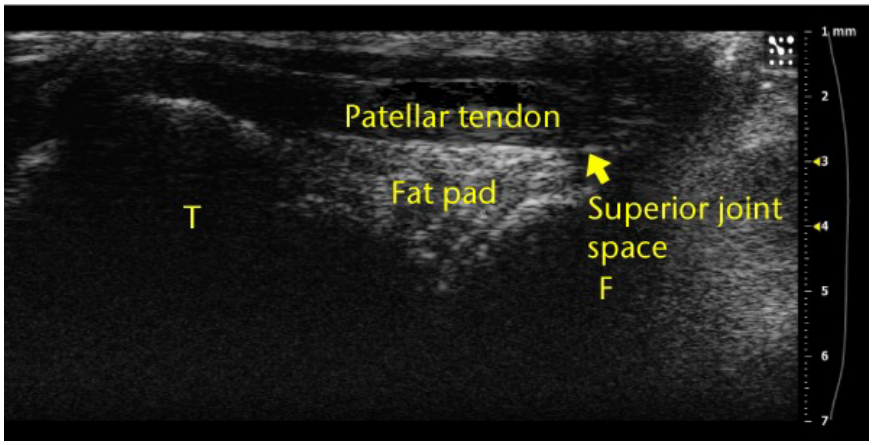

Figure 4.2.: Example ultrasound image of a knee joint with labels over the femur ('F'), tibia ('T'), superior joint space and fat pad. These anatomical landmarks were observed for each injection.

probe to the animal. Moderate extension of the joint and firmly pushing the back of the leg against the transducer surface is crucial to visualize the tibial plateau, medial femoral condyle and fat pad at the same time. We further refined the joint position until lucent lines separating the fat pad and tibia and fat pad and femur, representing joint space and articular cartilage, were clearly distinguishable (Figure 4.2). The needle was inserted at an angle of 45 ° to the long axis of the ultrasound transducer in order to image the entire joint, including the femur, tibia and fat pad. Once an acceptable orientation was obtained, a 500-frame B-mode cine loop of approximately five seconds was acquired during the 100 μL injection of aggrecan mimic or PBS (control). For each animal, one knee received aggrecan mimic injections while the contralateral joint received PBS injections. We then assessed our ability to visualize 1) important anatomical landmarks, 2) the needle and 3) anatomical changes due to the injection.

4.4 Results and Discussion

Anatomical landmarks of the knee joint could be distinguished from the ultrasound images in all animals (Figure 4.2) and clearly visualized 75% of the injections (Table

4.1). We defined 'visualized' injections as those where separation, movement, or expansion due to the build-up of intra-articular fluid was observed of the fat pad, of the joint space dorsal to the patella and trochlea, or of the patellar tendon. Separation of the fat pad was identified when the fat pad was physically pushed away from the femur or tibia (Figure 4.3). Dorsal joint expansion was identified when fluid or bubbles moved into the joint space proximal to the patella or trochlea. Finally, movement of the patellar tendon was identified as injections that led to a pressure increase that caused the tendon to bend or arch. No differences between injections of aggrecan mimic or PBS were observed. Table 4.1 summarizes our results by identifying and characterizing several anatomical features and observed movement due the injections.

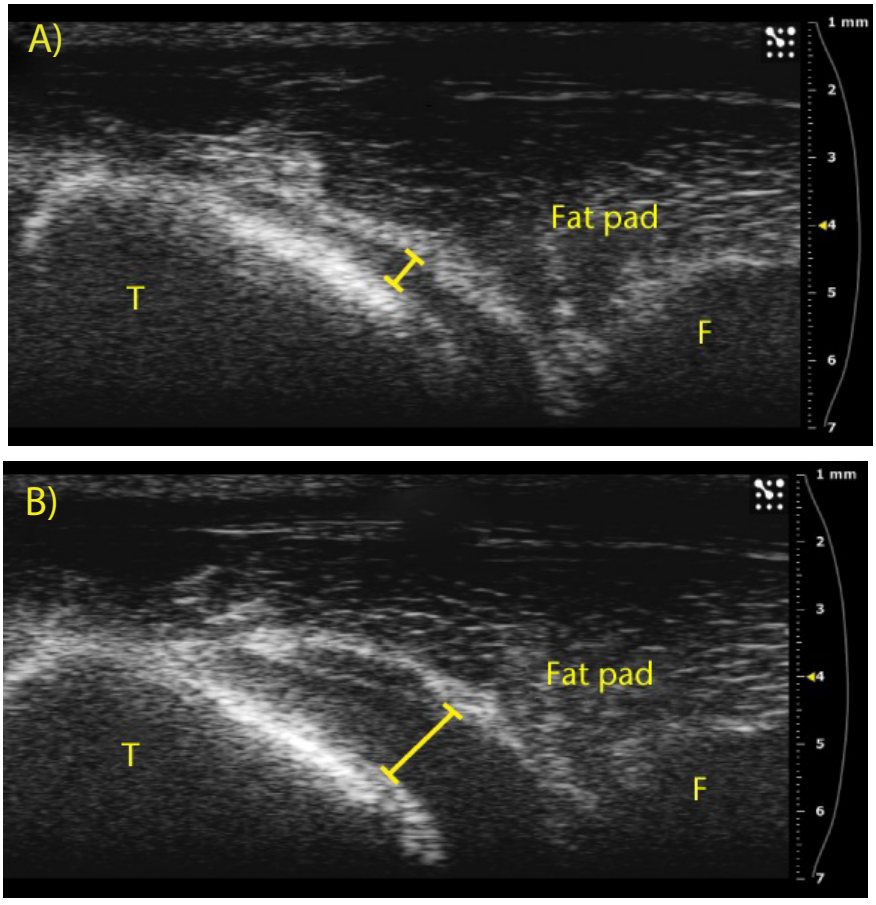

Figure 4.3.: Ultrasound images showing substantial separation of the fat pad from the tibia (A) before and (B) after an injection.

Table 4.1.: Summary of total injections visualized and anatomical landmarks observed. We quantified the number and percentage of injections where the needle or movement of the fat pad, superior joint space and/or patellar tendon was clearly observed.

	Number of Injections	Visualized	Needle Observed	Fat Pad Observed	Separation of Fat Pad	Superior Joint Space Observed	Superior Joint Space Expansion	Patellar Tendon Observed	Patellar Tendon Movement
n (%)	216	162 (*75.0*)	21 (*9.7*)	205 (*95.0*)	145 (*67.1*)	108 (*50.0*)	50 (*23.1*)	92 (*42.6*)	22 (*10.2*)

The vast majority of the ultrasound images where the injection was visualized also showed separation of the fat pad (145 of 162; 89.5%), providing confidence that the injected fluid was delivered to the correct location. Furthermore, proximal/superior joint expansion was observed both with and without separation of the fat pad. Only 12 of the 50 injections where dorsal joint space expansion was observed occurred without separation of the fat pad. We also observed small bubbles in 28 of the images (Figure 4.4A), an occurrence that increased echogenicity of the injected fluid and helped with visualization. Finally, five injections led to subcutaneous expansion below the skin surface but above the patellar tendon (Figure 4.4B).

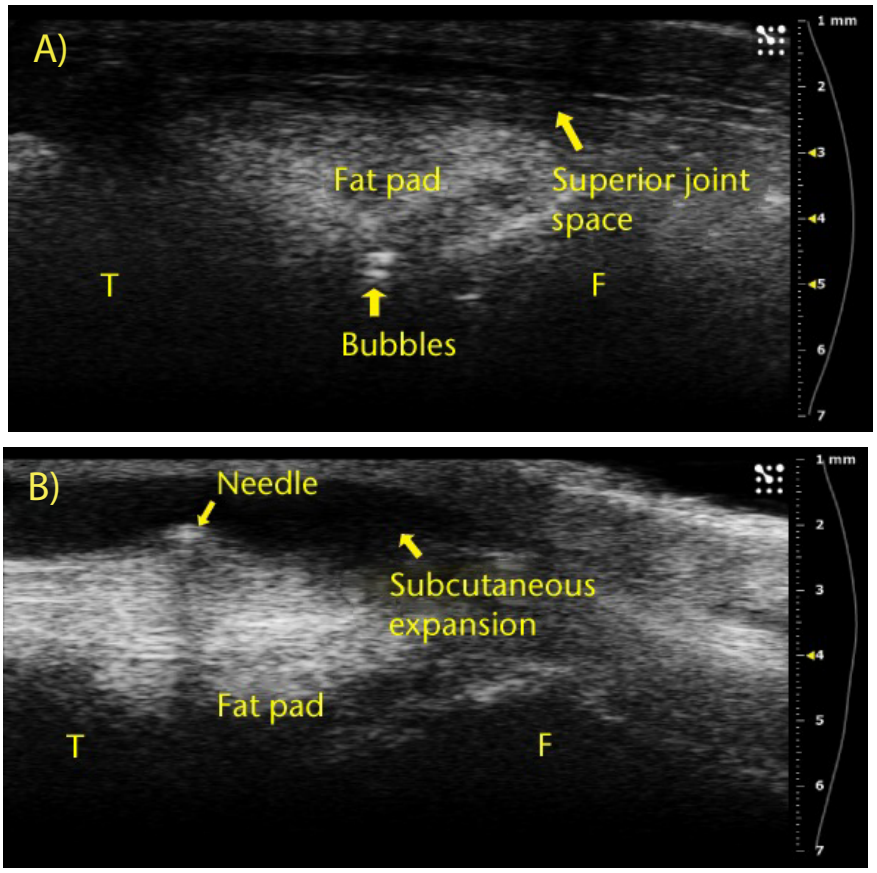

Figure 4.4.: Ultrasound images showing (A) that bubbles helped visualize the injections and were clearly observed in the joint space between femur and fat pad. The needle (B) and subsequent metal shadow are clearly seen during an injection that created subcutaneous expansion.

The results of this study suggest that high frequency ultrasound can be used to measure the accuracy of intra-articular injections in the knee joints of Dunkin Hartley guinea pigs. Because of the size of the stifle joint and the need to maintain aseptic technique, insertion of the needle under ultrasound guidance was not possible. However, we were able to demonstrate that 75% of the injections were deposited intra-articularly. The small knee joint size, difficulties with probe positioning, variation in the location of the needle tip and unanticipated animal limb movement during the injection are likely reasons why we were not able to visualize 25% of the injections. Furthermore, even though we made a strong effort to keep the ultrasound probe position consistent, the innate variation between animals and the fast injection times meant that visualization was not always possible. In future studies, longer cine loops of more than 500 frames can be obtained to help ensure the exact time of injection is acquired with the ultrasound system.

We realized during this study that several small changes could be made to improve visualization of the injection. First, we began adding a small amount of air into the syringes in order to create bubbles during the injection. These bubbles helped us distinguish exactly where the injected fluid appeared and spread. Similarly, contrast-enhanced ultrasound using gas-filled microbubbles has become common in clinical imaging [15]. Second, the knee joints were also placed on the left side of the image such that both the fat pad and superior joint space could be visualized at the same time. This joint placement facilitated observation of injections that spread from the center of the joint into the superior joint space. Finally, small movements of the needle, before the injection, allowed us to localize the tip location by either visualization of the metal artifact caused by the needle, or from movement of adjacent tissue. While the 90° orientation difference between the probe and needle reduced our ability to directly visualize the tip, small amounts of movement of the needle helped to ensure tip placement near the cartilage surface. Our experience also suggests that both the success of the injection and quality of the image improves with practice.

This high frequency technique of ultrasound injection could be used to help guide intra-articular needle placement for studies that focus on developing treatments for osteoarthritis with a variety of animal models. While we focused on the knee in this study, the hip, shoulder, elbow, or any other joint where arthritis is common, could also benefit from the use of ultrasound to improve the accuracy of injections. This is particularly important as advancements in protein and tissue engineering have led to exciting new potential candidates that may one day slow, prevent, or even reverse cartilage damage [5, 6].

The choice of animal models and anatomy will influence the ideal ultrasound frequency and position of the probe. Larger animals or joints deep within the body would likely require transducer frequencies of <40 MHz due to the inverse relationship between frequency and depth. In other words, lower frequency ultrasound can penetrate deeper into the body, but then produces images with a lower resolution. Furthermore, joint anatomy and positioning are important to consider as ultrasound does not easily penetrate calcified bone. The dense femur and tibia comprising the knee required us to place the joint in moderate flexion such that the intra-articular space could be visualized. Thus, ultrasound probe placement, in addition to needle insertion, may require some adjustments depending on the size, depth and orientation of the region of interest. If the desired location is not reached, an injection can always be repeated to ensure proper administration. Indeed, clinical studies have shown that the use of ultrasound improves the accuracy of injection in the knee [7, 10] and hip [9].

4.5 Conclusion

In conclusion, these data suggest that high frequency ultrasound can be used to visualize intra-articular needle placement and injections in small animals. Separation of the fat pad from the cartilage surface showed that fluid accumulates in the correct location within the knee joint. This method could also be used with different fre-

quency probes for other animal models to ensure the correct positioning of injections when developing anti-osteoarthritic therapies.

4.6 Acknowledgements

This work was supported by the Purdue Research Foundation Trask Innovation Fund. A. Panitch reports that monies have been received by the NIH and Symic Biomedical to Purdue University which is not related to this article.

4.7 References

[1] Reva C. Lawrence, Charles G. Helmick, Frank C. Arnett, Richard A. Deyo, David T. Felson, Edward H. Giannini, Stephen P. Heyse, Rosemarie Hirsch, Marc C. Hochberg, Gene G. Hunder, Matthew H. Liang, Stanley R. Pillemer, Virginia D. Steen, and Frederick Wolfe. Estimates of the prevalence of arthritis and selected musculoskeletal disorders in the United States. *Arthritis and Rheumatism*, 41:778–799, 1998.

[2] David T Felson. Clinical practice. Osteoarthritis of the knee. *The New England Journal of Medicine*, 354:841–848, 2006.

[3] Andrea J. Boon, Jay Smith, Diane L. Dahm, Eric J. Sorenson, Dirk R. Larson, Patrick D. Fitz-Gibbon, Dennis D. Dykstra, and Jasvinder A. Singh. Efficacy of intra-articular Botulinum Toxin type A in painful knee osteoarthritis: A pilot study. *PM and R*, 2:268–276, 2010.

[4] Elizaveta Kon, Roberto Buda, Giuseppe Filardo, Alessandro Di Martino, Antonio Timoncini, Annarita Cenacchi, Pier Maria Fornasari, Sandro Giannini, and Maurilio Marcacci. Platelet-rich plasma: Intra-articular knee injections produced favorable results on degenerative cartilage lesions. *Knee Surgery, Sports Traumatology, Arthroscopy*, (18):472–479, 2010.

[5] Jonathan C. Bernhard and Alyssa Panitch. Synthesis and characterization of an aggrecan mimic. *Acta Biomaterialia*, pages 1543–1550, 2012.

[6] Shaili Sharma, Alyssa Panitch, and Corey P. Neu. Incorporation of an aggrecan mimic prevents proteolytic degradation of anisotropic cartilage analogs. *Acta Biomaterialia*, (9):4618–4625, 2013.

[7] Erika L. Daley, Sarvottam Bajaj, Leslie J. Bisson, and Brian J. Cole. Improving injection accuracy of the elbow, knee, and shoulder: Does injection site and imaging make a difference? A systematic review. *American Journal of Sports Medicine*, 39:656–662, 2011.

[8] Douglas W. Jackson, Nicholas A. Evans, and Bradley M. Thomas. Accuracy of needle placement into the intra-articular space of the knee. *Journal of Bone and Joint Surgery. American volume*, 84-A:1522–1527, 2002.

[9] Mikel Sánchez, Jorge Guadilla, Nicolás Fiz, and Isabel Andia. Ultrasound-guided platelet-rich plasma injections for the treatment of osteoarthritis of the hip. *Rheumatology (Oxford)*, (51):144–150, 2012.

[10] W. L. Sibbitt, L. G. Kettwich, P. A. Band, N. R. Chavez-Chiang, S. L. DeLea, L. J. Haseler, and A. D. Bankhurst. Does ultrasound guidance improve the outcomes of arthrocentesis and corticosteroid injection of the knee? *Scandinavian Journal of Rheumatology*, 41:66–72, 2012.

[11] K Shung, Jonathan Cannata, Member Qifa Zhou, and Jungwoo Lee. High frequency ultrasound: A new frontier for ultrasound. *Conference proceedings : ... Annual International Conference of the IEEE Engineering in Medicine and Biology Society. IEEE Engineering in Medicine and Biology Society. Conference*, 2009:1953–1955, 2009.

[12] K. Kirk Shung. High Frequency Ultrasonic Imaging. *Journal of Medical Ultrasound*, (17):25–30, 2009.

[13] J.-M. Grégoire, S. Serrière, G. Georgesco, F. Jamet, A. Bleuzen, F. Ossant, F. Levassort, F. Tranquart, and F. Patat. Techniques and applications of noninvasive high-resolution ultrasound imaging. *Journal de Radiologie*, 87:1920–1936, 2006.

[14] P A Jimenez, S S Glasson, O V Trubetskoy, and H B Haimes. Spontaneous osteoarthritis in Dunkin Hartley guinea pigs: histologic, radiologic, and biochemical changes. *Laboratory animal science*, (47):598–601, 1997.

[15] Shiva Dindyal and Constantinos Kyriakides. Ultrasound microbubble contrast and current clinical applications. *Recent Patents on Cardiovascular Drug Discovery*, pages 27–41, 2011.

5. CONCLUSIONS AND FUTURE WORK

5.1 Conclusions

Articular cartilage tissue engineering aims to repair damaged cartilage by introducing a combination of cells, scaffold, and bioactive factors that altogether mimic articular cartilage. This thesis took into account the articular cartilage components and the protective role of aggrecan in cartilage degradation to develop scaffolds composed of collagen type I or blends of collagen type I and II that also incorporate the aggrecan mimic. The ultimate goal was to develop a scaffold that could halt the progression of OA and stimulate cartilage repair.

Collagen type I has been extensively used in articular cartilage tissue engineering for over 20 years. However, instead of collagen type I, collagen type II makes up the majority of the collagen present in articular cartilage [1, 2]. Previous studies have shown that collagen type II is able to stabilize chondrocyte morphology [3–6] and stimulate collagen type II synthesis [7–14], but it also exhibits poor mechanical properties [15, 16]. Collagen type II gels have been known to be difficult to synthesize due to collagen type II's lesser ability to form fibrils and incorporate into hydrogels [17]. The focus of Chapter 2 was to create hydrogels composed of different ratios of collagen type I to collagen type II to elucidate their unique properties. The collagen blend hydrogels were able to incorporate both types of collagen and retain chondroitin sulfate (CS) and hyaluronic acid (HA). Using cryoscanning electron microscopy images, we were able to show the 3:1 ratio of collagen type I to type II gels had a lower void space percentage (36.4%) than the 1:1 gels (46.5%). The complex modulus was larger for the 3:1 gels (G*=5.0 Pa) compared to the 1:1 gels (G*=1.2 Pa). Our results demonstrated that the addition of collagen type II alters gel formation, network structure, and mechanical properties. The 3:1 collagen type I to collagen type II ratio blend

formed consistent gels with superior mechanical properties compared to the other blends studied. For this reason, the 3:1 collagen gels were used in subsequent studies.

In Chapter 3, we explored whether an aggrecan mimic, CS-GAH$_b$, composed of CS and HA binding peptides, GAH, and not its separate components, is able to prevent glycosaminoglycan (GAG) and collagen release when incorporated into chondrocyte-embedded collagen gels. Previously, the aggrecan mimic was synthesized using a BMPH crosslinker and was named CS-BMPH-GAH [17]. In Chapter 3, we introduce a new chemistry to synthesize CS-GAH$_b$ without the crosslinker. Bovine chondrocytes were cultured and embedded in collagen type I scaffolds with CS, GAH, CS and GAH, or CS-GAH$_b$ molecules. Gels composed of 3:1 collagen type I and II with CS or CS-GAH$_b$ were also studied. Our findings show that the incorporation of CS-GAH$_b$ in chondrocyte-embedded collagen gels with HA, and not its separate comoponents, is able to prevent GAG and collagen release. CS-GAH$_b$ also stimulated cytokine production during the initial days of scaffold culture. CS-GAH$_b$, however, did not affect the chondrocytes' ECM protein expression in the gels. The incorporation of collagen type II into the collagen type I scaffolds did not significantly affect GAG and cytokine production and ECM protein expression in the gels, but did increase collagen release. The results suggest the complex interaction between CS-GAH$_b$, the chondrocytes, and the gel matrix make these scaffolds promising constructs for articular cartilage repair.

In Chapter 4, we used Dunkin Hartley guinea pigs, commonly used as an animal model of osteoarthritis, to determine whether high frequency ultrasound can ensure intra-articular injections are accurately positioned in the knee joint. A high-resolution small animal ultrasound system with a 40 MHz transducer was used for image-guided injections of 1x PBS or the aggrecan mimic. We assessed our ability to visualize important anatomical landmarks, the needle, and anatomical changes due to the injection. From the ultrasound images, we were able to visualize clearly the movement of anatomical landmarks in 75% of the injections. Separation of the fat pad from the cartilage surface, observed in 67.1% of the injections, showed that fluid accumulates

in the correct location within the knee joint. We also observed dorsal joint expansion (23%) and patellar tendon movement (10%) in a smaller subset of injections. Our results demonstrated that high frequency ultrasound can be used to visualize intra-articular needle placement and injections in small animals. This method could also be used with different frequency probes for other animal models to ensure the correct positioning of injections when developing anti-osteoarthritic therapies.

All of the work presented here suggests that the aggrecan mimic, CS-GAH$_b$, is able to protect collagen and GAGs in the gels and prevent them from being released into the scaffold surroundings, thus, maintaining the scaffold composition. Moreover, the results obtained with the aggrecan mimic could be attributed to an early attempt at repair and could be a signal of anabolic activities in the ECM. Since we are able to effectively inject the aggrecan mimic into the knee joints in small animals, the aggrecan mimic has shown a strong potential for use in cartilage repair, molecular therapy design, and articular cartilage tissue engineering.

5.2 Future Work

Future work will further explore the chondrocyte-embedded collagen type I gels with HA and the aggrecan mimic to determine whether the addition of collagen type II to the gels helps maintain chondrocyte morphology and stimulate cartilaginous tissue synthesis. We will also study the collagen content in the gels and culture medium to determine the amount of collagen incorporated in the gels and the amount released into the surroundings. These experiments will help us further understand the role and effects of collagen type II in these chondrocyte-embedded scaffolds. Moreover, the effects of the aggrecan mimic incorporation into the chondrocyte-embedded collagen gels will be assessed by analyzing the proteins remaining in the collagen gels via LC MS/MS. The collagen type I and collagen type I and II gels with CS, GAH, CS and GAH, and CS-GAH$_b$ will be analyzed after a 7 day culture period. These experiments

will help us better understand these scaffolds and their potential for articular cartilage tissue engineering.

5.3 References

[1] M A Cremer, E F Rosloniec, and A H Kang. The cartilage collagens: a review of their structure, organization, and role in the pathogenesis of experimental arthritis in animals and in human rheumatic disease. *Journal of molecular medicine (Berlin, Germany)*, 76(3-4):275–88, mar 1998.

[2] Hemanth Akkiraju and Anja Nohe. Role of chondrocytes in cartilage formation, progression of osteoarthritis and cartilage regeneration. *Journal of Developmental Biology*, 3:177–192, 2015.

[3] Stefan Nehrer, Howard A. Breinan, Arun Ramappa, Sonya Shortkroff, Gretchen Young, Tom Minas, Clement B. Sledge, Ioannis V. Yannas, and Myron Spector. Canine chondrocytes seeded in type I and type II collagen implants investigated in vitro. *Journal of Biomedical Materials Research*, 1997.

[4] S. Nehrer, H.A. Breinan, A. Ramappa, H-P. Hsu, T. Minas, S. Shortkroff, C.B. Sledge, I.V. Yannas, and M. Spector. Chondrocyte-seeded collagen matrices implanted in a chondral defect in a canine model. *Biomaterials*, 19:2313–2328, 1998.

[5] J. S. Pieper, P. M. Van Der Kraan, T. Hafmans, J. Kamp, P. Buma, J. L C Van Susante, W. B. Van Den Berg, J. H. Veerkamp, and T. H. Van Kuppevelt. Crosslinked type II collagen matrices: Preparation, characterization, and potential for cartilage engineering. *Biomaterials*, 23:3183–3192, 2002.

[6] Vincent Irawan, Tzu-Cheng Sung, Akon Higuchi, and Ikoma Toshiyuki. Collagen Scaffolds in Cartilage Tissue Engineering and Relevant Approaches for Future Development. *Tissue Engineering and Regenerative Medicine*, 15(6):673–697, 2018.

[7] C. W. Chen, Y. H. Tsai, W. P. Deng, S. N. Shih, C. L. Fang, J. G. Burch, W. H. Chen, and W. F. Lai. Type I and II collagen regulation of chondrogenic differentiation by mesenchymal progenitor cells. *Journal of Orthopaedic Research*, 23(2):446–453, 2005.

[8] D Bosnakovski, M Mizuno, G Kim, S Takagi, M Okumura, and T Fujinaga. Chondrogenic differentiation of bovine bone marrow mesenchymal stem cells (MSCs) in different hydrogels: Influence of collagen type II extracellular matrix on MSC chondrogenesis. *Biotechnology and Bioengineering*, 93:1152–1163, 2006.

[9] Elise Duval, Sylvain Leclercq, Jean Marc Elissalde, Magali Demoor, Philippe Galéra, and Karim Boumédiene. Hypoxia-inducible factor 1α inhibits the fibroblast-like markers type I and type III collagen during hypoxia-induced chondrocyte redifferentiation: Hypoxia not only induces type II collagen and aggrecan, but it also inhibits type I and type III collagen i. *Arthritis and Rheumatism*, 2009.

[10] Anne-Marie Freyria, Marie-Claire Ronzière, Delphine Cortial, Laurent Galois, Daniel Hartmann, Daniel Herbage, and Frédéric Mallein-Gerin. Comparative phenotypic analysis of articular chondrocytes cultured within type I or type II collagen scaffolds. *Tissue Engineering Part A*, 15:1233–1245, 2009.

[11] Z. F. Lu, B. Zandieh Doulabi, P. I. Wuisman, R. A. Bank, and M. N. Helder. Influence of collagen type II and nucleus pulposus cells on aggregation and differentiation of adipose tissue-derived stem cells. *Journal of Cellular and Molecular Medicine*, 2008.

[12] Amos Matsiko, John P. Gleeson, and Fergal J. O'Brien. Scaffold Mean Pore Size Influences Mesenchymal Stem Cell Chondrogenic Differentiation and Matrix Deposition. *Tissue Engineering Part A*, 2014.

[13] Henrique V. Almeida, Binulal N. Sathy, Ivan Dudurych, Conor T. Buckley, Fergal J. O'Brien, and Daniel J. Kelly. Anisotropic Shape-Memory Alginate Scaffolds Functionalized with Either Type I or Type II Collagen for Cartilage Tissue Engineering. *Tissue Engineering Part A*, 23:55–68, 2017.

[14] M. Tamaddon, M. Burrows, S. A. Ferreira, F. Dazzi, J. F. Apperley, A. Bradshaw, D. D. Brand, J. Czernuszka, and E. Gentleman. Monomeric, porous type II collagen scaffolds promote chondrogenic differentiation of human bone marrow mesenchymal stem cells in vitro. *Scientific Reports*, 2017.

[15] Laura Calderon, Estelle Collin, Diego Velasco-Bayon, Mary Murphy, Damien O'Halloran, and Abhay Pandit. Type II collagen-hyaluronan hydrogel: a step towards a scaffold for intervertebral disc tissue engineering. *European cells & materials*, 20:134–148, 2010.

[16] Nelda Vazquez-Portalatín, Claire E Kilmer, Alyssa Panitch, and Julie C Liu. Characterization of Collagen Type I and II Blended Hydrogels for Articular Cartilage Tissue Engineering. *Biomacromolecules*, 17:3145–3152, 2016.

[17] Jonathan C. Bernhard and Alyssa Panitch. Synthesis and characterization of an aggrecan mimic. *Acta Biomaterialia*, 8:1543–1550, 2012.

APPENDICES

A. CHARACTERIZATION OF COLLAGEN AND ELASTIN BLEND HYDROGELS

A.1 Abstract

Collagen and elastin networks are present in the extracellular matrix (ECM) of many organs including the skin, blood vessels, and lungs. Thus, collagen and elastin composites have been proposed for use in vascularisation, wound repair, and the development of alveolar and lung replacements. In this study, we characterized gels composed of collagen and elastin blends (1:0, 2:1, 1:1, 2:3, 1:2, and 1:5) to elucidate their unique properties. We demonstrated that the addition of varying amounts of elastin alters collagen fibrillogenesis and D-banding pattern. The addition of elastin in varying ratios does not seem to affect fibril diameter, but has shown to decrease storage modulus. The work presented here serves as a deeper understanding of how varying amounts of elastin affect collagen constructs. This knowledge will prove useful when developing collagen and elastin composites for tissue engineering in the future.

A.2 Introduction

Collagen has been extensively used in tissue engineering due to its biocompatibility, abundant presence in body tissues, and wide clinical approval [1–5]. However, collagen constructs do not fully mimic the complex composition and network as well as the biological and mechanical properties observed in native tissues [4]. Previous work has focused on the introduction of other ECM components to their construct to develop more complex materials that possess strong mechanical and biological properties and are reminiscent of native tissue composition and network organization [4, 6–24].

Elastin is a structural protein present in connective, vascular, and load-bearing tissues [6, 25, 26] that has also been used in tissue engineering due to its elastic mechanical properties [4,9,27–31]. Collagen and elastin networks are present in the ECM of many organs including the skin, blood vessels, and lungs [25, 26, 30]. Thus, collagen and elastin composites have been proposed for use in vascularisation [6,10,31,32], wound repair [30,31,33,34], and the development of alveolar and lung replacements [9].

In the work presented here, we characterized gels composed of collagen and elastin blends to better understand the effect of elastin addition to collagen fibril formation and the mechanical properties of collagen constructs.

A.3 Materials and Methods

A.3.1 Gel Preparation

Rat tail collagen type I with neutralization solution was purchased from Advanced Biomatrix (San Diego, CA). Soluble elastin from bovine neck ligament was purchased from Elastin Products Company, Inc (Owensville, MO). Stock collagen solutions were prepared on ice by combining 1 part of the neutralizing solution and 9 parts of the collagen type I solution for the desired volume. Stock elastin solutions were prepared in 1x PBS at a concentration of 100 mg/mL. The stock collagen and elastin solutions were used to prepare collagen type I:elastin mixtures with ratios of 1:0, 2:1, 1:1, 2:3, 1:2, and 1:5 (Table A.1). The collagen and elastin mixtures were dispensed into 8 mm diameter silicone molds, covered with glass slides, and incubated overnight at 37 °C and 5% CO_2. The gels were stored in 1x PBS for a day at 4 °C before measuring their mechanical properties.

A.3.2 Fibrillogenesis Assay

Collagen and elastin hydrogel mixtures (n=9) were prepared on ice and diluted 1:10 in 1x PBS for the fibrillogenesis assay. Samples of 200 μL were dispensed into 96-

Table A.1.: Concentration of collagen type I and elastin in different ratio hydrogels.

Gel Ratio	Collagen (mg/ml)	Elastin (mg/ml)
1:0 C	3.6	0
2:1	3.6	1.8
1:1	3.6	3.6
2:3	3.6	5.4
1:2	3.6	7.2
1:5	3.6	18

well plates and the fibrillogenesis of the samples was measured as described previously [35]. Briefly, the turbidity of the samples was monitored at 313 nm every 30 s for 3 h in a SpectraMax M5 spectrophotometer set at 37 °C (Molecular Devices, San Jose, CA).

A.3.3 Transmission Electron Microscopy (TEM)

A subset (1:0 C, 1:1, and 1:5) of the collagen and elastin hydrogel solutions was prepared on ice and diluted 1:10 in 1x PBS. Samples of 7 μL were added to 200 mesh copper-coated grids and allowed to settle for 10 min. The sample excess was removed and 10 μL of a 2% uranyl acetate stain were added and removed immediately. A Talos L120C transmission electron microscope (FEI, Hillsboro, OR) was used to image the samples after allowing them to air dry.

Collagen D-banding patterns ($n \geq 46$) were measured using ImageJ software (National Institutes of Health, Bethesda, MD). A parallel line was drawn along a fibril, over a light and a dark band, to obtain a measurement. ImageJ software was also used to measure the fibril diameter ($n \geq 46$) as described previously [14]. A perpendicular line was drawn across a fibril to obtain the diameter.

A.3.4 Rheological Measurements

A DHR-3 rheometer (TA Instruments, New Castle, DE) was used to perform rheological analysis with an 8 mm crosshatched plate geometry. Gels ($n \geq 16$) were placed on a crosshatched bottom plate surrounded by 1x PBS to prevent dehydration. Temperature sweeps were performed from 20 °C to 40 °C with a frequency of 0.1 Hz and a controlled stress of 0.3 Pa.

A.3.5 Statistical Analysis

Results are represented as a mean with error bars corresponding to the standard deviation. Statistical analysis was performed using GraphPad Prism (GraphPad Software, San Diego, CA) with $\alpha = 0.05$ and significance was determined with p value < 0.05. All results were analyzed using single factor analysis of variance (ANOVA) and Tukey's *post hoc* tests or Dunnett's multiple comparisons tests.

A.4 Results

A.4.1 Elastin increases the rate of fibrillogenesis

The collagen and elastin solutions for the different blends (1:0 C, 2:1, 1:1, 2:3, 1:2, and 1:5) were used to measure their turbidity. The addition of elastin to the collagen gel solutions increases the rate of fibrillogenesis and the optical density at 313 nm when compared to a collagen only solution (Figure A.1). All of the collagen and elastin blend gel solutions showed a significantly higher rate of fibrillogenesis than control, but were not significantly different to each other.

A.4.2 Elastin addition decreases the collagen D-banding pattern

TEM images were used to measure the D-banding pattern of collagen fibrils present in a subset (1:0 C, 1:1, and 1:5) of the collagen and elastin blend hydro-

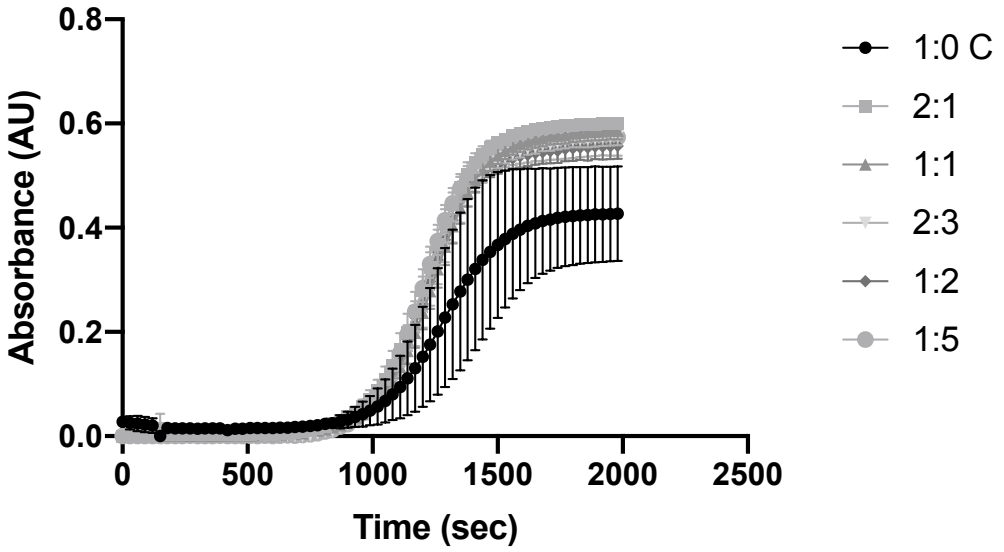

Fig. A.1.: Turbidity measurements during fibrillogenesis for collagen and elastin blend gel solutions. Addition of elastin significantly increases the rate of fibrillogenesis ($p < 0.05$). Data represents average ± standard deviation (n=3).

gels (Figure A.2). A parallel line to the collagen fibril was drawn over the D-banding pattern (a light and a dark band) to obtain a measurement. The results were compared to the control and showed the addition of elastin to the 1:5 collagen and elastin solutions significantly decreased the D-banding pattern observed in the collagen fibrils with respect to the D-banding pattern observed in the control gels (Figure A.3 and Table A.2). No significant difference was observed betweeen the 1:0C and 1:1 collagen and elastin blends.

A.4.3 Elastin addition does not affect collagen fibril diameter

The fibril diameter of the collagen fibrils present in the collagen and elastin solutions was measured by using TEM images (Figure A.2) and drawing a perpendicular line across a fibril. The results obtained showed no significant differences among the collagen and elastin blends (1:1 and 1:5) and control (Figure A.4). Table A.3 shows

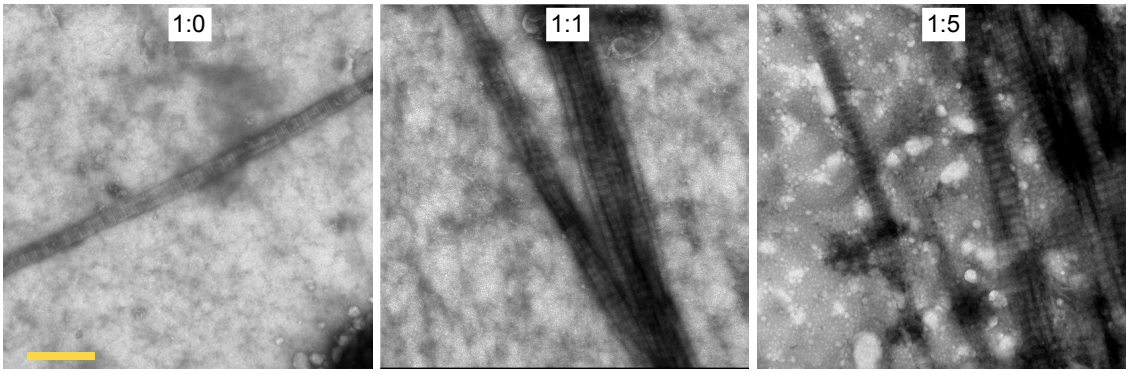

Fig. A.2.: Representative TEM images of collagen fibrils observed in 1:0, 1:1, and 1:5 collagen and elastin blend gels. TEM images were used to measure D-banding pattern and fibril diameter. Scale bar: 500 nm.

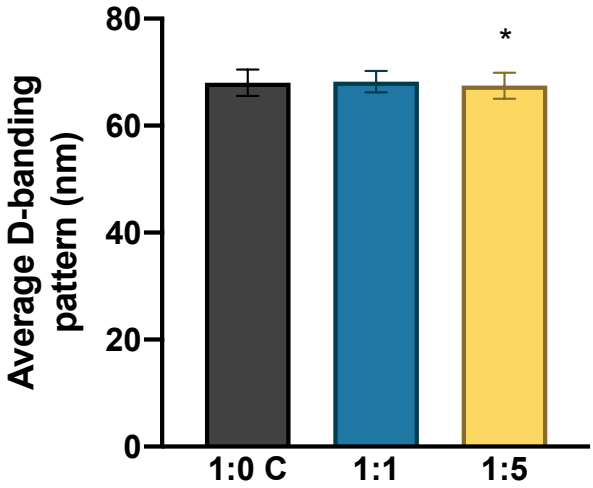

Fig. A.3.: Average D-banding pattern and standard deviation values for fibrils observed in gels ($n \geq 46$) prepared from mixtures of 1:0 C, 1:1, and 1:5 collagen type I to elastin. One-way ANOVA and Dunnett's method for comparisons with control were performed. A significant difference ($p < 0.05$) was observed between 1:0 C and 1:5 collagen and elastin blends.

the average fibril diameter, standard deviation, and p-values for fibrils present in the 1:0 C, 1:1, and 1:5 gels.

Table A.2.: Average D-banding pattern, standard deviation, and p values for fibrils observed in gels prepared from mixtures of 1:0 C, 1:1, and 1:5 collagen type I to elastin. P-values were obtained by performing Dunnett's method for comparisons with control.

Gel Type	N	Avg D-banding Pattern (nm)	Standard Deviation	p value
1:0 C	62	68.15	1.582	
1:1	46	68.25	1.992	0.9409
1:5	48	67.30	2.087	0.0366

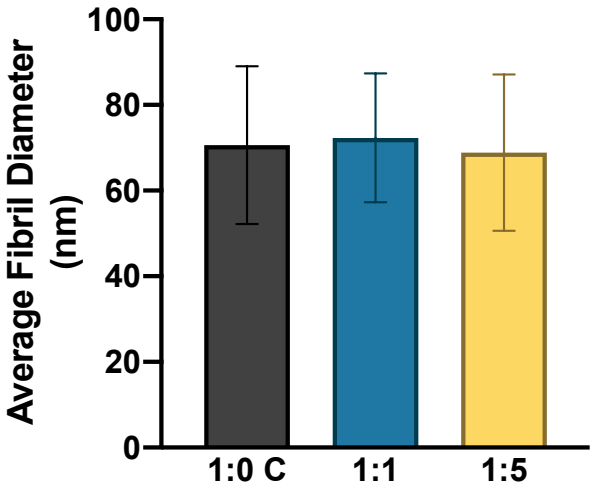

Fig. A.4.: Average fibril diameter and standard deviation values for fibrils present in gels ($n \geq 46$) prepared from mixtures of 1:0 C, 1:1, and 1:5 collagen type I to elastin. One-way ANOVA and Dunnett's method for comparisons with control were performed. No significant differences ($p < 0.05$) were observed between 1:0 C, 1:1, and 1:5 blend gels.

A.4.4 Addition of elastin alters storage modulus

The storage moduli of the collagen and elastin gels was measured and the results showed the addition of elastin to the collagen gels decreases the storage modulus (Figure A.5). All of the collagen and elastin gels showed a significantly different

Table A.3.: Average fibril diameter, standard deviation, and p values for fibrils present in gels prepared from mixtures of 1:0 C, 1:1, and 1:5 collagen type I to elastin. P-values were obtained by performing Dunnett's method for comparisons with control.

Gel Type	N	Avg Fibril Diameter (nm)	Standard Deviation	p value
1:0 C	62	70.62	18.44	
1:1	46	72.32	15.04	0.8740
1:5	48	68.90	18.25	0.8035

storage modulus from the control (1:0 C) gels, except for the 2:1 collagen to elastin blend (Table A.4).

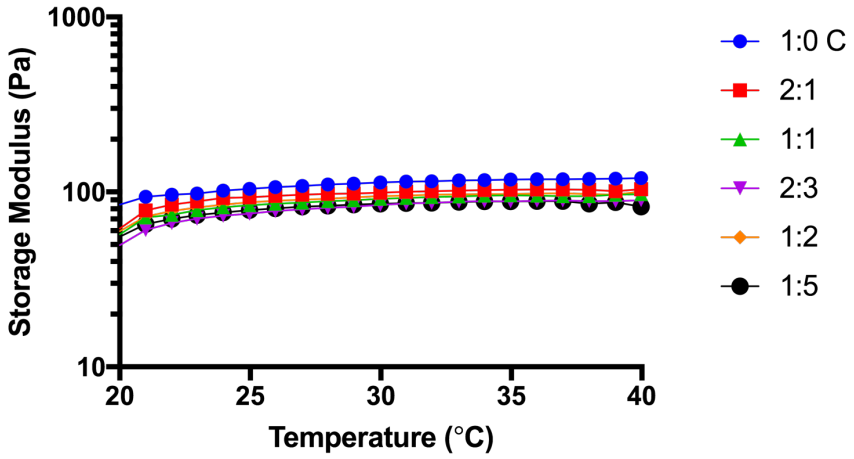

Fig. A.5.: Storage moduli of gels prepared from mixtures of 1:0 C, 2:1, 1:1, 2:3, 1:2, and 1:5 collagen type I to elastin. Data (n = 16-18) are represented as the mean ± the standard deviation.

A.5 Discussion

In the work presented here, we characterized gels composed of collagen and elastin blends to better understand the effect of elastin addition to collagen constructs. First, the collagen fibril formation was studied to determine whether the elastin addition to collagen affects the rate of fibrillogenesis. The rate of fibrillogenesis was measured

Table A.4.: Average storage moduli and standard deviation values for gels prepared from mixtures of 1:0 C, 2:1, 1:1, 2:3, 1:2, and 1:5 collagen type I to elastin. ANOVA and Dunnett's method for comparisons with control were performed. A significant difference ($p < 0.05$) was observed between 1:0 C and the rest of the mixtures except for 2:1.

Gel Type	N	Avg Storage Modulus (Pa)	Standard Deviation	p value
1:0 C	17	109.4	13.8	
2:1	17	99.2	13.7	0.0807
1:1	16	91.2	14.0	0.0039
2:3	16	86.4	9.5	0.0003
1:2	18	94.8	11.7	<0.0001
1:5	18	85.7	12.0	<0.0001

turbidimetrically [35, 36]. Previous studies have shown that addition of molecules to collagen solutions can alter the collagen fibril rate of fibrillogenesis [35]. However, to our knowledge, this is the first study to determine whether elastin addition affects collagen fibril fibrillogenesis. Our findings demostrated that addition of elastin to collagen gel solutions increases their rate of fibrillogenesis and their optical density at 313 nm (Figure A.1).

Next, we performed TEM imaging on a subset of the collagen and elastin gel blend solutions (1:0 C, 1:1, and 1:5) to obtain images of the fibrils present (Figure A.2). With these images, we were able to measure the D-banding pattern associated with collagen fibrils. The D-banding pattern is a repeating banding pattern of a D-periodicity distance of 64-67 nm that is characteristic of fibrillar collagens [5, 37–41]. This pattern occurs when tropocollagen molecules are organized in a staggered formation that produces overlap and gap regions [37, 38, 41, 42]. The overlap regions are observed as dark bands while the gap regions are observed as light bands [38, 39, 41]. Our results showed that 1:0 C and 1:1 collagen and elastin blends had average D-banding patterns of 68.15 nm and 68.25 nm, respectively (Table A.2). The 1:5 solutions, however, had a significantly smaller average D-banding pattern of 67.30

nm (Figure A.3 and Table A.2). This slight difference observed in D-banding pattern size in our control gels and previous studies could be attributed to the manipulation of the samples, which can cause the spacing in the fibrils to increase or decrease [39]. The use of control samples in experiments is, thus, encouraged to determine the effect of the variables being studied on the D-banding pattern. The cause for the difference in D-banding pattern between the 1:0 C and 1:5 solutions needs to be further elucidated.

Using the TEM images, we also analyzed the fibril diameter of the collagen fibrils present in the solutions. The diameter of collagen fibrils ranges from 10-500 nm and depends on several factors such as tissue location, age, and animal species [40]. Our results showed a fibril diameter range of 68-72 nm. The results also showed that elastin addition does not affect collagen fibril diameter (Figure A.4 and Table A.3). Even though the elastin addition affected the D-banding pattern, it did not affect the collagen fibril diameter. This observation is consistent with previous studies that have shown that fibril diameter is independent from D-banding pattern [43].

Finally, we studied the mechanical properties of the collagen and elastin blend hydrogels. We measured the storage moduli of the gels and determined that the addition of elastin to the collagen gels decreases their storage moduli. Similarly, Nguyen *et al* detected a decrease in strength and stiffness with the addition of elastin to collagen fibers [44]. However, Berglung *et al* and Bax *et al* saw increases in stiffness in collagen and elastin constructs when compared to collagen only contructs [4, 10]. These contrasting results could be caused by the isolation process used to obtain the elastin product as well as the scaffold fabrication process and the concentration of elastin used [4].

Many groups have focused their attention on studying collagen and elastin constructs and their uses in tissue engineering. However, to our knowledge, this work is the first to present the effect of elastin on collagen fibrillogenesis, D-banding pattern, and fibril diameter.

A.6 Conclusions

In this study, we characterized gels composed of collagen and elastin blends to elucidate their unique properties. We demonstrated that the addition of varying amounts of elastin alters collagen fibrillogenesis and D-banding pattern. The addition of elastin in varying ratios does not seem to affect fibril diameter, but has shown to affect storage modulus. The work presented here serves as a deeper understanding of how varying amounts of elastin affect collagen constructs. This knowledge will prove useful when developing collagen and elastin constructs for tissue engineering in the future.

Future work will focus on performing second harmonic generation (SHG) to study the effect of elastin addition on the collagen network organization. Fluorescence lifetime imaging (FLIm) will also be performed to retrieve fluorescence spectral and lifetime (LT) properties from the collagen and elastin blend gels.

A.7 Acknowledgments

The authors thank Dr. Alba Alfonso García from the Marcu Lab at University of California, Davis for providing the collagen and elastin materials used for the work presented here.

A.8 References

[1] Brian J Huang, Jerry C Hu, and Kyriacos A Athanasiou. Cell-based tissue engineering strategies used in the clinical repair of articular cartilage. *Biomaterials*, 98:1–22, 2016.

[2] E. B. Hunziker. Articular cartilage repair: Basic science and clinical progress. A review of the current status and prospects. *Osteoarthritis and Cartilage*, 2002.

[3] Vincent Irawan, Tzu-Cheng Sung, Akon Higuchi, and Ikoma Toshiyuki. Collagen Scaffolds in Cartilage Tissue Engineering and Relevant Approaches for Future Development. *Tissue Engineering and Regenerative Medicine*, 15(6):673–697, 2018.

[4] Daniel V. Bax, Helen E. Smalley, Richard W. Farndale, Serena M. Best, and Ruth E. Cameron. Cellular response to collagen-elastin composite materials. *Acta Biomaterialia*, 86:158–170, 2019.

[5] Alfonso Gautieri, Simone Vesentini, Alberto Redaelli, and Markus J. Buehler. Hierarchical structure and nanomechanics of collagen microfibrils from the atomistic scale up. *Nano Letters*, 11(2):757–766, 2011.

[6] K. Numata and D. L. Kaplan. Biologically derived scaffolds. In *Advanced Wound Repair Therapies*, pages 524–551. 2011.

[7] Calogero Fiorica, Fabio S. Palumbo, Giovanna Pitarresi, Mario Allegra, Roberto Puleio, and Gaetano Giammona. Hyaluronic acid and α-elastin based hydrogel for three dimensional culture of vascular endothelial cells. *Journal of Drug Delivery Science and Technology*, 46:28–33, 2018.

[8] Tristan De Chalain, John H. Phillips, and Aleksander Hinek. Bioengineering of elastic cartilage with aggregated porcine and human auricular chondrocytes and hydrogels containing alginate, collagen, and κ- elastin. *Journal of Biomedical Materials Research*, 44(3):280–288, 1999.

[9] Siobhá E Dunphy, Jessica AJ Bratt, Khondoker M Akram, Nicholas R Forsyth, and Alicia J El Haj. Hydrogels for lung tissue engineering: Biomechanical properties of thin collagen-elastin constructs. 2014.

[10] Joseph D Berglund, Robert M Nerem, and Athanassios Sambanis. Incorporation of Intact Elastin Scaffolds in Tissue-Engineered Collagen-Based Vascular Grafts. *Tissue Engineering*, 10(9/10):1526–1535, 2004.

[11] Amos Matsiko, John P. Gleeson, and Fergal J. O'Brien. Scaffold Mean Pore Size Influences Mesenchymal Stem Cell Chondrogenic Differentiation and Matrix Deposition. *Tissue Engineering Part A*, 2014.

[12] Leena-Stiina Kontturi, Elina Järvinen, Virpi Muhonen, Estelle C Collin, Abhay S Pandit, Ilkka Kiviranta, Marjo Yliperttula, and Arto Urtti. An injectable, in situ forming type II collagen/hyaluronic acid hydrogel vehicle for chondrocyte delivery in cartilage tissue engineering. *Drug Deliv. and Transl. Res.*, 4:149–158, 2014.

[13] Lu Yuan, Bao Li, Jirong Yang, Yilu Ni, Yingying Teng, Likun Guo, Hongsong Fan, Yujiang Fan, and Xingdong Zhang. Effects of composition and mechanical property of injectable collagen I/II composite hydrogels on chondrocyte behaviors. *Tissue Engineering Part A*, 22:899–906, 2016.

[14] Nelda Vazquez-Portalatín, Claire E Kilmer, Alyssa Panitch, and Julie C Liu. Characterization of Collagen Type I and II Blended Hydrogels for Articular Cartilage Tissue Engineering. *Biomacromolecules*, 17:3145–3152, 2016.

[15] Henrique V. Almeida, Binulal N. Sathy, Ivan Dudurych, Conor T. Buckley, Fergal J. O'Brien, and Daniel J. Kelly. Anisotropic Shape-Memory Alginate Scaffolds Functionalized with Either Type I or Type II Collagen for Cartilage Tissue Engineering. *Tissue Engineering Part A*, 23:55–68, 2017.

[16] Mariana Lazarini, Pedro Bordeaux-Rego, Renata Giardini-Rosa, Adriana S. S. Duarte, Mariana Ozello Baratti, Alessandro Rozim Zorzi, João Batista de Miranda, Carlos Lenz Cesar, Ângela Luzo, and Sara Teresinha Olalla Saad. Natural Type II Collagen Hydrogel, Fibrin Sealant, and Adipose-Derived Stem Cells as a Promising Combination for Articular Cartilage Repair. *CARTILAGE*, 8(4):439–443, 2017.

[17] M. Tamaddon, M. Burrows, S. A. Ferreira, F. Dazzi, J. F. Apperley, A. Bradshaw, D. D. Brand, J. Czernuszka, and E. Gentleman. Monomeric, porous type II collagen scaffolds promote chondrogenic differentiation of human bone marrow mesenchymal stem cells in vitro. *Scientific Reports*, 2017.

[18] Yongli Gao, Bao Li, Weili Kong, Lu Yuan, Likun Guo, Chuan Li, Hongsong Fan, Yujiang Fan, and Xingdong Zhang. Injectable and self-crosslinkable hydrogels based on collagen type II and activated chondroitin sulfate for cell delivery. *International journal of biological macromolecules*, 118:2014–2020, 2018.

[19] Timothy Douglas, Sascha Heinemann, Carolin Mietrach, Ute Hempel, Susanne Bierbaum, Dieter Scharnweber, and Hartmut Worch. Interactions of collagen types I and II with chondroitin sulfates A-C and their effect on osteoblast adhesion. *Biomacromolecules*, 8:1085–1092, 2007.

[20] Kate Stuart and Alyssa Panitch. Influence of chondroitin sulfate on collagen gel structure and mechanical properties at physiologically relevant levels. *Biopolymers*, 89:841–851, 2008.

[21] Kate Stuart and Alyssa Panitch. Characterization of gels composed of blends of collagen l, collagen III, and chondroitin sulfate. *Biomacromolecules*, 10:25–31, 2009.

[22] Tyler Novak, Sherry L Voytik-Harbin, and Corey P Neu. Cell encapsulation in a magnetically aligned collagen GAG copolymer microenvironment. *Acta Biomaterialia*, 11:274–282, 2015.

[23] Shaili Sharma, Aeju Lee, Kuiwon Choi, Kwangmeyung Kim, Inchan Youn, Stephen B. Trippel, and Alyssa Panitch. *Macromolecular Bioscience*.

[24] Shaili Sharma, Alyssa Panitch, and Corey P. Neu. *Acta Biomaterialia*.

[25] J.H. Kristensen and M.A. Karsdal. *Elastin*. Elsevier Inc., 2016.

[26] A Sionkowska, J Skopinska-Wisniewska, M Gawron, J Kozlowska, and A Planecka. Chemical and thermal cross-linking of collagen and elastin hydrolysates. *International Journal of Biological Macromolecules*, 47:570–577, 2010.

[27] J. Skopinska-Wisniewska, J. Kuderko, A. Bajek, M. Maj, A. Sionkowska, and M. Ziegler-Borowska. Collagen/elastin hydrogels cross-linked by squaric acid. *Materials Science and Engineering C*, 60:100–108, 2016.

[28] Aditee Kurane, Dan T. Simionescu, and Narendra R. Vyavahare. In vivo cellular repopulation of tubular elastin scaffolds mediated by basic fibroblast growth factor. *Biomaterials*, 28(18):2830–2838, 2007.

[29] Raquel Silva, Raminder Singh, Bapi Sarker, Dimitrios G Papageorgiou, Judith A Juhasz-Bortuzzo, Judith A Roether, Iwona Cicha, Joachim Kaschta, Dirk W Schubert, Konstantinos Chrissafis, Rainer Detsch, and Aldo R Boccaccini. Hydrogel matrices based on elastin and alginate for tissue engineering applications. *International Journal of Biological Macromolecules*, 114:614–625, 2018.

[30] J. Carlos Rodríguez-Cabello, I. González de Torre, A. Ibañez-Fonseca, and M. Alonso. Bioactive scaffolds based on elastin-like materials for wound healing. *Advanced Drug Delivery Reviews*, 129:118–133, 2018.

[31] Giselle C Yeo, Suzanne M Mithieux, and Anthony S Weiss. The elastin matrix in tissue engineering and regeneration This review comes from a themed issue on Tissue Engineering and Regenerative Medicine: The Future of Tissue Engineering. *Current Opinion in Biomedical Engineering*, 6:27–32, 2018.

[32] Eugene D. Boland, Jamil A. Matthews, Kristin J. Pawlowski, David G. Simpson, Gary E. Wnek, and Gary L. Bowlin. Electrospinning collagen and elastin: Preliminary vascular tissue engineering. *Frontiers in Bioscience*, 9:1422–1432, 2004.

[33] Jasper Killat, Kerstin Reimers, Claudia Y. Choi, Sabrina Jahn, Peter M. Vogt, and Christine Radtke. Cultivation of keratinocytes and fibroblasts in a three-dimensional bovine collagen-elastin matrix (Matriderm®) and application for full thickness wound coverage in vivo. *International Journal of Molecular Sciences*, 2013.

[34] Oscar Castaño, Soledad Pérez-Amodio, Claudia Navarro-Requena, Miguel Ángel Mateos-Timoneda, and Elisabeth Engel. Instructive microenvironments in skin wound healing: Biomaterials as signal releasing platforms. *Advanced Drug Delivery Reviews*, 129:95–117, 2018.

[35] John E. Paderi and Alyssa Panitch. *Biomacromolecules*.

[36] Timothy Douglas, Sascha Heinemann, Susanne Bierbaum, Dieter Scharnweber, and Hartmut Worch. Fibrillogenesis of Collagen Types I, II, and III with Small Leucine-Rich Proteoglycans Decorin and Biglycan. 2006.

[37] Meisam Asgari, Neda Latifi, Hossein K. Heris, Hojatollah Vali, and Luc Mongeau. In vitro fibrillogenesis of tropocollagen type III in collagen type i affects its relative fibrillar topology and mechanics. *Scientific Reports*, 7(1):1–10, 2017.

[38] A. Miller. Molecular packing in collagen fibrils. *Trends in Biochemical Sciences*, 7(1):13–18, 1982.

[39] Francis O. Schmitt, Cecil E. Hall, and Marie A. Jakus. Electron microscope investigations of the structure of collagen. *Journal of Cellular and Comparative Physiology*, 20(1):11–33, 1942.

[40] Tatsuo Ushiki. Collagen Fibers, Reticular Fibers, and Elastic Fibers. A Comprehensive Understanding from a Morphological Viewpoint. *Arch. Hist. Cytol.*, 65(2):109–126, 2002.

[41] A Chapman. The Staining Pattern of Collagen Fibrils. *Journal of Biological Chemistry*, 254(21):10710–10714, 1979.

[42] Jazli Aziz, Hafiz Shezali, Zamri Radzi, Noor Azlin Yahya, Noor Hayaty Abu Kassim, Jan Czernuszka, and Mohammad Tariqur Rahman. Molecular Mechanisms of Stress-Responsive Changes in Collagen and Elastin Networks in Skin. *Skin Pharmacology and Physiology*, 29(4):190–203, 2016.

[43] Laurent Bozec, Gert Van Der Heijden, and Michael Horton. Collagen Fibrils: Nanoscale Ropes. *Biophysical Journal*, 92:70–75.

[44] Thuy-Uyen Nguyen, Chris A Bashur, and Vipuil Kishore. Impact of elastin incorporation into electrochemically aligned collagen fibers on mechanical properties and smooth muscle cell phenotype. *Biomedical Materials*, 11(2):025008, mar 2016.

B. CHARACTERIZATION AND INCORPORATION OF BONE MORPHOGENETIC PROTEIN-2 AND AGGRECAN MIMETIC MOLECULES IN COLLAGEN I AND II HYDROGELS

B.1 Introduction

The bone morphogenetic protein-2 (BMP-2) is a growth factor that belongs to the transforming growth factor-β (TGF-β) family. Previous studies with BMP-2 have shown that this growth factor is involved in cartilage formation [1]. BMP-2 is also involved in chondrocyte proliferation and differentiation and matrix maturation [2]. Additionally, BMP-2 is able to stimulate collagen type II and aggrecan expression in chondrocytes [3, 4]. BMP-2 has also been used in bone healing and osteogenesis [5]. Furthermore, BMP-2 has been used to differentiate human mesenchymal stem cells (hMSCs) into chondrocytes for cartilage repair [6].

Recently, a peptide (KIPKASSVPTELSAISTLYL) derived from residues 73-92 of the knuckle epitope of BMP-2 has been used to differentiate hMSCs into chondrocytes [6, 7]. This BMP-2 peptide, or BMP, has also shown to increase collagen and glycosaminoglycan (GAG) production as well as expression of anabolic factors in cartilage. It has also shown little increase in collagen type X, a hypertrophic marker, when compared to BMP-2 [6].

Tissue engineering efforts aim towards the development of cartilage repair strategies that mimic articular cartilage. With this in mind, this work takes into account the articular cartilage architecture, the protective role of aggrecan in cartilage degradation, and the importance of growth factors, specifically BMP-2, in cartilage production and homeostasis. Previously, our lab designed and synthesized an aggrecan mimic (CS-BMPH-GAH) composed of HA binding peptides attached to a CS backbone [8].

This mimetic molecule has shown to bind to extracellular matrix (ECM) components, resist proteolytic degradation, protect collagen type II, and lower catabolic protein and gene expression [8, 9].

In this work, we proposed a new peptidoglycan (CS-BMP-GAH) composed of HA binding and BMP peptides attached to a CS backbone via a new 4-(4,6-dimethoxy-1,3,5-triazin-2-yl)-4-methyl-morpholinium chloride (DMTMM) chemistry that does not require the BMPH crosslinker. Collagen type I and II gels were synthesized with hyaluronic acid (HA) and CS, CS-GAH, or CS-BMP-GAH to evaluate the catabolic and anabolic effects of these mimetic molecules on chondrocytes embedded within these scaffolds in healthy or inflamed environments. We hypothesized the addition of CS-GAH would decrease the catabolic activities involved in cartilage degradation while the addition of CS-BMP-GAH would stimulate the anabolic activities involved in ECM synthesis. The ultimate goal of this work was to design a scaffold construct that was expected to overcome the limitations of current matrices and was likely to promote repair of articular cartilage. We hypothesized these molecules would resist proteolytic degradation, stimulate chondrocyte anabolic activities, and prove useful for cartilage repair.

B.2 Materials and Methods

B.2.1 Peptide Synthesis

The HA binding peptide was modified and biotinylated as described in Section 3.3.1. Similarly, the BMP peptide (KIPKASSVPTELSAISTLYL) synthesis with an additional GSG spacer and a hydrazide group at the C terminus (KIPKASSVPTEL-SAISTLYLGSG -$NHNH_2$) was loosely based on the method described by Zheng *et al* [10].

Resin Modification

The 2-Chlorotrityl chloride (2-ClTrt) resin was modified as described in Section 3.3.1.

Automated Peptide Synthesis and Biotinylation

The HA binding peptide was synthesized and biotinylated as described in Section 3.3.1. For the BMP peptide, the amino acid coupling step was run at 37 °C for 45 min. Afterwards, the resin was washed with DMF and deprotected with piperidine. The next six amino acids were coupled similarly. However, the last 15 amino acids were double coupled. The amino acid double coupling step was run at 37 °C for 45 min, the resin was washed, and another coupling step took place at 37 °C for 30 min. The subsequent amino acids were added until the sequence was completed. Finally, the resin was washed, deprotected, collected, and dried as described in Section 3.3.1.

Peptide Cleavage and Purification

The peptides were cleaved and purified as described in Section 3.3.1.

B.2.2 Biomimetic Molecule Synthesis

The CS-GAH and CS-BMP-GAH molecules were synthesized by following the steps described in Section 3.3.2. For the CS-BMP-GAH molecules, the CS backbone was functionalized with 1 mole of BMP peptide per 1 mole of CS. Once the BMP peptide had been conjugated to the CS backbone for 12 h and lyophilized, the steps were repeated with the CS-BMP molecule and GAH, the HA binding peptide. The CS-BMP molecule was functionalized further with an average of 10.5 moles of GAH per 1 mole of CS. These BMP and GAH peptide conjugated CS backbones were named CS-BMP-GAH. The CS-GAH and CS-BMP-GAH molecules were filtered, lyophilized, and stored at −80 °C for later use.

B.2.3 Peptide Quantification

To quantify the BMP peptide concentration attached to the CS backbone, a fluoraldehyde (OPA) assay was performed. Briefly, 20 μL of the CS-BMP molecule (without the GAH peptide) and 200 μL of the fluoraldehyde reagent solution were combined into a 96-well plate and mixed. The fluorescence of the samples was measured at 360nm excitation and 455 nm emission. A BMP peptide standard curve was used to calculate the peptide concentration in the samples. The final concentration of the GAH peptides attached to the CS backbone was quantified as described in Section 3.3.3.

B.2.4 Gel Preparation

Stock solutions of rat tail collagen type I (BD Biosciences, Franklin Lakes, NJ) and chicken sternal collagen type II (Millipore Sigma, Saint Louis, MO) were prepared in 20 mM acetic acid at a concentration of 5 mg/mL. The pH of the collagen solutions was raised to 7.4 with the addition of 10x phosphate buffered saline (PBS) and 1 M NaOH. The final concentrations of the collagen solutions were brought to 4 mg/mL with the addition of HA and the corresponding biomimetic molecule (e.g. CS-GAH or CS-BMP-GAH) in 1x PBS. The gels prepared consisted of a 3:1 collagen type I to collagen type II ratio with 0.2 mg/mL of added HA. HA (1.5 - 1.8 x 10^6 Da) (Millipore Sigma, Saint Louis, MO) was dissolved in 1x PBS to 10 mg/mL. The biomimetic molecule and CS stock solutions were dissolved in 1x PBS to a final concentration of 65 mg/mL. Gels were made with CS, CS-GAH, or CS-BMP-GAH at a final concentration of 47 μM of added CS or mimetic molecule. Gels with a final volume of 100 μL were allowed to polymerize in a 96-well plate for 30 min at 37 °C in a 5% CO_2 humidified incubator as previously described [11]. After polymerization, 150 μL of 1x PBS were added to each gel. The 1x PBS supernatants were collected and replaced on days 7, 14, and 21. Gels were collected at days 7, 14, and 21. Gels

and supernatants were stored at −80 °C until further testing. Table A.1 describes the experimental groups used.

Table B.1.: Experimental design for the collagen type I and II gels with biomimetic molecules.

Samples	Collagen (mg/mL)		Molecules (mg/mL)			
	Type I	Type II	CS	BMP	CS-GAH	CS-BMP-GAH
3:1 Control	3	1	-	-	-	-
3:1 CS	3	1	1.88	-	-	-
1:0 CS-GAH	4	-	-	-	2.44	-
3:1 CS-GAH	3	1	-	-	2.44	-
3:1 CS-GAH, BMP	3	1	-	0.11	2.44	-
3:1 CS-BMP-GAH	3	1	-	-	-	2.62

B.2.5 Molecule Retention

The gels and 1x PBS supernatants stored at −80 °C were used in a DMMB assay to quantify the amount of CS or biomimetic molecule retained in the gels and the amount released into the solutions. The DMMB assay was performed as described in Section 3.3.7. The frozen gels were lyophilized and digested with a papain digestion buffer, as described in Section 3.3.6, prior to performing the DMMB assays.

B.2.6 Chondrocyte Isolation and Culture

Fetal bovine chondrocytes were isolated from bovine knees as described in Section 3.3.4.

B.2.7 Chondrocyte-embedded Gel Preparation

Collagen type I, collagen type II, CS, and HA stock solutions and gels were prepared as indicated in Section 3.1.1. The biomimetic stock solutions (e.g. CS-GAH

or CS-BMP-GAH) were dissolved in 1x PBS to a final concentration of 65 mg/mL. Collagen type I and II stock solutions were used to prepare stock solutions of 1:0 and 3:1 collagen type I to collagen type II with biomimetic molecules (CS-GAH or CS-BMP-GAH) and HA. Chondrocytes were added to the stock solutions at a final concentration of 5 x 10^5 cells/mL. Gels were allowed to polymerize 30 min and equilibrate for 3 days. Live/Dead assays were performed at days 3 and 21 to verify the viability of the cells within the gels. The experimental design for this study is shown in Table A.1.

B.2.8 IL-1β Stimulation of Gels

IL-1β was used to simulate an osteoarthritic environment. The different chondrocyte embedded gels were incubated at 37 °C with or without 20 ng/mL of IL-1β in chondrocyte growth medium. The culture medium was replaced every 2 days for 21 days with gel evaluation time periods at days 0, 7, 14, and 21. The gels were stored at −80 °C until further testing.

B.2.9 GAG Retention and Molecule Release and Retention

Percentage of molecule released and retained as well as amount of GAGs retained in the chondrocyte embedded gels were detected with DMMB assays as described in Section 3.3.7.

B.2.10 Collagen Retention

Collagen retention in the gels was studied as described in Section 3.3.8.

B.3 Results

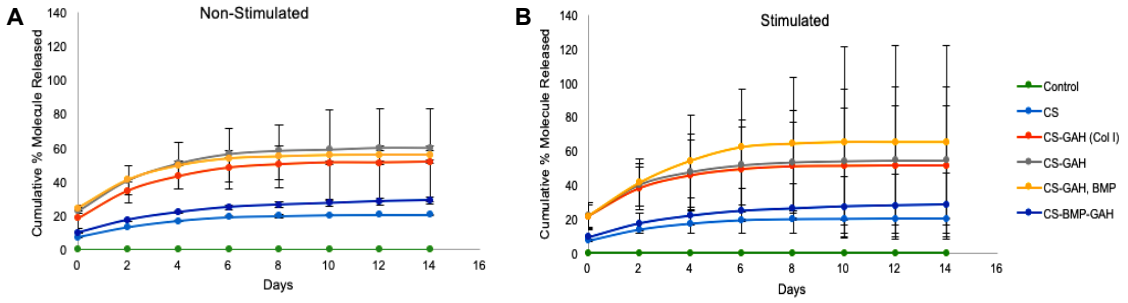

Figure B.1.: Percentage of molecules released from collagen gels into 1x PBS over a 14-day culture period. Percentage of molecule released is reported as cumulative measurements and was quantified with a DMMB assay. Gels were (A) non-stimulated or (B) stimulated with IL-1β to recreate healthy and OA environments, respectively, and analyze their effects on molecule release. Data is shown as the mean $\pm$ standard deviation (n = 6-9).

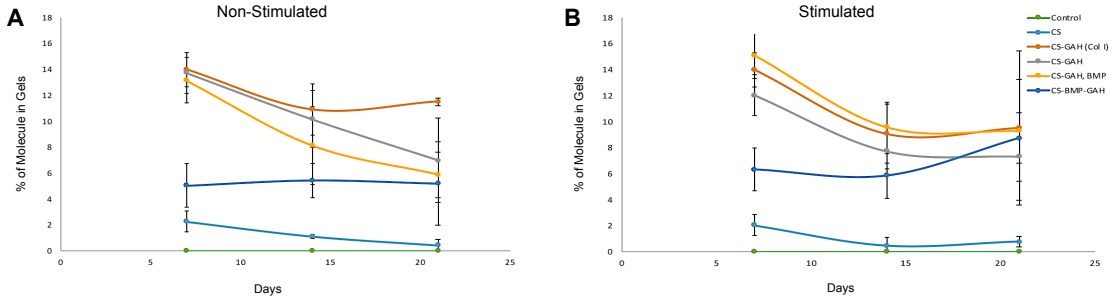

Figure B.2.: Percentage of molecules retained in the collagen gels over a 21-day culture period. Percentage of molecule retained is reported as day to day measurements and was quantified with a DMMB assay. Gels were (A) non-stimulated or (B) stimulated with IL-1β. Data is shown as the mean $\pm$ standard deviation (n = 6-9).

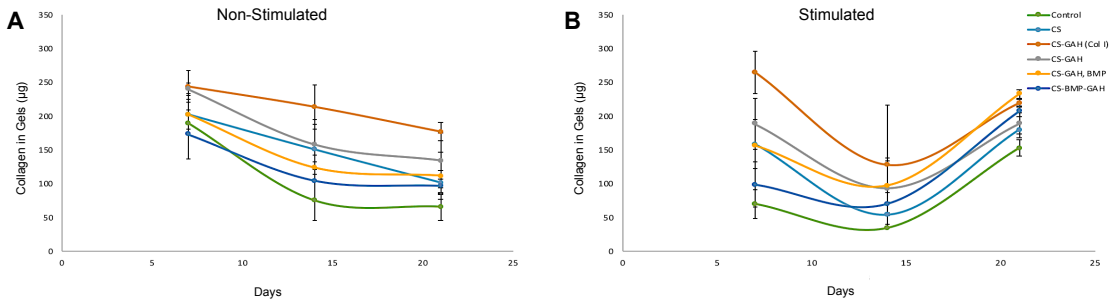

Figure B.3.: Amount of collagen retained in the gels over a 21-day culture period. Collagen retained in the gels is reported as day to day measurements and was quantified with a Sircol assay. Gels were (A) non-stimulated or (B) stimulated with IL-1β. Data is shown as the mean $\pm$ standard deviation (n = 6-9).

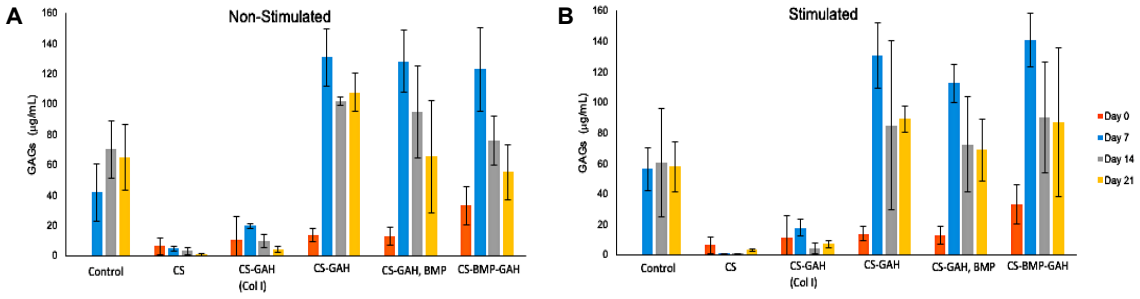

Figure B.4.: GAGs retained in the chondrocyte embedded collagen gels over a 21-day culture period. Data is reported as day to day measurements and was quantified with a DMMB assay. Gels were (A) non-stimulated or (B) stimulated with IL-1β. Data is shown as the mean $\pm$ standard deviation (n = 6-9).

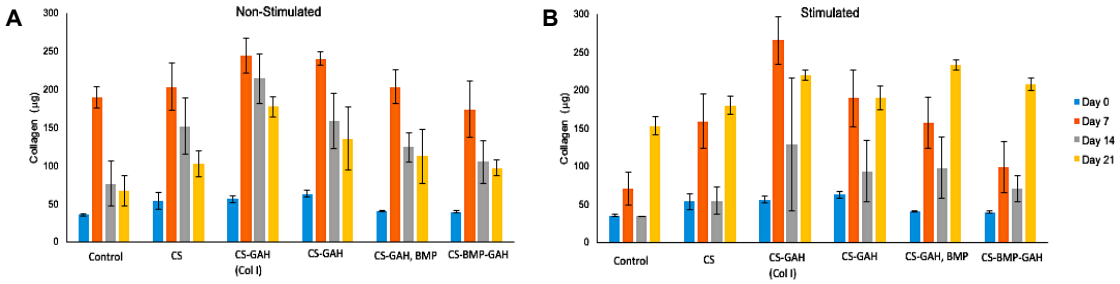

Figure B.5.: Collagen retained in the chondrocyte embedded gels over a 21-day culture period. Data is reported as day to day measurements and was quantified with a Sircol assay. Gels were (A) non-stimulated or (B) stimulated with IL-1β. Data is shown as the mean $\pm$ standard deviation (n = 6-9).

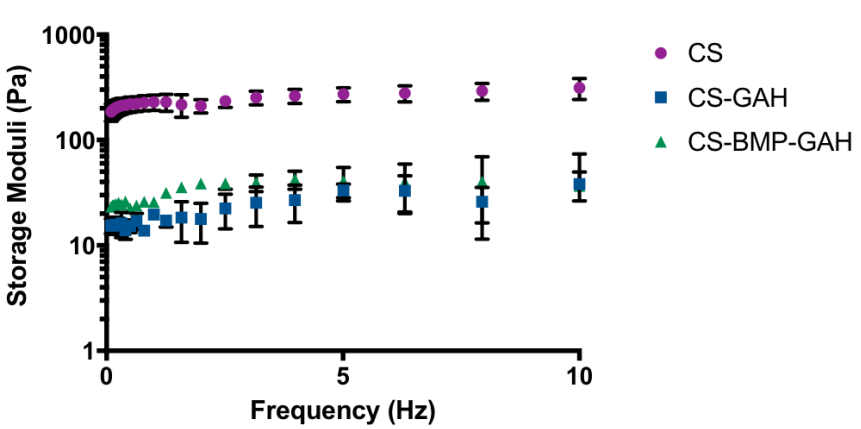

Figure B.6.: Frequency sweeps of storage moduli of collagen I and II hydrogels prepared with chondroitin sulfate (CS), CS-GAH and CS-BMP-GAH. Data (n = 2-3) are represented as the mean $\pm$ the standard deviation.

B.4 References

[1] E N Blaney Davidson, E L Vitters, P M van der Kraan, and W B van den Berg. Expression of transforming growth factor-beta (TGFbeta) and the TGFbeta signalling molecule SMAD-2P in spontaneous and instability-induced osteoarthritis: role in cartilage degradation, chondrogenesis and osteophyte formation. *Annals of the rheumatic diseases*, 65(11):1414–21, 2006.

[2] Bing Shu, Ming Zhang, Rong Xie, Meina Wang, Hongting Jin, Wei Hou, Dezhi Tang, Stephen E Harris, Yuji Mishina, Regis J O'Keefe, Matthew J Hilton, Yongjun Wang, and Di Chen. BMP2, but not BMP4, is crucial for chondrocyte proliferation and maturation during endochondral bone development. *Journal of cell science*, 124(Pt 20):3428–40, oct 2011.

[3] Y. Park, M. Sugimoto, A. Watrin, M. Chiquet, and Ernst B. Hunziker. BMP-2 induces the expression of chondrocyte-specific genes in bovine synovium-derived progenitor cells cultured in three-dimensional alginate hydrogel. *Osteoarthritis and Cartilage*, 13(6):527–536, 2005.

[4] Tatiana Gründer, Christoph Gaissmaier, Jürgen Fritz, Reinout Stoop, Peter Hortschansky, Jürgen Mollenhauer, and Wilhelm K Aicher. Bone morphogenetic protein (BMP)-2 enhances the expression of type II collagen and aggrecan in chondrocytes embedded in alginate beads. *Osteoarthritis and Cartilage*, 12(7):559–567, jul 2004.

[5] Xuezhong He, Junyu Ma, and Esmaiel Jabbari. Effect of grafting RGD and BMP-2 protein-derived peptides to a hydrogel substrate on osteogenic differentiation of marrow stromal cells. *Langmuir*, 24(21):12508–12516, 2008.

[6] Julie N. Renner, Yeji Kim, and Julie C. Liu. Bone Morphogenetic Protein-Derived Peptide Promotes Chondrogenic Differentiation of Human Mesenchymal Stem Cells. *Tissue Engineering Part A*, 18(23-24):2581–2589, dec 2012.

[7] Atsuhiro Saito, Yoshihisa Suzuki, Shin ichi Ogata, Chikara Ohtsuki, and Masao Tanihara. Activation of osteo-progenitor cells by a novel synthetic peptide derived from the bone morphogenetic protein-2 knuckle epitope. *Biochimica et biophysica acta*, 1651(1-2):60–7, sep 2003.

[8] Jonathan C. Bernhard and Alyssa Panitch. Synthesis and characterization of an aggrecan mimic. *Acta Biomaterialia*, 8:1543–1550, 2012.

[9] Shaili Sharma, Aeju Lee, Kuiwon Choi, Kwangmeyung Kim, Inchan Youn, Stephen B. Trippel, and Alyssa Panitch. *Macromolecular Bioscience*.

[10] Ji-Shen Zheng, Shan Tang, Yun-Kun Qi, Zhi-Peng Wang, and Lei Liu. Chemical synthesis of proteins using peptide hydrazides as thioester surrogates. *Nature Protocols*, 8(12):2483–2495, dec 2013.

[11] Ulrich Nöth, Lars Rackwitz, Andrea Heymer, Meike Weber, Bernd Baumann, Andre Steinert, Norbert Schütze, Franz Jakob, and Jochen Eulert. Chondrogenic differentiation of human mesenchymal stem cells in collagen type I hydrogels. *Journal of Biomedical Materials Research Part A*, 83A(3):626–635, dec 2007.

VITA

VITA

EDUCATION

Ph.D., Biomedical Engineering Purdue University, August 2019

Dissertation Title: The Use of Biopolymers for Tissue Engineering

Research Advisor: Dr. Alyssa Panitch, Edward Teller Professor in Biomedical Engineering, Executive Associate Dean and Associate Dean for Academic Personnel and Planning

B.S., Industrial Biotechnology University of Puerto Rico: Mayagüez, June 2012

RESEARCH EXPERIENCE

2016-2019 **Visiting Graduate Student**, University of California, Davis

Advisor: Alyssa Panitch, Ph.D.

- Incorporation of aggrecan mimetic molecules in collagen hydrogels

2012-2019 **Graduate Research Assistant**, Purdue University

Advisor: Alyssa Panitch, Ph.D.

- The Use of Biopolymers for Tissue Engineering

2011-2012 **Undergraduate Research Assistant**, University of Puerto Rico Mayagüez

Advisor: Magda Latorre Esteves, Ph.D.

- Identifying programmed cell death pathways employed by human breast adenocarcinoma cells in response to magnetic fluid hyperthermia treatments

2011 **Summer Research Opportunities Program**, Purdue University

Advisor: Alyssa Panitch, Ph.D.

- Development of collagen-targeted thermoresponsive nanoparticles

2010 **Summer Research Opportunities Program**, The Ohio State University

Advisor: Thomas Mitchell, Ph.D.

- Comparative analysis of three fungi genomes with respect to conidiation, circadian rhythms, avirulence, appressorial formation and virulence determinants

2009 **Summer Research Opportunities Program**, The Ohio State University

Advisor: Pierluigi Bonello, Ph.D.

- Investigations into tree-pathogen and tree-insect interactions

SERVICE ACTIVITIES

Biomedical Engineering Society

2015-Present Volunteer Manager, BMES Annual Meeting

Purdue Biomedical Engineering Graduate Students Association

2014-2015 Vice-President

2013-2014 Graduate Student Advisory Committee representative

2013-2014 Second year graduate student representative

Purdue Women in Engineering Program

2015 Team Coordinator, I2D2: K-5 Outreach Program

2015 Team Coordinator, Access Engineering: K-8 Summer Outreach

	Program
2014-2016	Program Coordinator, BME Graduate Womens Gatherings
2013-2016	Team Member, I2D2: K-5 Outreach Program
2013	Team Member, Access Engineering: K-8 Summer Outreach Program

Science on Tap

2014-2016	Program Coordinator
2013-2014	Public Relations & Marketing Coordinator

PUBLICATIONS AND PATENTS

Peer-Reviewed Journal Articles

1. Vázquez-Portalatín, N., Kilmer, C., Panitch, A., and Liu, J. (2016) Characterization of collagen type I and II blended hydrogels for articular cartilage tissue engineering. Biomacromolecules 17(10): 31453152.

2. Sharma, S., Vázquez-Portalatín, N., Calve, S., and Panitch, A. (2015) Biomimetic molecules lower catabolic expression and prevent chondroitin sulfate degradation in an osteoarthritic ex vivo model. ACS Biomater Sci Eng 2(2): 241250.

3. Vázquez-Portalatín, N., Breur, G. J., Panitch, A., and Goergen, C. J. (2015) Accuracy of ultrasound-guided intra-articular injections in guinea pig knees. Bone Joint Res 4(1): 1-5.

Patents

1. Panitch, A., Paderi, J.E., Sharma, S., Stuart, K.A., and Vázquez-Portalatín, N. Extracellular matrix-binding synthetic peptidoglycans U.S. Patent 9200039, issued December 1, 2015.

Conference Proceedings and Presentations

1. Vázquez-Portalatín, N. Effects of matrix factors on chondrocytes embedded in collagen type I and II scaffolds for cartilage repair. Preliminary Exam Oral Presentation. West Lafayette, IN. 2016.

2. Vázquez-Portalatín, N., Kilmer, C., Liu, J., and Panitch, A. Characterization of collagen type I and II gels for articular cartilage tissue engineering. Biomedical Engineering Society Annual Meeting. Poster. Tampa, FL. 2015.

3. Vázquez-Portalatín, N., and Panitch, A. Biomimetic peptidoglycan lowers friction levels in articular cartilage. Biomedical Engineering Graduate Student Association Research Symposium. Poster. West Lafayette, IN. 2015.

4. Vázquez-Portalatín, N., Sharma, S., and Panitch, A. Characterization and animal model development for the study of an aggrecan mimic in osteoarthritis. Biomedical Engineering Summer Seminar Oral Presentation. West Lafayette, IN. 2014.

5. Vázquez-Portalatín, N., and Panitch, A. Biomimetic peptidoglycan lowers friction levels in articular cartilage.5th Annual Biomaterials Day. Poster. Cleveland, OH. 2013.

6. Vázquez-Portalatín, N., and Panitch, A. Biomimetic peptidoglycan lowers friction levels in articular cartilage. Biomedical Engineering Society Annual Meeting. Poster. Seattle, WA. 2013.

7. Vázquez-Portalatín, N., McMasters, J., and Panitch, A. Collagen-targeted thermoresponsive nanoparticles. Student Research Opportunities Program Research Symposium. Oral Presentation. West Lafayette, IN. 2011.

8. Vázquez-Portalatín, N., McMasters, J., and Panitch, A. Collagen-targeted thermoresponsive nanoparticles. 25th Annual CIC Student Research Opportunities Program Conference. Poster. Columbus, OH. 2011.

9. Vázquez-Portalatín, N., and Mitchell, T. K. Comparative analysis of three genomes with respect to conidiation, circadian rhythms, avirulence, appressorial formation, and virulence determinants. Student Research Opportunities Program Research Symposium. Oral Presentation. Columbus, OH. 2010.

10. Vázquez-Portalatín, N., and Mitchell, T. K. Comparative analysis of three genomes with respect to conidiation, circadian rhythms, avirulence, appressorial formation, and virulence determinants. 24th Annual CIC Student Research Opportunities Program Conference. Poster. Columbus, OH. 2010.

11. Vázquez-Portalatín, N., Nagle, A., Whitehill, J., and Bonello, P. Investigations into tree-pathogen and tree-insect interactions. Student Research Opportunities Program Research Symposium. Oral Presentation. Columbus, OH. 2009.

12. Vázquez-Portalatín, N., Nagle, A., Whitehill, J., and Bonello, P. Investigations into tree-pathogen and tree-insect interactions. 23th Annual CIC Student Research Opportunities Program Conference. Poster. Ann Arbor, MI. 2009.

AWARDS AND HONORS

2016	Purdue University College of Engineering Outstanding Service Award
2015	Purdue University Joe Bourland Travel Award
2014	Federation of American Societies for Experimental Biology (FASEB) Travel Award
2012	Purdue University George Washington Carver Fellowship
2008	Xerox/SHPE Scholarship

PROFESSIONAL AFFILIATIONS

2012-Present	Biomedical Engineering Society
2009-2012	International Society for Pharmaceutical Engineering
2007-2012	Society of Hispanic Professional Engineers